CROP STRESS DURING THE 2018 DROUGHT
CASE STUDY: NORTH BRABANT, THE NETHERLANDS.

AKE JOSIANE UWUMUKIZA
July 2021

SUPERVISORS:
Dr. Ir. C. van der Tol
Dr. Ir. R. van der Velde

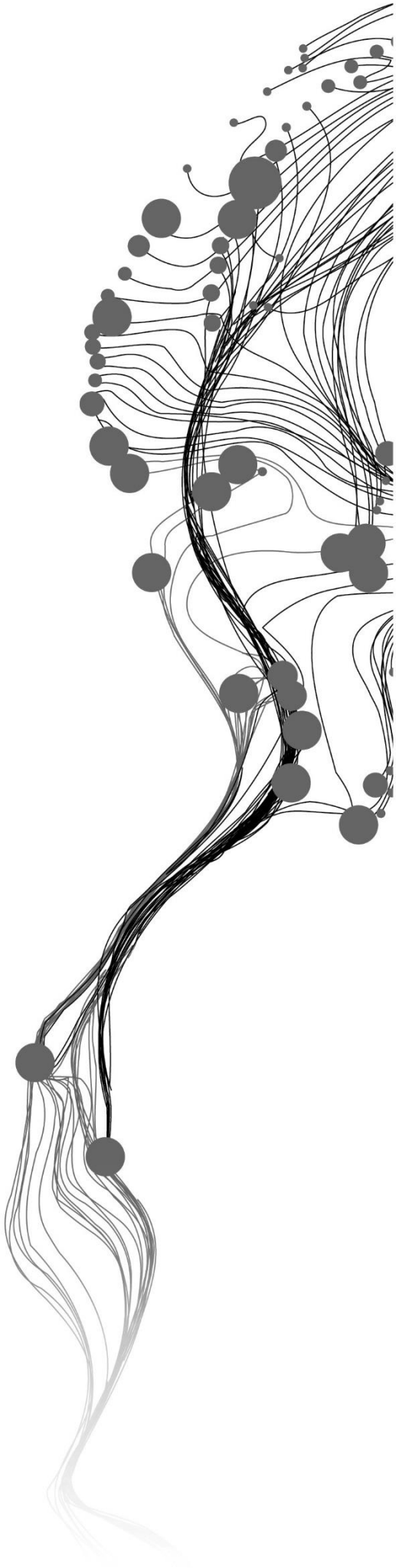

CROP STRESS DURING THE 2018 DROUGHT
STUDY AREA: NORTH BRABANT, THE NETHERLANDS

AKE JOSIANE UWUMUKIZA
Enschede, The Netherlands, July 2021

Thesis submitted to the Faculty of Geo-Information Science and Earth Observation of the University of Twente in partial fulfilment of the requirements for the degree of Master of Science in Geo-information Science and Earth Observation.

Specialization: Water Resources and Environmental Management

SUPERVISORS:
Dr. Ir. C. van der Tol _ First supervisor
Dr. Ir. R. van der Velde _ Second supervisor

THESIS ASSESSMENT BOARD:
Prof. Dr. T.H.M Rientjes (Chair)
Dr. Ir. A. Vrieling (External examiner, UT-ITC-NRS)
Ir. A.M. van Lieshout (Procedural advisor)

DISCLAIMER

This document describes work undertaken as part of a program of study at the Faculty of Geo-Information Science and Earth Observation of the University of Twente. All views and opinions expressed therein remain the sole responsibility of the author and do not necessarily represent those of the Faculty.

ABSTRACT

Water shortage is a severe environmental constraint to plant productivity and food security worldwide. Due to the severity and duration of drought, it can exceed all other causes of crop yield reduction. Crop growth and yield production are negatively affected by deficient water supply and abnormal temperature due to physical damages and biochemical changes. For better management, it is vital to understand the physiological, ecological, and biological processes related to drought stress. Drought stresses reduce leaf area, leaf water content, root proliferation, and CO_2 assimilation by leaves due to the stomatal closure.

This study aims to develop a method to monitor drought stress on potatoes and differentiate this from other effects such as diseases, wildfires, lack of fertilizers, and floods by using multiple indices and considering physical processes related to drought. Satellite data combined with in-situ data have been used to achieve the objectives. The first step was to identify the drought period, based on the time series of 20 years Normalized Difference Vegetation Index (NDVI), four current years' time series of precipitation deficit, and comparative analysis of two different growing seasons (2017 and 2018) of the temperature difference between the surface and air(dTsa). The second step was to retrieve the vegetation properties ((leaf area index (LAI), leaf water content(Cw), chlorophyll content(Cab), and dry matter content(Cdm)) from a radiative transfer model for solar radiation in vegetation (RTMo), which is part of the 'Soil Canopy Observation of Photosynthesis and Energy fluxes' model (SCOPE),' then evaluated whether their seasonal course can be used as stress indicators. This retrieval is based on Sentinel-2 reflectance data. The simulated vegetation properties coupled with weather data from climate reanalysis data produced by the computer simulation model (ERA5) have been used in the SCOPE to simulate photosynthesis and evapotranspiration, which are the variables used to assess the severity and duration of the 2018 agricultural drought in the Raam region. The results obtained have been compared with groundwater levels, rainfall, leaf area index, and the estimated root zone soil moisture based on the weighted average method. The approach has been made by relating two different growing seasons: non-stressed toward water-stressed crops conditions 2017 versus 2018.

This analysis showed that the critical period that indicates drought was the 2018 summer in the Raam region. The time series of NDVI was related to in-situ data of annual agricultural crop yield from 2000 to 2020 as documented by CBS. The NDVI time series demonstrates a significant relationship between the 2018 NDVI maturity stage and the seasonal 2018 annual yield reduction production. Most vegetation properties show the stress indicators in their season course, except chlorophyll content due to the insufficient cloud-free data in 2017. The simulated photosynthesis indicated drought in the 2018 summer as expected. The in situ data used for comparison were first analyzed to check if they show drought at the same period. The data used for root zone soil moisture of potato are for 40cm and 80 cm depth as potato roots can go shallow or deeper depending on where they are cultivated.

In conclusion, the Sentinel-2 reflectance data can be relied on in agricultural drought monitoring of a specific crop. It has a high spatial resolution to provide accurate and detailed data that can be used to retrieve relevant vegetation properties. In this study, the combination of various indicators which react on all aspects of drought (meteorological, remote sensing indices, vegetation properties, and in-situ data) was used to develop a reliable method for agricultural drought monitoring on potato. This approach was based on multispectral Sentinel-2 data of 20m spatial resolution, which provided reliable photosynthesis results that matched with the hydrological drought as indicated by the in-situ data of groundwater and soil moisture.

Keywords: Agricultural drought Monitoring, Sentinel-2 reflectance data, Radiative transfer inversion Model (RTMo), Vegetation properties, SCOPE Model, Photosynthesis, Evapotranspiration, Root zone soil moisture, Groundwater level

ACKNOWLEDGEMENTS

First and foremost, I would like to extend my gratitude to the almighty God for his blessing and protection during this journey.

I would like to thank the Dutch Government for providing the financial means through the Orange Knowledge Program to pursue a Masters' course at the University of Twente (ITC).

I would like to express my sincere appreciation to my supervisors; Dr. Ir. C. van der Tol and Dr. Ir. R. van der Velde; for their professional guidance, for supervising my work with interest, providing valuable suggestions and feedback, and for allowing me to benefit from their enormous experience. This thesis would not be completed without their support.

I would like to thank mentor Ir.A.M. Van Lieshout for his advice, motivation, and ensuring a good study environment during this program.

I would like to thank the University of Twente and the Faculty of Geoinformation Science and Earth Observation, mainly the Department of Water Resources Management, for the knowledge and skills they provided through lectures and staff.

My appreciation goes to my classmates, mainly our class representative Ranit De and Ransford Nii Ayitey Welbeck, for their support during this master's program.

Special thanks to my family, friends, and countrymates for moral support and encouragement.

Last but not least, I would like to thank my big sister Ingabire Antoinette and my best friend Tumukunde Clarisse for always being my supporting system, always being there for me, encouraging, and praying for me. Special thanks to everyone out there; I didn't mention who supported me and prayed for me; I am really grateful.

Contents

LIST OF FIGURES

LIST OF TABLES

LIST OF ABBREVIATION

KNMI: Koninklijk Nederlands Meteorologisch Instituut (Royal Dutch Meteorological Institute)
NDVI: Normalized difference vegetation index
LST: Land surface temperature
LAI: Canopy leaf area index
Cw: Equivalent leaf water thickness
Cab: Leaf chlorophyll content
N: Mesophyll structure parameter
Cdm: Leaf mass per area (dry matter)
Cs: Senescent material (brown pigments)
Cant: Leaf anthocyanin content
Cca: Leaf carotenoid content
LIDFa: Leaf inclination distribution
LDFb: Function parameters a, b
RTMo: Radiative transfer model for solar radiation in vegetation
ERA5: Climate reanalysis data produced by the computer simulation model
ECMWF: The European Centre for Medium-Range Weather Forecasts
SCOPE: The soil canopy observation of photosynthesis and Energy flux
SPI: Standardized precipitation index
VHI: Vegetation health index
ADCI: Agricultural dry condition index
NDWI: The normalized difference water index
VCI: Vegetation condition index
TCI: Temperature condition index
ET_o: Reference evaporation
ET_a: Actual evapotranspiration
ET_p: Potential evapotranspiration
FAO: Food Agriculture Organisation
MODIS: Moderate Resolution Image Spectroradiometer
GEE: Google Earth Engine
Dinoloket: Data en Informatie van de Nederlandse Ondergrond
RZSM: Root zone soil moisture
MSI: Multispectral Instrument
dTsa: The temperature difference between the land surface and air

1. INTRODUCTION

1.1. Background

Drought is a major natural hazard, which varies spatially and temporally; it fluctuates in severity, duration, intensity, and extent. Nevertheless, it is expected to increase in occurrence and severity due to climate change (Dai, 2013; Thornes, 2002). Drought is defined as a prolonged time of abnormally low water supply, leading to water shortage. Precipitation is the most dominant factor influencing drought. It is a phenomenon that manifests itself gradually and impacts regions and societies in different ways, mainly on agricultural production, water resources, environment, and ultimately economic development of the countries (Fathi & Tari, 2016; Sheffield, Wood, & Roderick, 2012).

The climatological scientific community has defined four different types of drought: 1) Meteorological drought, 2) Hydrological drought, 3) Agricultural drought, 4) Socio-economic drought (Do Amaral Cunha et al., 2019). Meteorological drought is defined by precipitation deficiency, it occurs when atmospheric moisture is inadequate to provide rain, resulting in an abnormally dry period in a specific area, and then dry weather patterns dominate an area. Hydrological drought occurs after many months of meteorological drought. It is characterized by low streamflow, which supplies less water into the water bodies, and groundwater reduction due to less recharge to the saturated zones. The soil moisture deficit causes plant stress, which leads to agricultural drought, the condition in which the root zone soil moisture available cannot meet the plant's growth demands. Socio-economic drought relates to water supply and water demand for various human activities; it is associated with the demad and supply of economic goods (D. A. Wilhite & Glantz, 2019; Hayes et al., 2011).

This study focuses on agricultural drought monitoring because agriculture is usually the first economic sector affected by drought (Ruíz, 2015). Agricultural drought is one of the significant abiotic stress constraints to crop production and food security worldwide, and it is affecting societies in various ways. For example, it reduces food production, increases food prices, affects the export system, disturbs the country's economy, and even causes famine in developing countries (Fahad et al., 2017). Crops are exposed to water stress when the amount of water supply to the tissue is less than the required water for crop growth and sometimes when the evapotranspiration is very high (Peng, Di, Deng, Han, & Yagci, 2013). This phenomenon causes crop stress, which leads to a significantly lower crop production yield.

Regions in Europe regularly experience droughts throughout the course of time, where a severe one occurred in 1976, especially in the Northern and Western parts of Europe (Feyen & Dankers, 2009; Weijers, 2020; W. Peters et al., 2020). The Royal Netherlands Meteorological Institute (KNMI, 2020) and Weijers (2020) published that among the dry years that happened in the Netherlands (1976, 1983, 1995, 2003, 2006, 2018, and 2019), 2018 was the second driest and the hottest year recorded after 1976. The 2018 drought negatively impacted various sectors in the Netherlands, especially the agricultural sector, where several crops experienced substantial yield reduction due to the low precipitation in combination with very high evapotranspiration (Prins, Jager, Stokkers, & van Asseldonk, 2018; Philip et al., 2020; Centraal Bureau Voor de Statistiek, 2020). The farmers, society, and the country have been affected by this agricultural drought as it reduced yield production, increased food price, affected the export due to the low production. Recreation areas have been affected too. In response, the government under the Ministry of Agriculture, nature and food quality took actions to compensate for some of the damage suffered. The total economic loss was

estimated between 450 and 2080 million euros (Prins et al., 2018; Philip et al., 2020). Table 1 shows the 2018 potato yield reduction by comparing the current twenty years data.

Table 1:Comparison of total potato yield production from 2000 to 2020 in the Netherlands, documented by Centraal Bureau voor de Statistiek, 2020.

Year	The cultivated area in hectare (ha)	Harvested area in hectare (ha)	Gross yield per ha (1000kg)	Total gross revenue ha (1000kg)
2000	180200	174929	46.5	8126799
2001	163934	161665	43.4	7015253
2002	165157	164308	44.8	7362738
2003	**158644**	**158518**	**40.8**	**6468762**
2004	163905	162821	46	7487652
2005	155784	155558	43.6	6776860
2006	**156499**	**155825**	**40**	**6239648**
2007	157174	156899	43.7	6859727
2008	151869	151865	46	6992690
2009	155233	154971	46.3	7180981
2010	158213	156969	43.6	6843529
2011	159686	159233	46.1	7333472
2012	149932	149770	45.2	6765618
2013	155822	155822	42.2	6576860
2014	156252	155502	45.7	7100258
2015	156511	155661	42.7	6651692
2016	157900	155594	42	6534338
2017	162671	160791	46	7391881
2018	**164973**	**164597**	**36.6**	**6025365**
2019	**167523**	**165733**	**42**	**6961230**
2020	165621	164504	42.7	7020062

The potato crop is chosen in this study because it is one of the most cultivated in the Netherlands and worldwide; it highly contributes to food security, but it is vulnerable to drought and most affected by the 2018 drought. It is documented by the central bureau of statistics. Based on Table 1, the 2018 drought was the most critical, even compared to the other dry years published by KNMI, such as 2003, 2006, and 2019.

The various drought indicators such as precipitation deficit, normalized difference vegetation index (NDVI), the temperature difference between the surface and air (dTsa), vegetation properties (Canopy leaf area index (LAI), Equivalent leaf water thickness (Cw), Leaf chlorophyll content (Cab), Mesophyll structure parameter (N), Dry matter content (Cdm), Senescent material (Cs), Leaf anthocyanin content (Cant), Leaf carotenoid content (Cca), Leaf inclination distribution (LIDFa), and Function parameters a, b (LDFb)), soil moisture, and groundwater level have been used in this study to monitor the 2018 agricultural drought in Raam catchment. This study developed an accurate algorithm for crop drought monitoring that exploits remote sensing data from specific crop and meteorological data, remote sensing indices, vegetation properties, and in situ data. The developed method can help the planners at the ministry of agriculture to identify the drought stress on crops and then provide early warning to the farmers. In addition, it will help decision-makers with mitigation measures and even how they can deal with similar droughts.

1.2. Research problem statement

A survey of the literature demonstrates that the field point measurement method is the main method used to analyze vegetation stress (Beersma & Adri Buishand, 2004). Normally, the meteorological data through the potential precipitation deficit is the common drought indicator used in the Netherlands for quantifying drought severity of previous significant dry years such as 1976, 2003, 2006, and even it is used in some studies for monitoring the current drought (Sluijter et al., 2018) This indicator uses point measurements which lacks the spatial resolution, and the data are often incomplete.

Earlier, studies were done without remote sensing techniques because there were insufficient sensors to provide data (Bressers & Bressers, 2016). At present, satellite data are adequate for drought modeling, but few studies on agricultural drought using remote sensing data have been carried out so far (Buitink et al., 2020). There is a lack of agricultural drought monitoring studies using the combination of various indicators (meteorological, remote sensed, vegetation indices, and in-situ data). Such methods involve the retrieval of vegetation properties using remote sensing data of sentinel-2, which have good spatial resolution are more specific and needed. The kinds of studies using that approach are needed mainly on particular crops as the farmers cultivate different crop types and because the crops react differently to drought, with some crops or varieties more sensitive to drought than others.

1.3. Research Objectives and Questions

The main objective of this study is to develop a method used to monitor drought stress in potatoes and differentiate this from other effects (of diseases, wildfire, insects, pesticides, lack of fertilizers, flood) by using multiple indices and considering plant physiologic processes related to drought.

1.3.1. Specific Objectives

1. To verify if 2018 was exceptional by comparing the unstressed vegetation with stressed, using MODIS NDVI time series of 20 years (2000 - 2020).

2. To retrieve multi-spectral reflectance data from Sentinel-2 and use it in RTMo to retrieve vegetation properties and evaluate whether anomalies in their seasonal dynamics can be used as stress indicators

3. To use the retrieved vegetation properties combined with the weather data as the input for the SCOPE model to simulate photosynthesis and actual evapotranspiration.

4. To assess the performance of SCOPE model output variables against the determined physical processes occurring during drought, such as root zone soil moisture.

5. To identify the phenological stage of potato affected during the drought period.

1.3.2. Research Questions

1. Was there an anomaly in the 2018 NDVI that can be attributed to agricultural drought?

2. Which of the vegetation properties that can be retrieved from Sentinel-2 are indicative of agricultural drought?

3. Which are output variables of the SCOPE model related to drought? And how were their reactions against the root zone soil moisture?

4. Which is the best combination of meteorological and remote sensed- vegetation indices used in agricultural drought monitoring and why?

5. At which stage of development and growth of potato is most affected by agricultural drought?

1.4. Thesis structure

The structure of this thesis is arranged in six chapters:
The first chapter is the introduction composed of background, along with research problems, research objective, research questions, and thesis structure. The second chapter is the literature review. The third chapter describes the study area, defines the location of the Raam catchment and specific potato farms, the climate of the region during the study period, the location of soil moisture stations, soil texture, and the piezometer's location. The fourth one is materials and method, explaining the data used, data sources, data processing, and study methodology. The fifth chapter contains the results and discussion; the sixth chapter presents the conclusion, the limitation, and recommendation following from this study; the seventh is the appendix.

2. LITERATURE REVIEW

2.1. Agricultural drought monitoring

Drought monitoring and early warning is an evaluation of the drought situation on time and alerting community and drought management teams by announcing the possibility of any coming drought event (Boken, 2009). Agricultural drought monitoring and early warning systems help in agricultural drought risk management plans. A comprehensive drought monitoring system that can determine drought severity and provide an early warning of drought's onset is needed to face the drought challenges. The severity and duration of the agricultural drought at the surface of the reference crop are indicated by numerous indicators of drought, such as precipitation deficit, high temperature, lower soil moisture content, and water losses through evapotranspiration (L. Zhang et al., 2019). Based on the mentioned indicators, several studies worldwide have been done to monitor agricultural drought using different indices. For example, the Normalized Difference Vegetation Index (NDVI), standardized precipitation index (SPI), vegetation health index (VHI), and the agricultural dry condition index (ADCI) have been used individually to monitor agricultural drought, with food crises early warning purposes in 6 different regions all over the world (Meroni, Fasbender, Rembold, Atzberger, & Klisch, 2019; Wu, Ma, & Yan, 2020; (Sur, Park, Kim, & Lee, 2019b). The combination of visible, near-infrared, and shortwave infrared remote sensing data from MODIS products was utilized to provide a highly accurate result on vegetation drought stress assessment in America, a case study of Iowa (Peng et al., 2013).

Peters et al. (2002); Vicente-Serrano et al. (2010); Huang et al. (2020) concluded that no single index could capture all aspects of agricultural drought because indices respond to different aspects of the drought. Some are based on precipitation, others on evaporation, some on soil moisture, and others on vegetation characteristics. This means each index has its limitations. For example, NDVI has been successfully used in agricultural drought monitoring due to its ability to respond to vegetation's presence, density, and greenness (Bhavani et al., 2017). In agricultural drought monitoring, NDVI has been related to change in water stress, which is sometimes not the case because NDVI responds to other factors like crop diseases, wildfire, insects, and lack of fertilizers.

The normalized difference water index (NDWI) reflects the moisture content of vegetation canopies (B.-C. Gao, 1995). Various studies (Serrano et al., 2019; JRC European Commission, 2011; Peng et al., 2013) have defined NDWI as a suitable satellite index to monitor agricultural drought. NDWI is derived from near-infrared (NIR) and short wave infrared (SWIR) channels, where the NIR band responds to the leaf structure and leaf dry matter content, while SWIR responds to the leaf water content and to the spongy mesophyll structure (JRC European Commission, 2011). NDWI is calculated as

$$\text{NDWI} = \frac{NIR-SWIR}{NIR+SWIR} \quad \text{(Eq1).}$$

Where the NIR located at 0.86 μm wavelength and SWIR at 1.24 μm wavelength (B. C. Gao, 1996).
NDWI can detect dryness and wilt of the vegetative canopy; it is more sensitive in assessing the health status of plants. High NDWI values indicate the high water content of the vegetation. On the other hand, it has a weakness in being affected by the soil reflectance effects (B. C. Gao, 1996).

Standardized precipitation index (SPI) is also an agricultural drought index that is based on precipitation and ignores other water sources, contributing to the plant's growth, such as irrigation water, groundwater,

and water from rivers (Livada & Assimakopoulos, 2007). The Vegetation Health index (VHI) is a vegetation drought monitoring index that is based on a strong inverse correlation between normalized difference vegetation index (NDVI) and brightness temperatures since land surface temperatures impact vegetation vigor (Badeck et al., 2004). When the land surface temperature increases, it negatively affected vegetation vigor leading to plant stress (White et al., 1997; Badeck et al., 2004). VHI is successful when applied in the low latitudes, which means where vegetation growth is primarily limited by water. Otherwise, it requires caution in humid regions of high latitudes, where energy is the main limiting factor for vegetation development(Karnieli et al., 2006).

The agricultural dry condition index (ADCI) is a weighted index that combines land surface temperature, soil moisture, and vegetation activity as the input data (Sur et al., 2019). ADCI has been a successful agricultural drought index in monitoring and predicting actual drought conditions in various studies (Sur et al., 2019; Kim et al., 2021). ADCI can be calculated using the following equation:

$$ADCI = 0.6 * SM + 0.2 * VCI + 0.2 * TCI \quad \text{(Eq2).}$$

Where 0.6, 0.2, and 0.2 are the weighted values of soil moisture (SM), VCI is vegetation condition index, and TCI is temperature condition index. VCI is estimated using the following equation of the maximum, and minimum values of the NDVI developed based on the concept that droughts cause water scarcity to plants (Kim et al., 2021).:

$$\text{VCI} = \frac{NDVI - NDVImin}{NDVImax - NDVImin} \quad \text{(Eq3).}$$

Temperature condition index(TCI) is a land surface temperature (LST) related index that is standardized based on the minimum and maximum LST due to the fact that LST affects soil moisture which leads to vegetation stress (Kim et al., 2021):

$$\text{TCI} = \frac{LSTmax - LST}{LSTmax - LSTmin} \quad \text{(Eq4).}$$

Table 2: shows the calculation, advantages, and disadvantages of some drought indices, mainly the ones used in the study.

Drought Index and their Calculation	**Advantages**	**Disadvantages**	**Reference**
$\text{NDWI} = \frac{NIR - SWIR}{NIR + SWIR}$	- NDWI is strongly related to the plant water content; it is an excellent commission for plant water stress. - It highly responds to vegetation properties	- NDWI is highly affected by the soil reflectance effects. - It is difficult to detect the stress type on the canopy using only NDWI.	(B. C. Gao, 1996). (JRC European Commissio n, 2011).
SPI	- SPI is a simple index - It only requires rainfall input data.	- SPI does not consider other drought indicators such as; temperature and soil moisture	(Mckee et al., 1993).

	- Its standardization ensures the frequency consistent of extreme events at any location and on any time scale. - SPI allows drought monitoring at different temporal scales. - It describes the dry and wet period in the same way	- Misleading SPI values when it is applied to regions of low seasonal precipitation (short time scales). - Different lengths of precipitation records of data impact the SPI results.	(Mishra & Singh, 2011).
$NDVI = \frac{NIR - RED}{NIR + RED}$	- NDVI is easy to use, no modeling; frequently works well as most errors are minimal. -It is used to minimize the impacts of variable irradiance levels. - It is limited to any segment of its functional relationship with vegetation properties.	- NDVI does not differentiate the cause of plant stress. - It tends to amplify atmospheric noise in its ration bands, which causes it to be very sensitive to background variation. - NDVI Saturates at high biomass content, which challenges it to differentiate plant cover levels.	(Bhavani et al., 2017). (Pettorelli et al., 2005).
$PD = Cum\ ET_0 - Cum\ R_n$	- Precipitation deficit (PD) is in situ related index using meteorological data. -It considers the main drought indicators (ET and Rainfall).	- No spatial resolution	(Sluijter et al., 2018). (Mallin et al., 1993).
$dTsa = LST - Ta$	- dTsa is immediately indicating the intensity and heat fluxes of land-atmosphere interaction. - It considers the impact of surface characteristics and air condition to detect drought.	- dTsa does not consider other drought indicators apart from temperature.	(Zhang et al., 2015a).

Therefore, it is crucial to adapt remote sensing techniques in agricultural drought monitoring, preferably on specific crops, because it provides detailed information to the farmers as they cultivate different crops. Additionally, it is vital to consider multiple indices based on various indicators while monitoring agricultural drought to avoid misunderstanding the cause of crop stress. (Peng et al.,2013; Sheffield et al., 2012).

The various agricultural drought indicators which respond to different aspects of drought (Precipitation deficit, NDVI, dTsa, vegetation properties, root zone soil moisture, and groundwater level) have been used in this study to monitor drought stress on potato by referring to the 2018 summer drought. In addition, multi-spectral imageries and reflectance from sentinel-2 have been explored; the information from the different bands helped in selecting the best data to be used, which produced a highly accurate result for drought monitoring.

2.1.1. Sentinel-2 product

Sentinel-2 satellite with the Multispectral Instrument (MSI) sensor onboard was launched in June 2015. It is the optical earth observation satellite in the European Copernicus program, and it was created and developed under the industrial leadership of the European Space Agency. Sentinel-2 has three different spatial resolutions (10, 20, and 60m), which cover the span of 13 spectral bands, from visible to shortwave infrared (Zheng et al., 2018). Band 2, 3, 4, and 8 are the four bands at 10m resolution secure continuity with other satellites such as Landsat-8 and address user needs. The six bands (band 5, 6, 7, 8A, 11, and 12) at 20m resolution fulfill needs for improved land-cover classification and retrieval of vegetation properties and other geophysical parameters; this resolution is suitable for agriculture. The three remaining bands at 60m resolution (band 1, 9, and 10) are mainly used for atmospheric correction and cloud inspection (Pettorelli, 2019). Table 3 demonstrates the spectral band, width, and spatial resolution of the mentioned Sentinel-2 MSI sensor.

Table 3: The spectral band, width and spatial resolution of Sentinel-2 MSI sensor (Zheng et al., 2018).

Sentinel-2 Bands	**Central Wavelength (nm)**	**Band Width (nm)**	**Spatial Resolution (m)**
Band 1 - Coastal aerosol	443 nm	20	60
Band 2 - Blue	490 nm	65	10
Band 3 - Green	560 nm	35	10
Band 4 - Red	665 nm	30	10
Band 5 – Vegetation Red Edge	705 nm	15	20
Band 6 - Vegetation Red Edge	740 nm	15	20
Band 7 - Vegetation Red Edge	783 nm	20	20
Band 8 - NIR	842 nm	115	10
Band 8A - Vegetation Red Edge	865 nm	20	20
Band 9 – Water vapour	945 nm	20	60
Band 10 - SWIR - Cirrus	1375 nm	30	60
Band 11 - SWIR	1610nm	90	20
Band 12 - SWIR	2190 nm	180	20

Sentinel-2 data have been successfully used in various applications. Among the ones related to drought monitoring, it has been used to assess the drought severity based on perpendicular drought index estimated by sentinel-2 data in the west of Texas, America, in 2017(Y. Chen et al. l., 2019). Sentinel-2 products have been used in developing a fusel vegetation temperature condition index for drought monitoring in Guanzhong plain, Shaanxi Province, China(Zhou et al., 2020).

2.1.2. Normalized difference vegetation index (NDVI)

The Normalized Difference Vegetation Index (NDVI) is a spectral index that is related to the quantity of photosynthetically absorbed radiation. It is used to determine the vigor of vegetation, and it is associated with the other vegetation properties such as leaf area index (LAI), total green biomass, and photosynthetic activity of plants in the red band (Borzuchowski & Schulz, 2010). NDVI ranges between -1 to 1, where the negative value indicates clouds and water, while the positive value indicates bare soil to good vegetation healthy (Dagnenet, 2019). The NDVI is estimated as a ratio between visible (red) and the near-infrared (NIR) bands:

$$NDVI = \frac{NIR-RED}{NIR+RED} \quad \text{(Eq5).}$$

RED is red band reflectance (0.6-0.7μm), while NIR is near-infrared band reflectance (0.75-1.4 μm).

2.1.3. Precipitation deficit

Precipitation deficit is one of the most common drought indicators used in quantifying drought severity and shows how long a water shortage period lasted, as the rainfall is the primary water source of agriculture (Mallin et al.,1993; Sluijter et al., 2018). It is defined as the cumulated difference between daily amounts of precipitation and the computed daily potential evapotranspiration in a specific area (Harmsen et al., 2009; Philip et al., 2020). Different studies in the Netherlands have used potential precipitation deficit to monitor drought. The maximum cumulative difference between precipitation and potential crop evaporation has been used to quantify the drought occurrence in six districts within the Netherlands (Beersma & Buishand, 2007). Based on the thirteen reference station data of average rainfall and evapotranspiration distributed in the country, KNMI used it to calculate the average precipitation deficit based on the growing season from 1st April to 30th September. The reference evaporation is estimated using makkink based evaporation method by reference to the well fedded short grass with sufficient soil moisture. The precipitation deficit of a specific location can be determined based on the station data within or around the location.

2.1.4. Land surface temperature (LST)

Land surface temperature is determined by physical processes that are sensitive to drought, and therefore related to drought. It is important in drought detection as it is used to detect the dynamics of processes on the land surface(Dash, Göttsche, Olesen, & Fischer, 2002). LST influence the temporal dynamic of soil moisture content (SMC), and as both of them (LST ad SMC) are the main physical indicators related to drought, each impact other, which results to the contribution of soil moisture emission (Pablos et al., 2016).

LST from Landsat-8 is calculated in six steps using ArcGIS:
The first step is to calculate the top of atmosphere (TOA) spectral radiance, then convert to TAO brightness temperature from Kelvin to Celsius. The 3rd step is to Calculate the NDVI and the proportion of vegetation, which is related to NDVI, then after estimation of emissivity (ε), finally apply the following Land surface temperature formula in raster calculator to obtain the surface temperature map

$$LST = (BT / (1 + (0.00115 * BT / c2) * Ln(\varepsilon))) \quad \text{(Eq6).}$$

Where BT is brightness temperature, c2 is a factor =1.4388, and (ε) is emissivity

2.2. SCOPE Model

The Soil Canopy Observation of Photosynthesis and Energy fluxes model (SCOPE) is designed to simulate photosynthetic, hydrological, and modeling of interactions between radiative and non-radiative fluxes among elements of the vegetation canopy (Yang et al., 2020). SCOPE relates remote sensing reflectance with biomass functioning (Bayat et al., 2019). This interaction provides reflectance, fluorescence, and thermal radiance as the remote sensing signal outputs. The vegetation reflectance simulated depends on the type of plant, plant phenological stage, and reflectance characteristics.

2.2.1. Some improvement of SCOPE to SCOPE 2.1 version

A recent improvement of the SCOPE model has been made in the main sub-models; this provided the additional outputs in the SCOPE-2.1 and the facilitation of achieving the new outputs without extra formulas (Yang et al., 2020). Some new outputs added are radiance in the viewing direction, including fluorescence, fluorescence scattering coefficient, spectrally integrated observed fluorescence, canopy electron transport rate, etc.

Van Der Tol et al. (2009) published the first version of the SCOPE Model; since then, improvements have been made to the model for the sake of the users. For example, with the formal SCOPE version, the users were supposed to measure some input variables such as the soil reflectance spectrum, which is now simulated due to the implementation of a soil reflectance model. The code has been improved to increase the computation speed. For this reason, it is possible to use the model for making maps (Yang et al., 2020).

2.2.2. SCOPE Model Structure

Figure 1 shows the SCOPE model structure. The SCOPE requires sub-models for radiative transfer (RTMs), modules for energy balance, input-output functions, and some supporting functions. Seven RTMs contain one for the soil, and another one for leaf, and five for the combined system of soil and foliage are included in SCOPE to simulate the spectrally resolved radiance originating from the vegetation (Yang et al., 2020). The energy balance module in SCOPE is used to minimize the energy balance closure error (Ebal) and is expressed in Wm^{-2} :

$$Ebal = Rn - H - \lambda E - G \qquad \text{(Eq7).}$$

Where is ***Rn*** is the net radiation, ***H***: Sensible heat flux, ***λE***: Latent heat flux, and ***G:*** Ground heat flux.

The inputs data required for the SCOPE model consist of soil data, vegetation properties (leaf and canopy), meteorological data, and Sun-observer geometry which is determined by the sun, zenith angles of the observer, and their absolute azimuth difference (Tol et al., 2009; Yang et al., 2020). The various output variables simulated by SCOPE Model, Photosynthesis of canopy which obtained from vegetation part, Latent heat flux of canopy, Latent heat flux of soil, and evapotranspiration from fluxes part are the most variables related to agricultural drought, and which are focussed on in this study.

Figure 1 describes the function of SCOPE. Down part (**A**) explains how the light interacts with soil and canopy; briefly, it is about simulation reflectance. The brightness shape moisture (BSM) models simulate soil, RTMo, RTMf, and RTMz, which is canopy part, which means are different spectral parts that provide reflectance fluorescence outputs and vegetation properties. The upper part (**B**) is about photochemistry and Energy balance. For this, different parameters such as radiation, temperature, wind speed, and air pressure are required to simulate all fluxes needed (Yang et al., 2020). The link between parts A and B is 'net radiation' because SCOPE can simulate very well how much incoming and outgoing radiation, and even what is remaining (net radiation) then partitioned it to transpiration, evaporation, and photosynthesis.

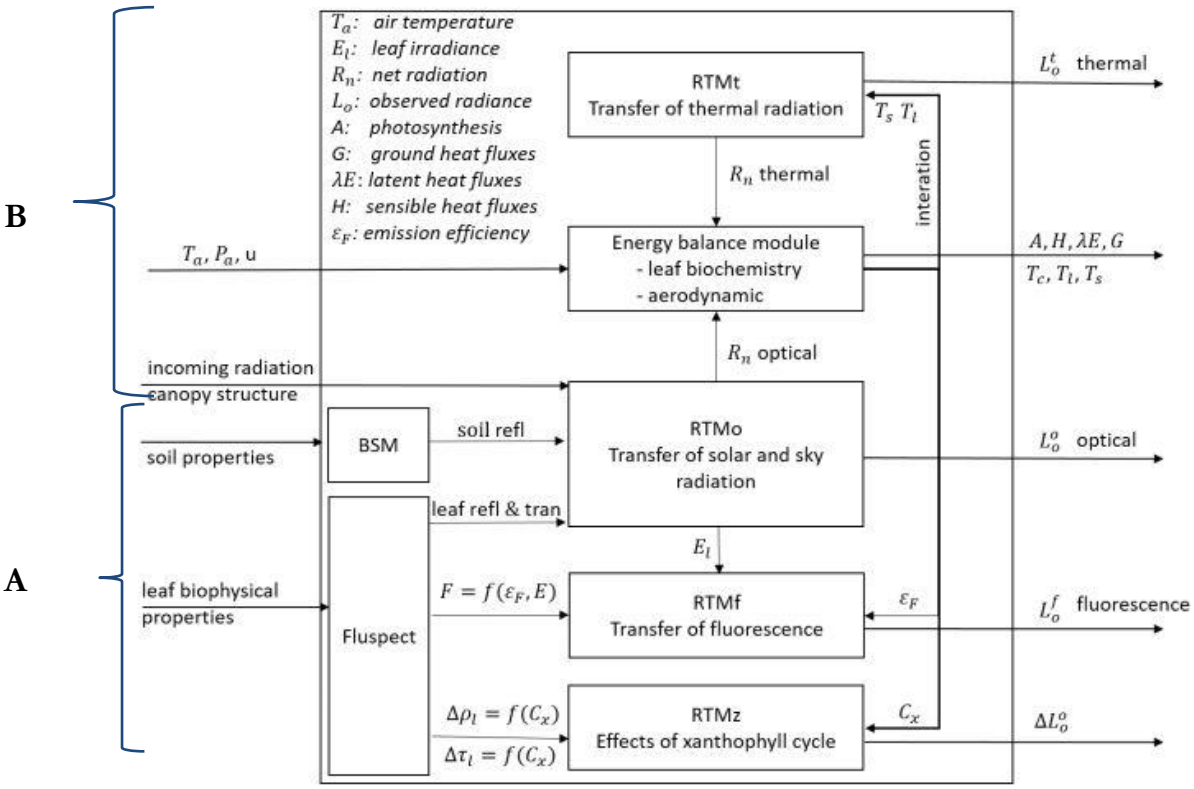

Figure 1: Diagram overview of the SCOPE model structure obtained from Yang et al., 2020.

2.3. Concept of Evapotranspiration (ET)

Evapotranspiration is a combined sum of water evaporated from the surface areas (such as open water bodies, bare soil, etc.) and transpiration from vegetation, person's body, or any other living that can release moisture to the atmosphere (Li et al., 2009). ET represents the water loss via evaporation heat, which is the energy used to transform water into gas and transmit it to the atmosphere. The rate of ET mainly depends on shortwave radiation, wind speed, and air temperature (Pereira et al., 1999). The following are different types of Evapotranspiration:

- **Reference evapotranspiration (ET_o):** is defined as the amount of evapotranspiration from grass, which is a theoretical reference crop, with an adopted crop height of 0.12 m, and bulk surface resistance of 70 sm^{-1}, and an albedo of 0.23. It is closely similar to the evapotranspiration from a wide surface of green grass of uniform height, vigorously growing with sufficient water and completely covering the ground (Allen et al., 1998). ET_o is estimated using meteorological data with the help of the FAO Penman-Monteith method as recommended by Allen et al. (1998). However, KNMI uses the Makkink equation to calculate ET_o because it shows the relationship between daily reference evaporation and the incoming shortwave radiation (Hiemstra et al., 2011).

$$ET_0 = 0.65. \frac{s}{s+\gamma} . \frac{R\downarrow_{day}}{\lambda * \rho} \quad \text{(Eq8).}$$

Where ET_0 is the Makkink reference evaporation (mm day^{-1}), s the slope of the curve of saturation water vapor pressure (kPa^o C^{-1}), γ the psychometric constant (kPa^o C^{-1}), $R\downarrow_{day}$ is the daily incoming shortwave radiation in (Joule $m^{-2}d^{-1}$) and ρ is the bulk density of water.

- **Potential evapotranspiration (ET_p):** is the amount of water evaporated and transmitted that would occur if there is a sufficient water source(Milly & Dunne, 2016). The major source of energy required for the evaporation and transpiration process is from the sun, which supplies sensible heat from elsewhere by advection and follows by the wind, which is the mechanism by which evaporated water is transported away from the surface.

- **Actual Evapotranspiration (ET_a)**: is the real amount of evaporation from the water sources available by considering the condition of the area. If the ET_p is the ability of evaporation and transpiration process, the ET_a is the quantity of water driven by the same process. Sun, wind, surface area, and air temperatures impact the process.

2.4. Relationship between Soil moisture, Photosynthesis, and Agricultural Drought

The main factors affecting photosynthesis are light, water (soil moisture content), temperature, and CO2.

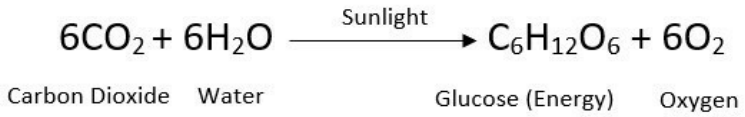

Soil moisture content is one of the main factors impacting the photosynthesis process, which is highly indicated and affected by drought because it is related to the current precipitation and describes drought potential within a region (Keyantash, 2002). The soil moisture content at the top layer profile is related to short-term precipitation, while the root zone soil moisture (RZSM) is related to long-term precipitation combined with the groundwater level, and it influences crop growth stages. RZSM is considered as a good measure of agricultural drought (Holzman et al., 2014).

Soil moisture availability depends on the soil moisture content, root zone depth, and water retention curve. Therefore, the reduction in the soil water content and increased rate of evapotranspiration resulting in soil moisture deficit (D. a. Wilhite, 2011; Vicente-Serrano et al., 2010). The soil moisture deficit affects photosynthesis, water potential dropping below a certain level causes plant water stress and reduces yield production leading to agricultural Drought (Wilhite, Sivakumar, & Pulwarty, 2014). Photosynthesis, soil moisture, and drought mainly depend on rainfall as it is the primary source of water for agricultural activities.

Figure2 explains well the relationship between those three phenomena.

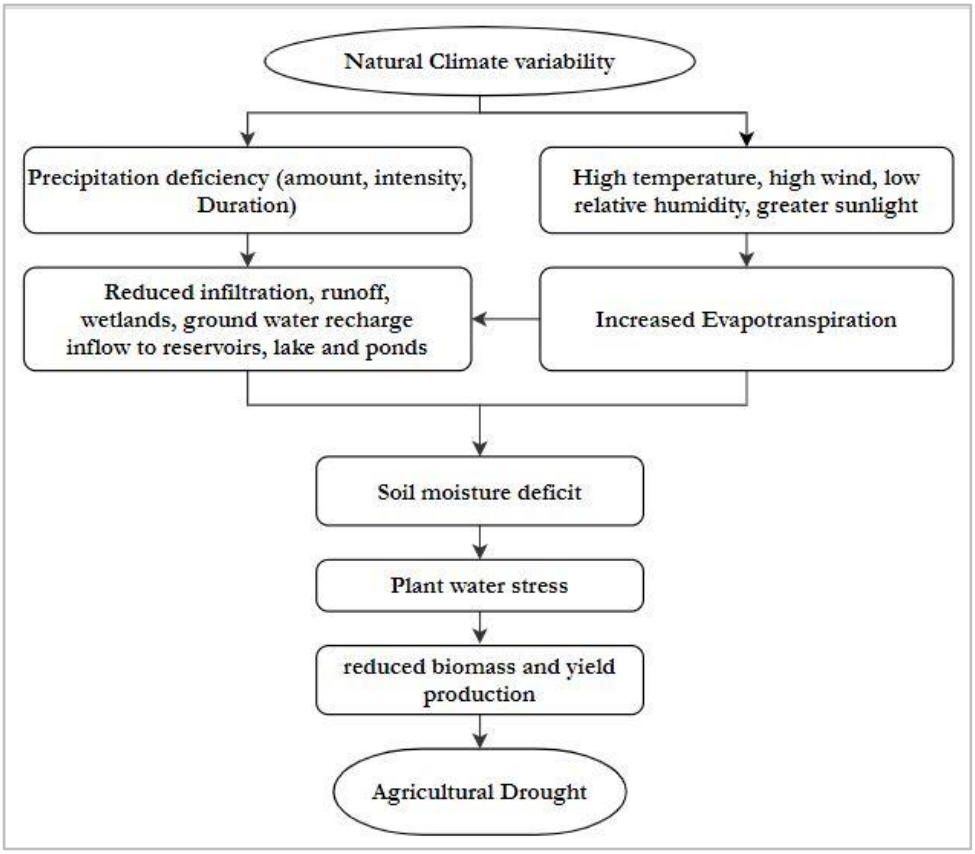

Figure 2: Relation between Soil moisture, photosynthesis, and drought for drought analysis.

2.5. Potato crop

Potato crops originated from the humid areas of high altitudes in the Andes (Beukema et al., 1990). It is the third most important crop globally after rice and wheat, and their production has increased in the last two decades, which shows its positive contribution to food security(Muthoni & Kabira, 2016). Potato crop produces the highest number of calories per unit water input: it is seven times as efficient as some cereals, like wheat, maize, etc. Potato is a C3 crop, and this study focuses on it because of the mentioned reasons, and even it is drought-sensitive with losses in yield that can reach 79% reduction if water requirements are not met. Hijmans, (2003) estimated 18 to 32% of potential potato yield reduction in 2040 to 2069 due to the agricultural drought. This vulnerability is mainly caused by shallow root system of potato, combined with the low ability of recovery after drought stress period (Vasquez-Robinet et al., 2008; Muthoni et al., 2016). Even short periods of water shortage can affect potatoes due to the sparse and shallow root zone ranging from 0.3 to 1m depth. 85% of the potato root is located on the upper part of the soil, around 0.3m (Mane et al., 2008; Muthoni & Kabira, 2016).

Potato yield and quality are influenced by soil moisture content and temperature, 15 to 18°C is the optimum soil temperature for tuber growth, and it can be sharply hampered when the temperature goes below 10°C or above 30°C (Allen et al., 1998). The soil moisture deficit highly impacts the 4th growth stage of potato (tuber bulking), where the water stress reduces the leaf expansion rate, prevents the development of new leaves, influences plant senescence, negatively affects the tube size and quality of potato, which lead to the reduction of the tuber yield production (Kumar & Minhas, 1999; Muthoni & Kabira, 2016; Aliche et al., 2018). The crop coefficient (Kc) of potato depends on the growing stage; during the sprout development stage, the Kc is 0.42, Tuber Initiation 0.85, Tuber Bulking 1.27, and Maturation 0.57. Therefore, FAO recommends using the Kc value of maturity (Kashyap & Panda, 2001).

3. STUDY AREA AND DATASET

3.1. Raam location

The North Brabant province, which lies on 5,082 km² (4,908 km² Land / 174 km² Water), within latitudes 51◦ 32' 59" N, and longitudes 5◦ 10' 27" E, is chosen as the study area because it is located in the southern region of the country, which is highly affected by the 2018 drought (Philip et al., 2020). The Raam catchment, a focused study area, is located in the northeast of the province (figure3), and it covers a total area of 223km². The main soil types in the region are sand, clay, and peat, with agriculture which is the primary land use. The water management at the location is mainly through the use of weirs and pumps. In drought years, mostly during the summer, the cumulative precipitation deficit can reach up to 250mm (figure 4). The regional water management authority operated a system of weirs and pumping stations used in irrigation to minimize droughts in the region (Benninga et al., 2018). Even though many parcels in the Raam catchment have irrigation facilities, the 2018 drought is highly affected the southern region at which the Raam catchment located which resulting in the high yield reduction of the region (Philip et al., 2020). The crop yield reduction in the region was high even more than the other dry years; see section 1.1, table 1.

Raam catchment had many potato farms during the 2018 growing season, and the farmers were expecting massive yield production. However, it was not the case because it provided a significant production loss compared to the other provinces (Centraal Bureau Voor de Statistiek, 2020). Therefore, during this research, 88 potato farms from the north Brabant_ Raam catchment have been selected for monitoring the effect of agriculture drought on the crop. Figure 3 represents the location and characteristics of the catchment, piezometers, and in-situ soil moisture stations located in the study area.

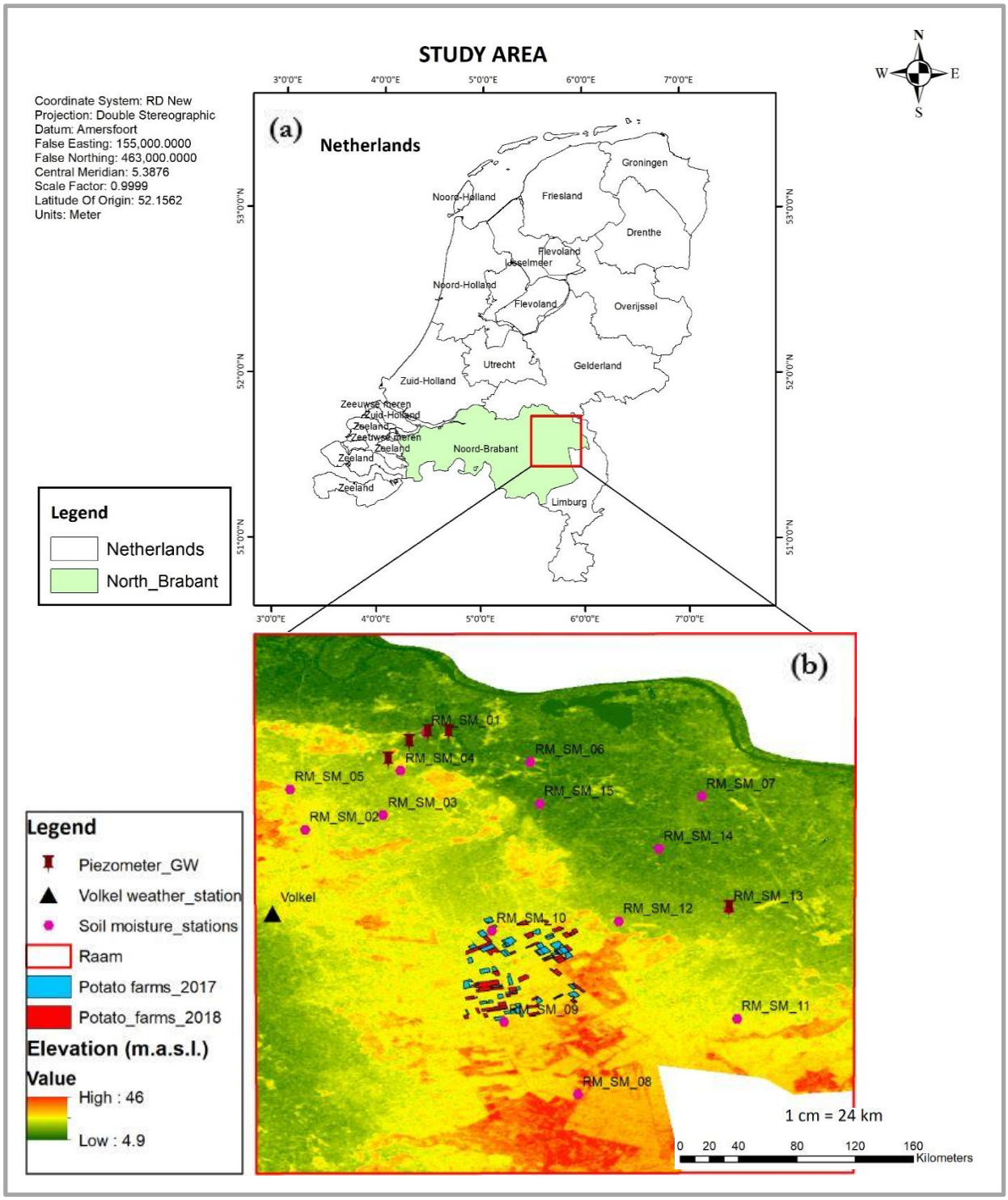

Figure 3: (a) The Netherlands with Raam study area in (red box), **(b)** Digital elevation model of Raam location obtained from (Actueel Hoogtebestand Nederland, 2016).

The selected plots for potato farms in 2017 and 2018 were not the same due to the crop rotation issue in the Netherlands, which means it is impossible to get the same farms of a similar crop type in two consecutive years. But the used potato farms data are from the same pixel of 10*10km climate reanalysis data (ERA5), which means their properties are pretty similar.

3.2. Climate in Raam

During the study period, the coldest time of 2017 was on 18th January with -3.35 ◦C, while the hottest time of 2017 was on 22nd June with 25.77 ◦C, and in 2018 was -5.23 ◦C, and 29.5 ◦C daily mean temperatures on 28th/February and 27th July, respectively. Figure 4 shows the cumulative precipitation deficit of the Raam location for the hydrological year 2018 and the normal year 2017, measured using the Volkel weather station at the Raam. The cumulative precipitation deficits were computed by subtracting daily precipitation from daily reference evapotranspiration and setting all negative precipitation deficit values to zero (0). The lack of precipitation events occurred from June to August 2018, which caused the 2018 summer in the Raam area to be drier than normal, which concluded as a drought.

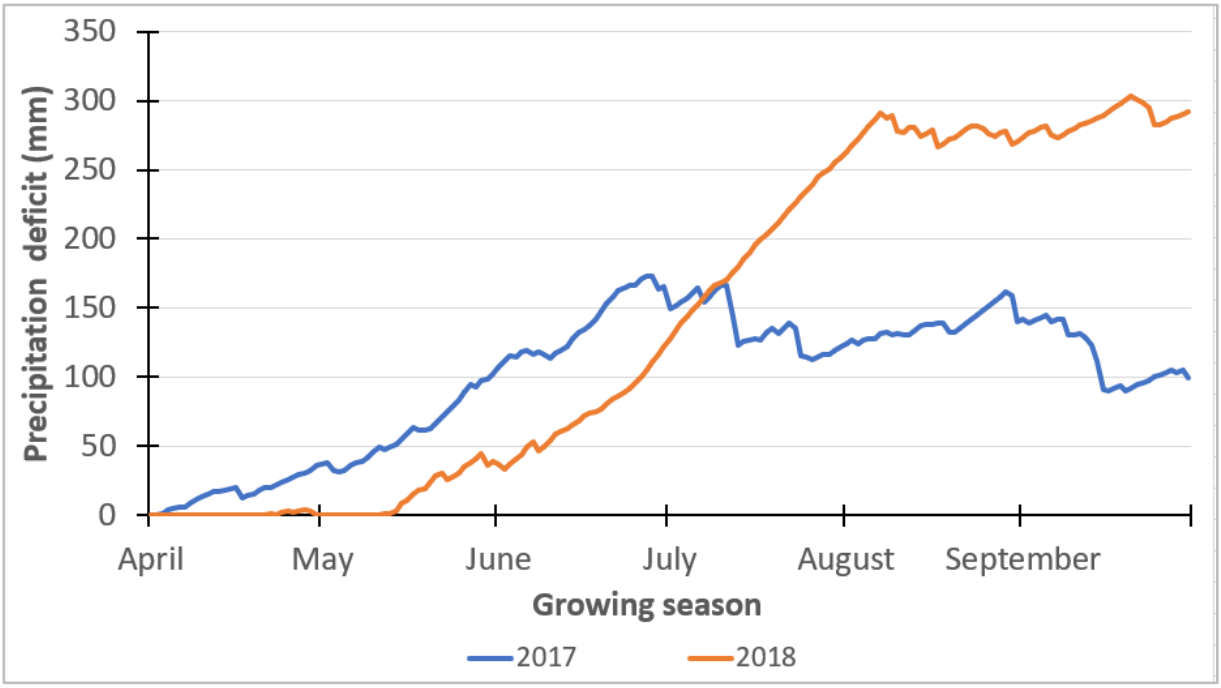

Figure 4: Precipitation deficit of the two growing season data (2017 _ 2018) from KNMI for the Raam location.

3.3. Station locations and Soil texture

In April 2016, 15 soil moisture stations were installed in the Raam region (Fig.3) and distributed over 495 km2. Stations 6 to 15 are located within the Raam catchment, while stations 1 to 5 are located in a closed sub-catchment of the Raam catchment, called the Hooge Raam catchment (The High Raam). The Raam catchment mainly holds sandy soils. Among 15 soil moisture stations, 13 are located in coarse sand soil, while the two remaining (6 and 7 stations) are located in clay and loamy sand, respectively (Benninga et al., 2018). BOFEK2012 provided the soil physical characteristics such as the soil texture, water retention curve, and hydraulic conductivity curve for the soil units in the Netherlands. The physical characteristic considered in this study are soil texture, which is described in the following in Table 4, and land cover types mentioned in section 4.3

Table 4:Characteristics of the soil moisture monitoring stations in Raam catchment, Soil description and classification were obtained from BOFEK2012 (Wösten et al., 2013).

Station	Soil description	Soil order	Sand fraction (> 50 µm) (%)	Silt fraction (50–2 µm) (%)	Clay fraction (< 2 µm) (%)	Organic matter fraction (%)
1	Weakly loamy sandy soil on subsoil of coarse sand (305)	Podzols	91.3	1.9	3.5	3.3
2	Weakly loamy sandy soil on subsoil of coarse sand (305)	Podzols	90.4	3.7	2.1	3.8
3	Weakly loamy Podzol soil (304)	Podzols	93.3	2.4	1.9	2.4
4	Weakly loamy sandy soil on subsoil of coarse sand (305)	Podzols	90.0	2.0	2.9	5.2
5	Weakly loamy sandy soil with thick man-made earth soil (311)	Anthrosols	93.1	2.3	1.1	3.5
6	Clayey sand on sand (fluvial) (409)	Anthrosols (Vague soils)	83.7	4.8	9.9	1.6
7	Loamy sandy soil with thick man-made earth soil (317)	Anthrosols	82.1	10.5	5.2	2.2
8	Weakly loamy Podzol soil (304)	Podzols	92.8	1.6	1.4	4.1
9	Weakly loamy Podzol soil (304)	Podzols	95.4	1.1	0.8	2.6
10	Weakly loamy Podzol soil (304)	Podzols	96.3	0.8	0.7	2.2
11	Weakly loamy Podzol soil (304)	Podzols	94.8	1.7	1.6	1.9
12	Weakly loamy Podzol soil (304)	Podzols	92.0	2.5	1.7	3.9
13	Weakly loamy soil partly on subsoil of coarse sand (309)	Podzols	96.7	1.1	0.8	1.4
14	Loamy Podzol soil (312)	Podzols	90.0	4.7	2.3	3.0
15	Weakly loamy sandy soil with thick man-made earth soil (311)	Anthrosols	88.6	5.5	2.8	3.1

3.4. Datasets

The data processed and used in this study are from two different growing seasons of the 01st April to 30th September of (non-stressed toward water-stressed crops conditions 2017 versus 2018), except NDVI time-series data of 20 years and four years' time series of precipitation deficit. This means that the temporal resolution is daily data from 2017 to 2018, daily NDVI data from 2000 to 2020, and daily precipitation data from 2017 to 2020. The collected datasets are listed in Table 5, with the different archives used to obtain the data.

Table 5: Datasets used for the study.

Acquired Data	Data type	Spatial resolution	Sources	Archives
Remote sensed data	-Reflectance data of Multi-spectral imagery	20m	Sentinel-2	https://code.earthengine.google.com/40fe18f5b76c400a87dd9b89f752bf76
	- Images	20m	Sentinel-2	https://code.earthengine.google.com/8c4f0fa8cd944885144fbad57e8cd3ad
	NDVI	250m	MODIS	https://code.earthengine.google.com/82cab3b485087c145916534479bfbeda
	Land surface temperature (LST)	30m	Landsat-8	http://landsat.usgs.gov
Meteorological data	-Rainfall -Reference crop evaporation - Air temperature - Wind speed - Sunshine radiation - Surface pressure	_	KNMI	https://www.knmi.nl/nederland-nu/klimatologie
Weather data	-Air temperature -Wind speed -Air pressure -Atmospheric vapor pressure -Integrated incoming shortwave radiation -Integrated incoming longwave radiation -Leaf air index _ low vegetation	10 km	ERA5	https://cds.climate.copernicus.eu/cdsapp#!/yourrequests?tab=form
Hydrological Data	Groundwater level	_	DINOloket	https://www.dinoloket.nl
In situ data	Soil moisture content (5,10,20,40, & 80cm)	_	Raam catchment	https://data.4tu.nl/articles/dataset/Regional_soil_moisture_monitoring_network_in_the_Raam_catchment_in_the_Netherlands_-_2017-04_2018-04/12712910/1

3.4.1. Sentinel-2 data

This study is based on sentinel-2 reflectance and image data, with a high spatial resolution of 20m and the capability of measuring multi-spectral data, which is crucial in vegetation monitoring as it helps collect specific data. The Sentinel-2 Level-2A products were obtained from the Google Earth Engine (GEE) (the link provided in table 3), where the reflectance data used was extracted from each pixel of potato farms. The Sentinel-2 provides the products in 10, 20, and 60 spatial resolution, with five (5) days temporal resolution, and it offers spectral data in 13 bands from 443 to 2190 nm (Pettorelli, 2019).

The three (3) cloud-free images collected on 26th May, 10th June, and 21st August 2017 with spectral wavelengths reflect vegetation spectrum were available and used for the 2017 growing season. While, in the 2018 growing season, the available and used images with vegetation spectrum reflectance were eight (8), collected on 26th May, 10th June, 27th June, 7th July, 17th July, 27th July, 6th August, and 21 August/2018). Some images from April and September were available for both years, but they did not used because they were reflecting soil spectrum, which makes sense since as April is the planting period of the growing season in the Netherlands, while September is the harvesting period, as mentioned by De Wit & Clevers, (2004) with the help of crop calendar they provided.

4. MATERIAL AND METHOD

Figure5 shows the methodology of the study. The first step was the identification of the critical period using remote sensing and meteorological data. After knowing that 2018 was a critical year over 20 current years, 2017, which was a normal year, was chosen for comparative analysis to the 2018 drought year. The second step was to retrieve multi-spectral crop reflectance from sentinel-2 using google earth engine (GEE). The third step was to retrieve vegetation properties such as (leaf area index, chlorophyll, water content, dry matter content, etc.) based on Sentinel-2 reflectance data, using a radiative transfer model (RTMo). The fourth step was to download weather data from ERA5 and convert it into the format the SCOPE model can read; then, use those downloaded weather data combined with vegetation properties in the SCOPE model to simulate photosynthesis and evapotranspiration. The fifth step was to evaluate the results by comparison analysis with in-situ data. Finally, identify the highly affected phenological stage of potatoes. Apart from the NDVI long time series and precipitation deficit of four years time series, the rest of the data collected and processed based on two growing seasons (2017 and 2018) in the Raam location. The links to the scripts used can be found in Table 5.

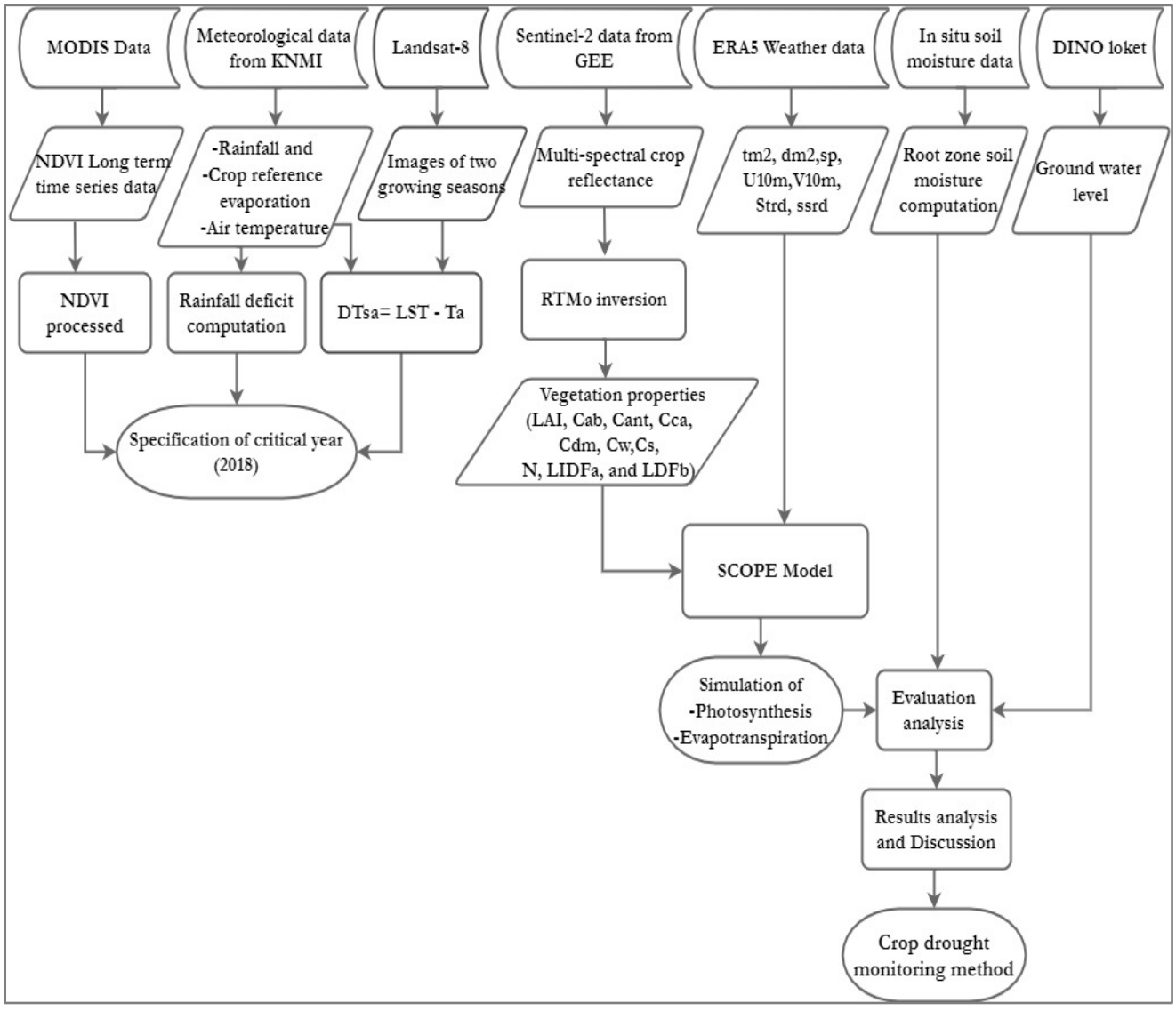

Figure 5: Flow chart of the study

4.1. Data acquisition and Data processing

Despite the information from different literature showing the severity of the 2018 drought (W. Peters et al., 2020; Buitink et al., 2020; Prins et al., 2018), this study used meteorological and satellite indicators to check if 2018 was an exceptional year. MODIS NDVI time series maps and precipitation deficit identified severe drought year, using the data from the study area (Raam catchment).

4.1.1. MODIS NDVI time series

With satellite data to show the exceptional year, the MODIS_MOD13Q1.006 of 250m spatial resolution and 16 days temporal resolution was used to determine the NDVI long-term time series of 20 years. After collecting the CSV file of daily NDVI data for the study area, with the help of the Google Earth Engine, the script used is described in table 5. The next step was the processing of data, where the outlier errors have been removed. The smoothing of NDVI values has been performed using the moving average filter method with the help of the RStudio script mentioned in the metadata. The trendline has been added to the map, and the two values are chosen to be combined for average smoothing. After processing, the time series map of multiple years (from 2000 to 2020) has been plotted using the North Brabant data to show the critical period defined as a drought year.

4.1.2. Precipitation deficit computation

Daily precipitation and reference evaporation data from 01st April to 30th September of 4 years (2017, 2018, 2019, and 2020) were used to calculate the precipitation deficit of the North Brabant province. The raw data downloaded from KNMI in the text format is then processed and saved in excel format to be used. Daily precipitation deficits were computed by subtracting cumulative precipitation from cumulative reference evapotranspiration and setting all negative precipitation deficit values to zero (0).

The data used are daily data for the growing seasons of 2017, 2018, 2019, and 2020. Those four years have been chosen because the three current ones (2018, 2019, and 2020) were the dry years in the Netherlands, which means are the best ones to use for analyzing the severity of the 2018 drought. The fourth one (2017) was used for comparison as it was the normal year. North Brabant province contains four weather data stations (Eindhoven, Gilze_Rijen, Volker, and Woensdrecht), but the precipitation deficit was computed using the data from two stations (Gilze Rijen and Volkel) because the two others contain data gaps during the study period.

4.1.3. Land surface temperature (LST)

The mentioned steps in section 2.1.4 of how to estimate LST have not been performed in this study because the data used are collected from Landsat 8 collection 2 level-2. Three (3) cloud-free images in 2017 and five (5) in 2018 of the study area were available and used to estimate the temperature difference between the surface and the air (dTsa). Those images provide a calculated LST in band 10, but also it requires adjustment using the related factors (U.S. Geological Survey, 2020).

Cloud-free images of two growing seasons(2017 and 2018) have been used to estimate land surface temperature. With the extracted image of the potato farm area, band 10 with the wavelength range of 10600 to 11190 nm has been opened in ArcMap, and using the raster calculator, LST has been calculated by

multiplying band 10 by a factor of 0.00341802 and an offset of 149 was added, and finally, LST was converted from Celsius to Kelvin (U.S. Geological Survey, 2020):

$$LST = (Band10 * 0.00341802 + 149) - 273.15 \quad \text{(Eq9)}$$

Based on the Volkel weather station data, the air temperature recorded at the time the Landsat 8 image was taken has been extracted from LST for evaporation measurement and drought analysis on the focussed area. The temperature difference between the surface and air (dTsa) is a good drought indicator as it directly illustrates the intensity and heat fluxes of land-atmosphere interaction (Zhang et al., 2015).

4.1.4. Weather data collection and analysis

SCOPE Model requires weather data combined with vegetation data. The weather data used are the climate reanalysis data, produced by an atmospheric circulation model with the help of the European Centre for Medium-Range Weather Forecasts (ECMWF). The meteorological variables from ERA5 used in the study are processed where the names and units are converted to the SCOPE model format, as shown in table 6.

The climate reanalysis data (ERA5) have been used in the study because it provides all the weather data required for the SCOPE, while the KNMI weather data station does not offer incoming longwave radiation data. However, KNMI and ERA5 data are highly correlated, as provided in appendix 7.1.

Table 6: Table shows the formulas used to convert the variable and units in the format SCOPE model can read.

SCOPE			**ERA**			
Names	**Abbreviation**	**Units**	**Names**	**Abbreviation**	**Units**	**Conversion**
Integrated incoming shortwave radiation	Rin	W m^{-2}	Surface solar radiation downward	ssrd	J m^{-2}	ssrd/ 60*60*24
Integrated incoming longwave radiation	Rli	W m^{-2}	Surface thermal radiation downward	strd	J m^{-2}	ssrd/ 60*60*24
Air temperature	Ta	^{0}C	2m temperature	t2m	K	t2m – 273.15
Atmospheric vapour pressure	ea	hPa	2m dew point temperature	d2m	K	Satvap(d2m – 273.15)
Air pressure	P	hPa	Surface pressure	sp	Pa	Sp * 0.01
Wind speed	u	m s^{-1}	-10m u-component of wind -10m v-component of wind	u10 v10	m s^{-1}	$\sqrt{u10^2 + v10^2}$

- 60*60*24: number of seconds in a day. Watt (W)=J S^{-1}

- Satvap () is a SCOPE model function that converts dewpoint temperature to atmospheric vapor pressure in the following way:

$$ea = 6.107 * 10^{\frac{7.5T}{237.3+T}} \quad \text{(Eq10)}$$

Where $\boldsymbol{ea}$ is a SCOPE function that converts dewpoint temperature to atmospheric vapor pressure, and $\boldsymbol{T}$ is dewpoint temperature in Celsius

The ERA5 land hourly data were downloaded as NetCDF file data, then converted into the daily mean of 24hours with the help of MATLAB script showed in the metadata, the resulting "era_dd CSV file," which contained the daily mean data with the variable names and unit SCOPE can read.

Light intensity, water content, and temperature are the main factors affecting photosynthesis and evapotranspiration; they are going to be focused on in the following data analysis, as they are among the collected weather data for simulating those variables (photosynthesis and Evapotranspiration). The following discussed variables are the main, which indicate crop stress

4.1.4.1 Integrated incoming shortwave radiation

Figure 6 shows that shortwave radiation in summer 2018 June to August) was high compared to 2017; by considering only radiation, the potential crop productivity was high in 2018 as the light is the primary driver of photosynthesis. The radiation in May and in the summer of 2017 was low, which indicates cloud days, and the clouds affect the satellite data collection.

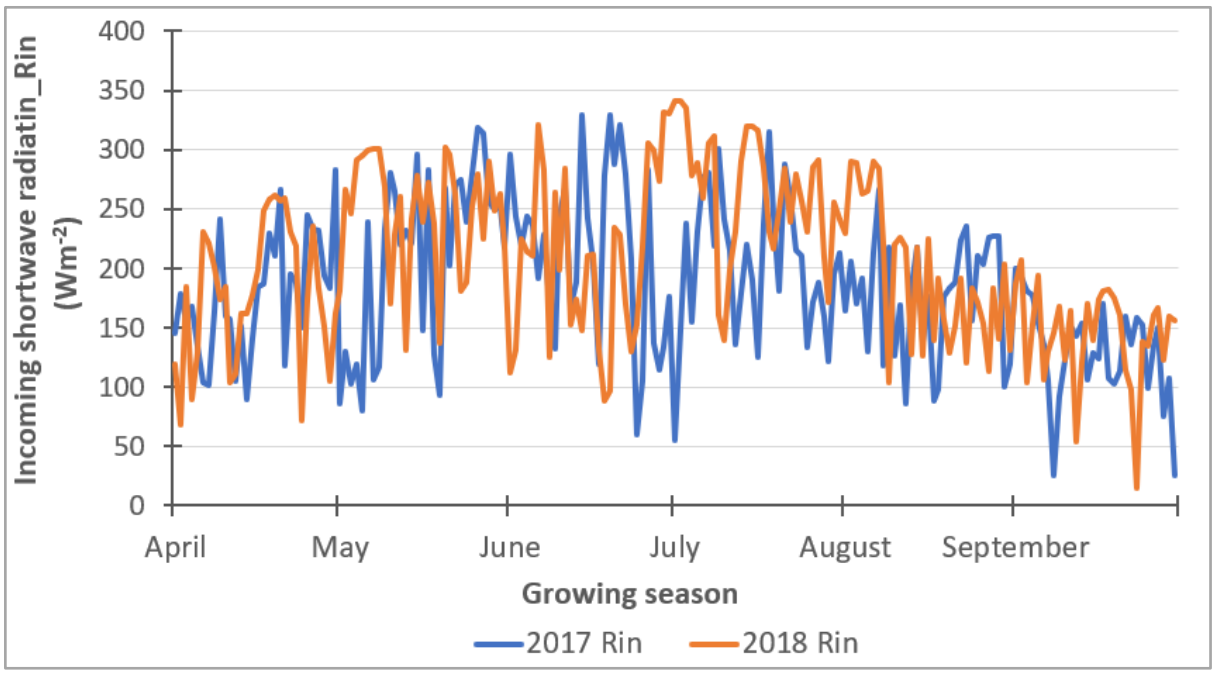

Figure 6: Daily mean incoming shortwave radiation of two growing seasons (2017 _ 2018) at the study area, data used are from ERA5

4.1.4.2 Air temperature

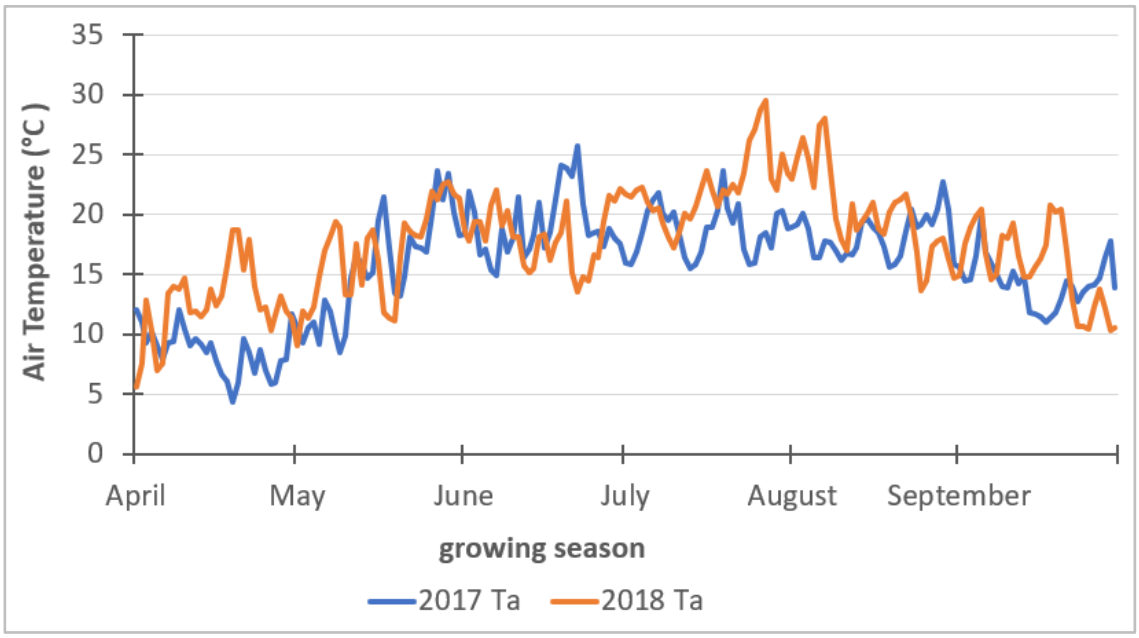

Figure 7: Daily mean air temperature of two growing seasons (2017 _ 2018) at the study area data used are from ERA5.

The air temperature was high in 2018, mainly in April and in the summer (from the end of July to September). Still, the air temperature in 2018 was not critical because the temperature affecting vegetation is above 35 °C or below 10 °C (Sage & Kubien, 2007). Ta figure above shows that the temperature of 2017 was critically low in April and the beginning of May, which is expected to influence the growth of the crop.

4.1.4.3 Precipitation

The precipitation is analyzed because it is the primary source of water used in agriculture. The rainfall data are obtained from KNMI on the Volkel weather station around the study area to analyze and define the precipitation impact on the 2018 drought.

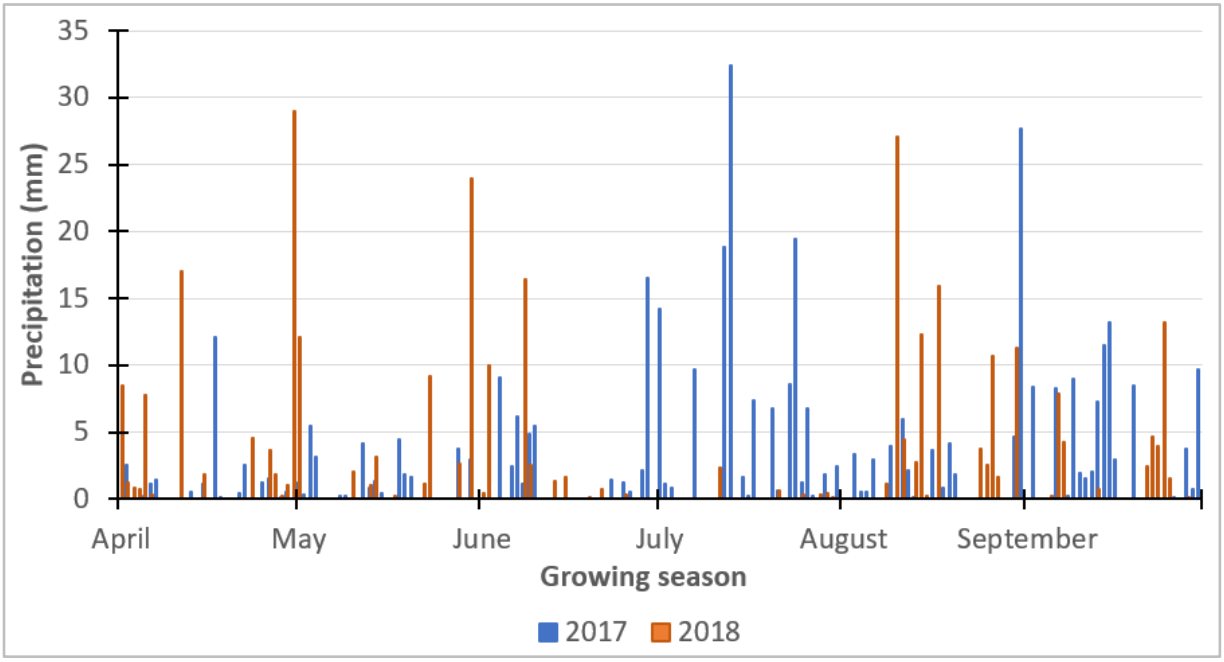

Figure 8: Daily precipitation of two growing seasons (2017 _ 2018) at the study area, data used are from KNMI.

Figure 8 shows that the rainfall availability in July and August 2018 was less than in those months in 2017. Thus, it affected crops and influenced agricultural drought. In the Netherlands, the crops are typically in good health in the summer period. However, if the water shortage becomes severe, it affected crop production, mainly because the crops require much water at that time. This is the case for potatoes because it requires sufficient water on the tuber bulking stage (on the 90th days) means July to August; it depends on when it is cultivated (Aliche et al., 2018; Muthoni & Kabira, 2016).

4.1.5. Vegetation data collection and analysis

4.1.5.1. Reflectance of Multispectral

Reflectance data of multi-spectral imagery from Sentinel-2 have been used in the radiative transfer inversion model (RTMo) to simulate the vegetation properties, which their seasonal course used as stress indicators. Reflectance data downloaded from sentinel-2, with the help of the Google Earth Engine (GEE), the link found in Table 5. Forty-four potato farms per growing season have been used to obtain the reflectance data, which is analyzed and processed to know the quality of the available data. The data quality assessment was based on cloud-free days data, cloud-free farms data, the type of spectral per single day, the position of farms, and the criteria of each farm due to its reflectance.

Due to cloud cover, vegetation data could be retrieved for only a small number of days in 2017, especially in July 2017, compared to 2018. This was proved by the following sentinel-2 imagery analysis and CSV file data from GEE. The link to the two GEE scripts provided in table 5, and in the metadata, the first script is used to collect the reflectance CSV data of less than 10% cloud cover from the selected farms, while the second script is used to collect sentinel-2 RGB images of the study area.

The CSV files of vegetation data obtained from GEE have been used in multi-spectral crop reflectance performance in order to analyze the data available then decide what to use for the following step. The sentinel-2 images of the 2017 and 2018 growing seasons have been used to analyze the data provided by the farms.

Figures 9, 10,11,12,13, and 14 illustrate the data selection and quality filtering for partly or fully clouded days. The spectrum represents the reflectance of potato farms on the specified day. Each spectral correspond to the specific farm, and they are plotted with the sentinel-2 bands on the X-axis, which means each star (×) symbol represents a band value. On the left side, there are RGB sentinel-2 images (Band4, Band3, and Band2) which show cloud situation at the study area and the location of potato farms for better reflectance analysis. Briefly, the spectral reflectance on the right side depends on the Sentinel-2 images in the left hand.

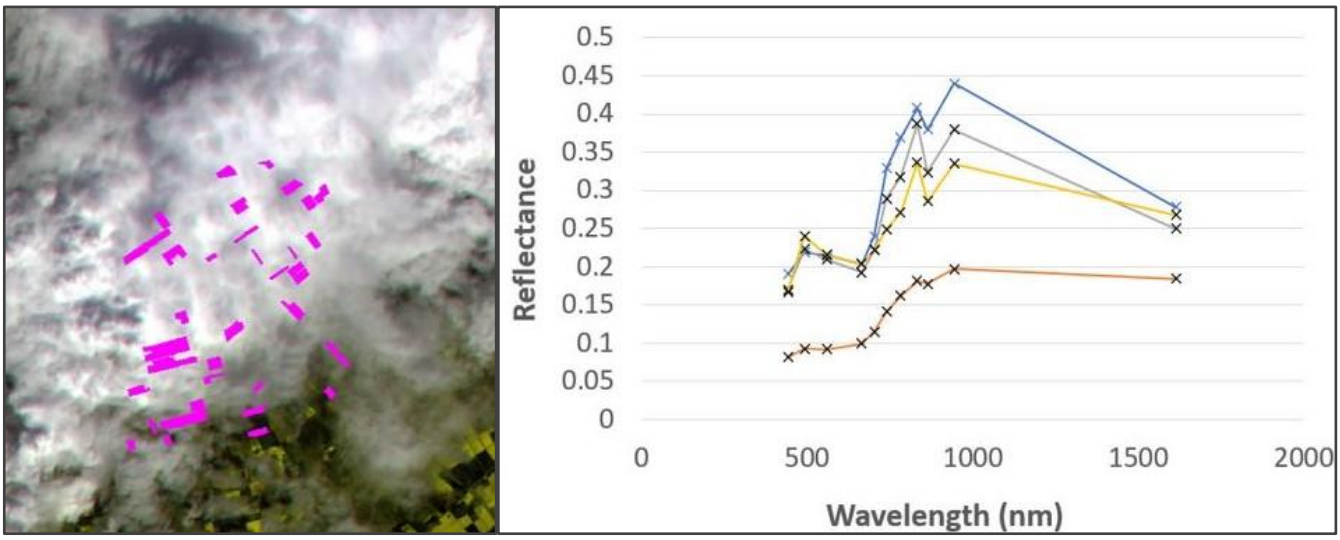

Figure 9: Spectrum reflectance of potato farms, based on the left-hand satellite image of 26th/April/2017.

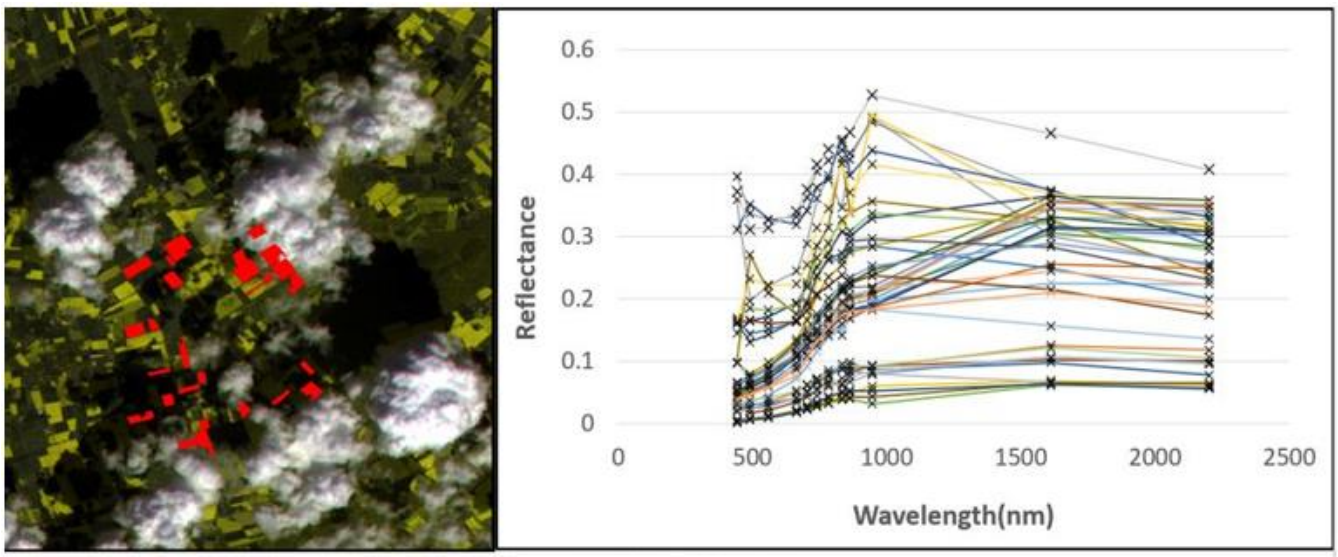

Figure 10: Spectrum reflectance of potato farms, based on the left-hand satellite image of 26th/April/2018.

The above spectrum represents the reflectance of potato farms on 26th April of 2017 and 2018; the cloud cover of 26th April 2017 corresponds to the weather data at the time. Where the shortwave radiation and air temperature were low (below 7°C), which means the sky was very clouded at the point the satellite was not able to record the data, that is why the spectrum is very few compared to the 44 potato farms analyzed.
On 26th April 2018, The farms located in the cloud cover reflect high in the blue band of spectral, and the lowest reflectance with dark color are located on cloud shadow area. The remaining farms located on the free-cloud area provide the soil spectrum because it was in the planting period, where the crops were not yet reflected like vegetation.

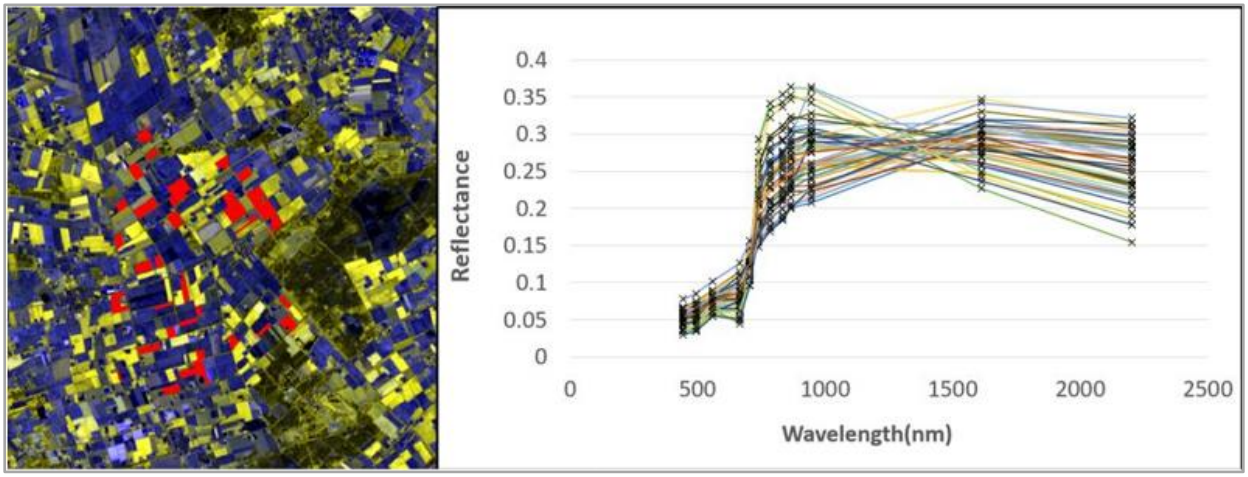

Figure 11: Spectrum reflectance of potato farms, based on the left-hand satellite image of 26th/May/2017.

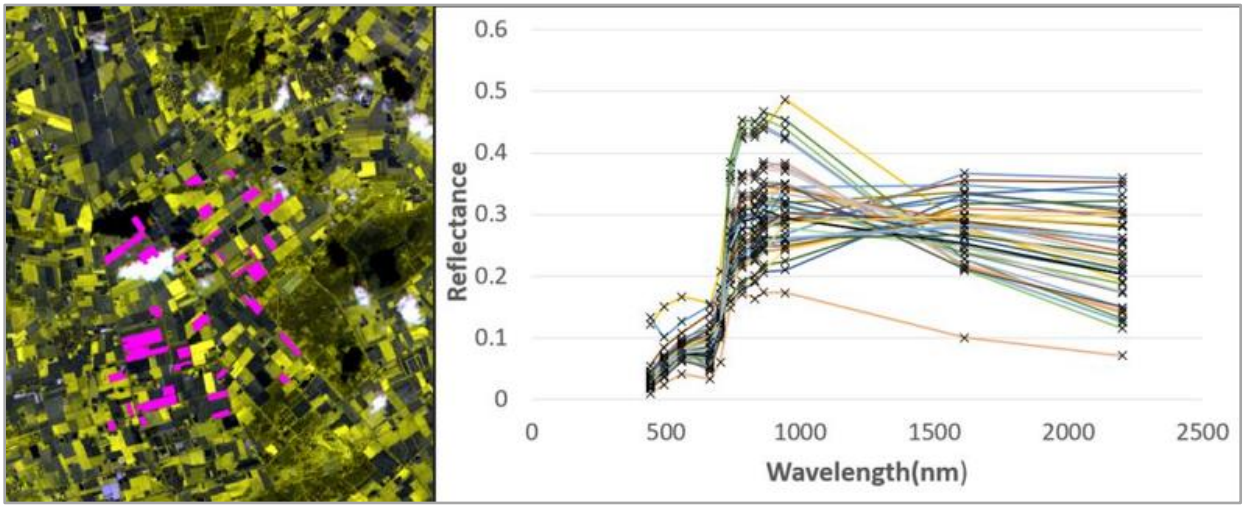

Figure 12: Spectrum reflectance of potato farms, based on the left-hand satellite image of 26th/May/2018.

26th/May/2017 and 2018 were the free clouded days, as shown in figures 11 and 12 above. Each spectrum corresponds to the individual farm. The crop provided vegetation spectrum, but which are not well-formed because the crop was on the 2nd growth stage (vegetation growth), only one month after planting time. Also, one farm in 2018 indicates cloud cover, as it reflects high in the blue band, and another one reflects low, indicating cloud shadow.

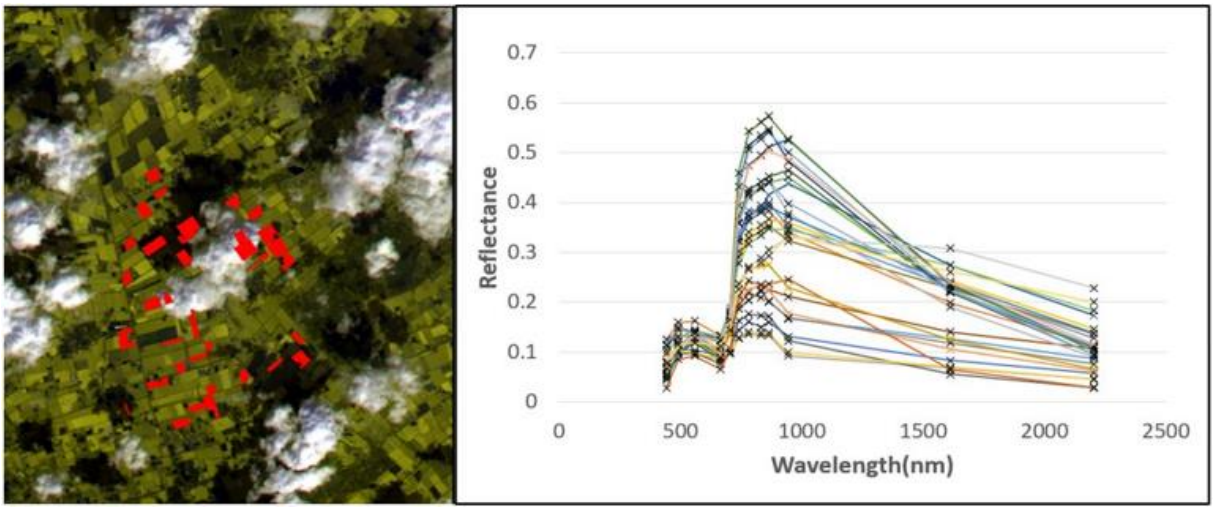

Figure 13:Spectrum reflectance of potato farms, based on the left-hand satellite image of 21st/August/2017.

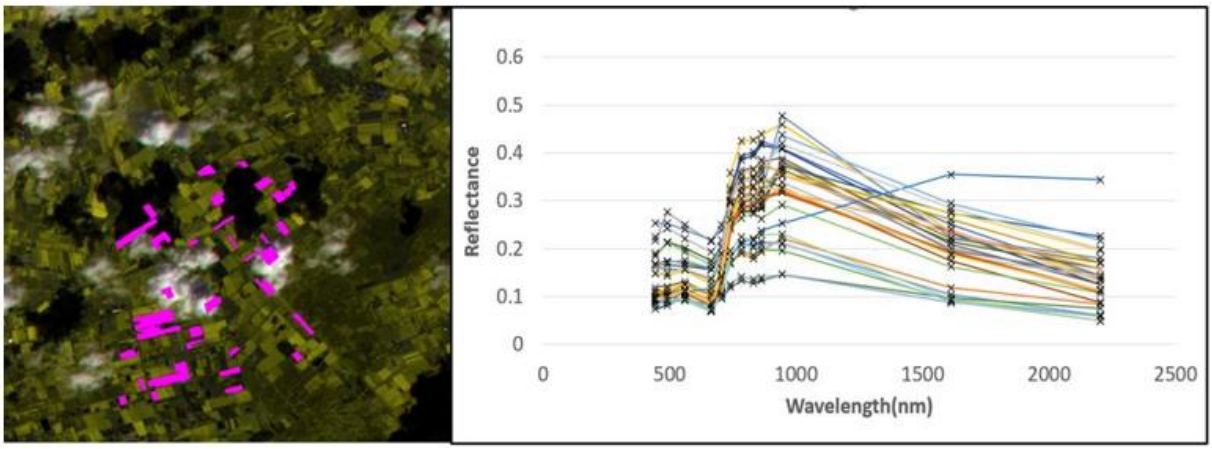

Figure 14: Spectrum reflectance of potato farms, based on the left-hand satellite image of 21st/August/2018.

On 21st/August/2017 and 2018, some potato farms were harvested due to planting time; others were located on the high cloud cover (above 10%), which are eliminated by the GEE script (shown in table5), the remaining ones were located on the cloud-free area as shown by figure 13 and 14. The cloud-free farms reflected the vegetation spectrum as they were on the maturity period of the crop due to the growing season of potatoes. Those cloud-free farms have been selected to be used in the analysis as they are expected to influence due to their growing stages.
Among the vegetation data available in the growing seasons, the free clouded data (farm by farm) and the ones which reflect the vegetation spectrum have been used in the analysis.

4.1.5.2. Retrieval of Vegetation Properties

The vegetation properties of the potato crops for both years were obtained using inverse modeling with the numerical optimization approach. The simulations of the RTMo were performed using time-series Sentinel-2 multi-spectral reflectance of the accurate chosen data from the same pixel obtained using Google Earth Engine. RTMo simulated ten vegetation properties (Cab, Cw, Cdm, Cca, Cant, Cs, N, LAI, LIDFa, and LIDFb) that have been used in the SCOPE model. Three of the simulated vegetation properties (LAI, Cab, and Cw) were analyzed to evaluate whether anomalies in their seasonal dynamics can be used as stress indicators. See section 5.2

4.2. Retrieval of Photosynthesis and Evapotranspiration

SCOPE photosynthesis model has been used in this study to simulate the assimilation and evapotranspiration of potatoes to know how much the crop is growing. The estimation of those variables is highly important as it provides the amount of CO2 uptake using photosynthesis and shows the crop situation based on the evapotranspiration. With this study, the SCOPE model used the daily-mean weather data from ERA5, together with the retrieved vegetation properties from Sentinel-2 (LAI, Cw, Cab, N, Cdm, Cs, Cant, Cca, LIDFa, and LDFb) to simulate the various output variables. Photosynthesis and evapotranspiration are the ones focussed on due to their indication of agricultural drought stress. The findings have been evaluated by in situ data and vegetation property.

4.3. Soil moisture monitoring network

The Raam network covers 15 stations of soil moisture and temperature sensors (Decagon 5TM), one by each station was installed at five levels (5, 10, 20, 40, and 80 cm depths), as shown by figure 15. The measurements were recorded every 15 min (Benninga et al., 2018). The agricultural is the dominated land cover type characteristics within the catchment area. At the station's location in the study period, the most common crop type was grass, followed by potato, corn, sugar beet, and other vegetable crops (Carranza et al., 2021). The mentioned varying plant type at the catchment have different active root zone depths, where grass may only be up to 20cm, as it has a shallow rooting system, while for potato and other crops, the root zone can extend deeper. For this study, the root zone soil moisture at 40 cm and 80cm depth have been used for analysis as the focussed crop is potato. Therefore, two different levels are estimated because the potato root zone can be shallow or deeper depending on where it is cultivated. Additionally, the weighted method applied in determining the rootzone soil moisture in this study could also be adapted for other depths that would suitably represent the root zone depths like 20cm of grass(Carranza et al., 2021; Dumedah et al. l., 2015).

Root zone soil moisture is estimated using the weighted method. This method considers the contribution of each layer from shallow to deep (5cm to 80cm). It is not a point measurement method because it covers the midway upper and down part of the instrument (Decagon 5TM), it averaged depth values based on the measurements and associated soil thicknesses (see Eq 11.). Each measurement depth (5, 10, 20, 40, and 80cm), its combined soil thickness according to the reached level, is based on the middle distance between two adjacent measurement points (Carranza et al., 2021). The following figure 16 shows the range of depth each instrument covers, while the figure15 shows the arrangement of the decagon 5TM into the soil.

$$\theta_{rz} = \frac{\sum_{j=1}^{n} \theta_j \Delta_{z_j}}{Z} \qquad \text{(Eq11).}$$

Where θj (in m3 m− 3) is the volumetric water content for measurement depth j (cm), Δzj (cm) is the thickness of soil associated with the measurement depth, and Z (cm) is the total averaging depth.

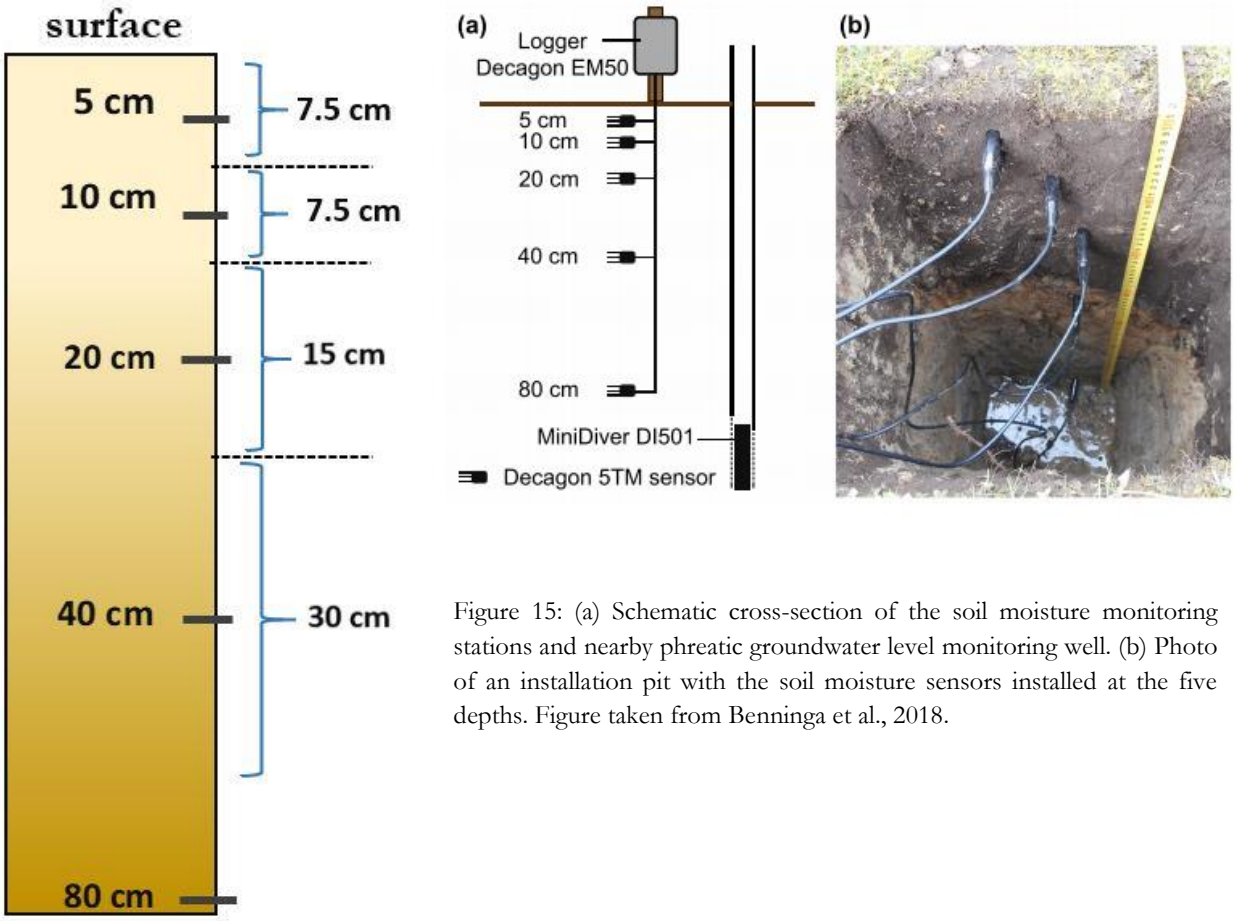

Figure 15: (a) Schematic cross-section of the soil moisture monitoring stations and nearby phreatic groundwater level monitoring well. (b) Photo of an installation pit with the soil moisture sensors installed at the five depths. Figure taken from Benninga et al., 2018.

Figure 16:Diagram of an installation set up of Decagon 5TM at each depth, and it covered area on each station .

The data from all 15 stations of 2017 and 2018 growing seasons were considered for the analysis. 15min soil moisture data have been aggregated to daily data in order to match the temporal resolution of developed meteorological and hydrological datasets (rainfall and groundwater) for better analysis, as the shallow depth 5 to 10 cm soil moisture content is corresponding to the rainfall, while the root zone soil moisture is related to groundwater. All the soil moisture stations have been considered because they are within the study area. The furthest station is located at 9.96 km distance far from the focussed potato farms.

Figures 17, 18, 19, 20, and 21 show the soil moisture variability of five (5) depths in two growing seasons, which define the severity of the 2018 summer drought as it compared with the regular growing season of 2017. The data used for those graphs are the average of four stations (stations 01, 02, 03, and 04) which provided the full dataset in the study period and which are not influenced by the irrigation system.

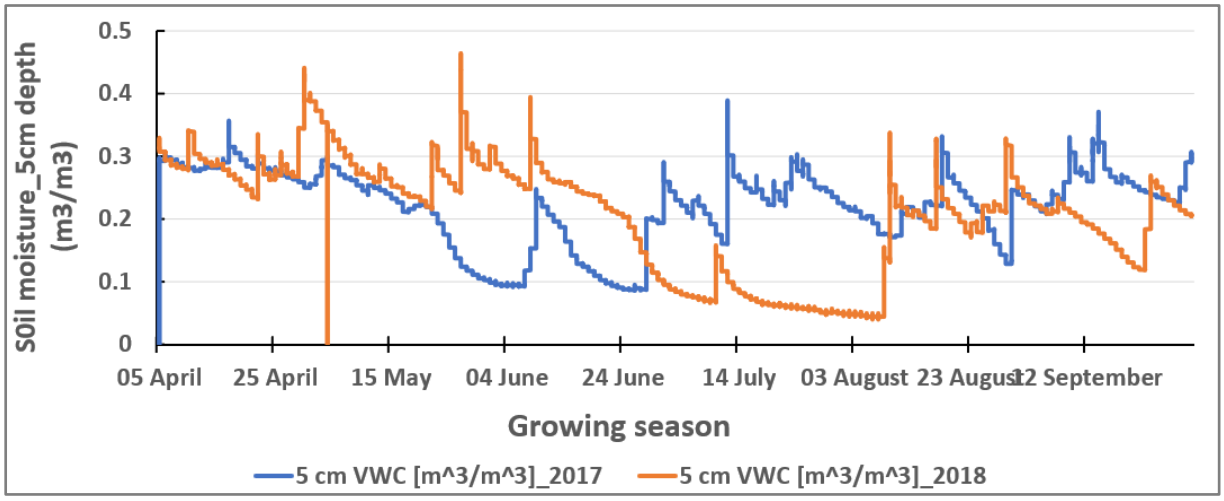

Figure 17: 5cm depth of soil moisture variability of two growing seasons (2017 versus 2018), based on the average data of four stations provided the full dataset, and which are not influenced by the irrigation system.

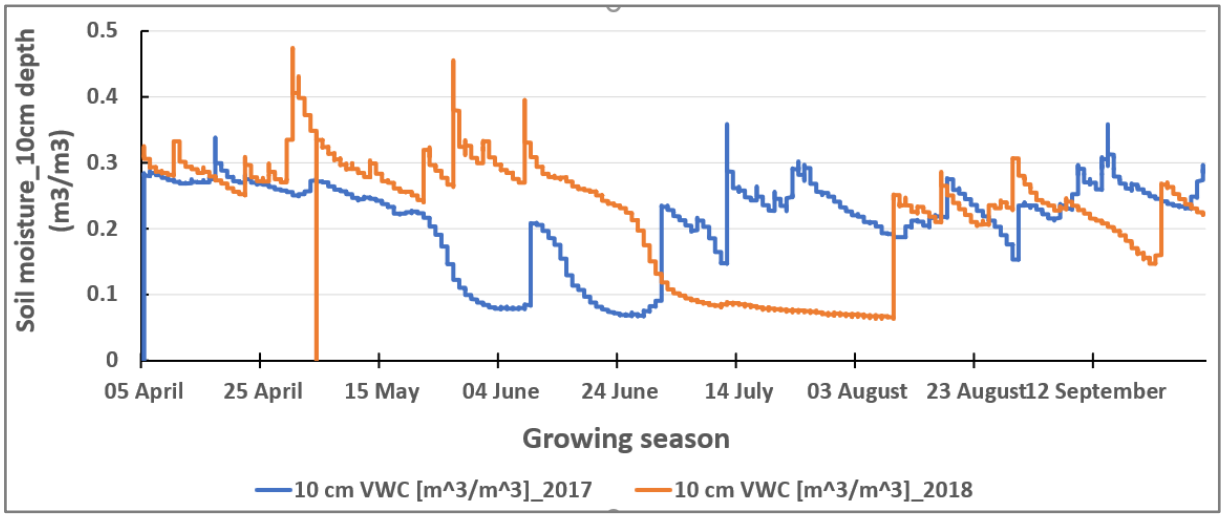

Figure 18: 10cm depth of soil moisture variability of two growing seasons (2017 versus 2018), based on the average data of four stations provided the full dataset, and which are not influenced by the irrigation system.

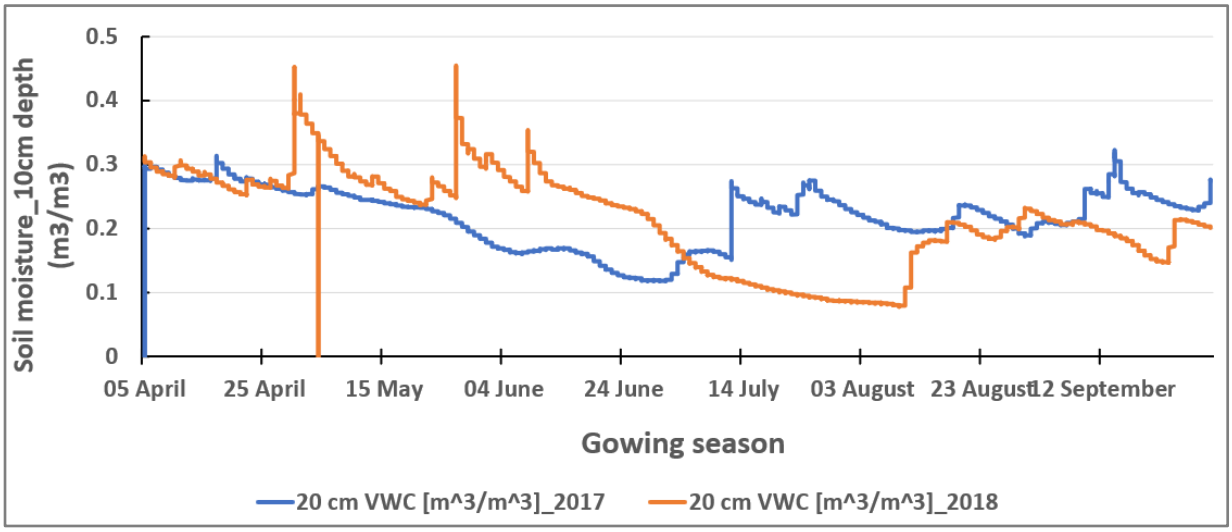

Figure 19: 20cm depth of soil moisture variability of two growing seasons (2017 versus 2018), based on the average data of four stations provided the full dataset, and which are not influenced by the irrigation system.

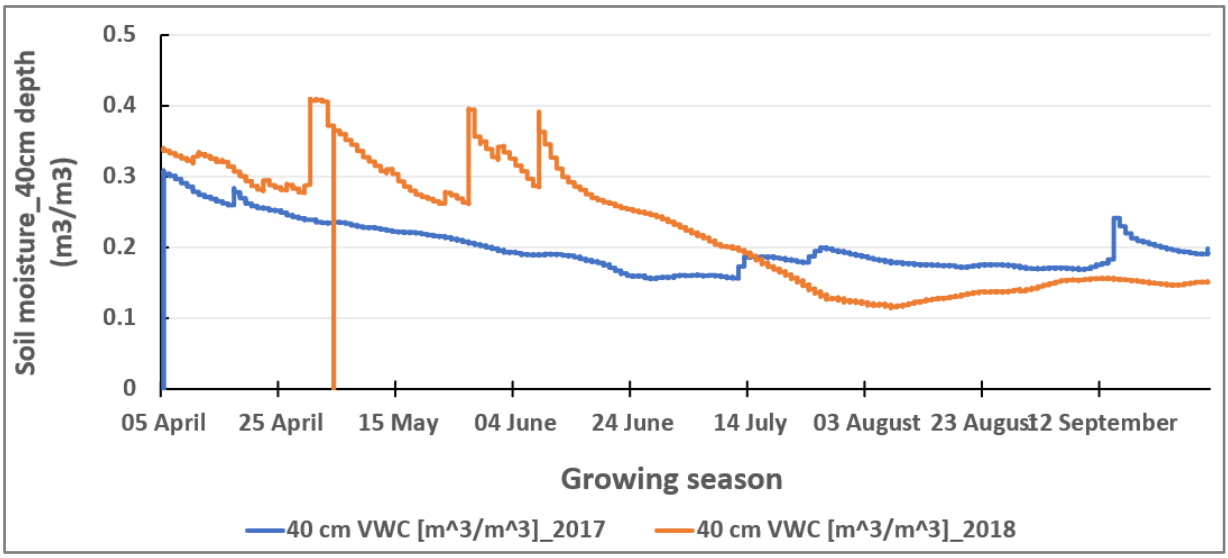

Figure 20: 40cm depth of soil moisture variability of two growing seasons (2017 versus 2018), based on the average data of four stations provided the full dataset, and which are not influenced by the irrigation system.

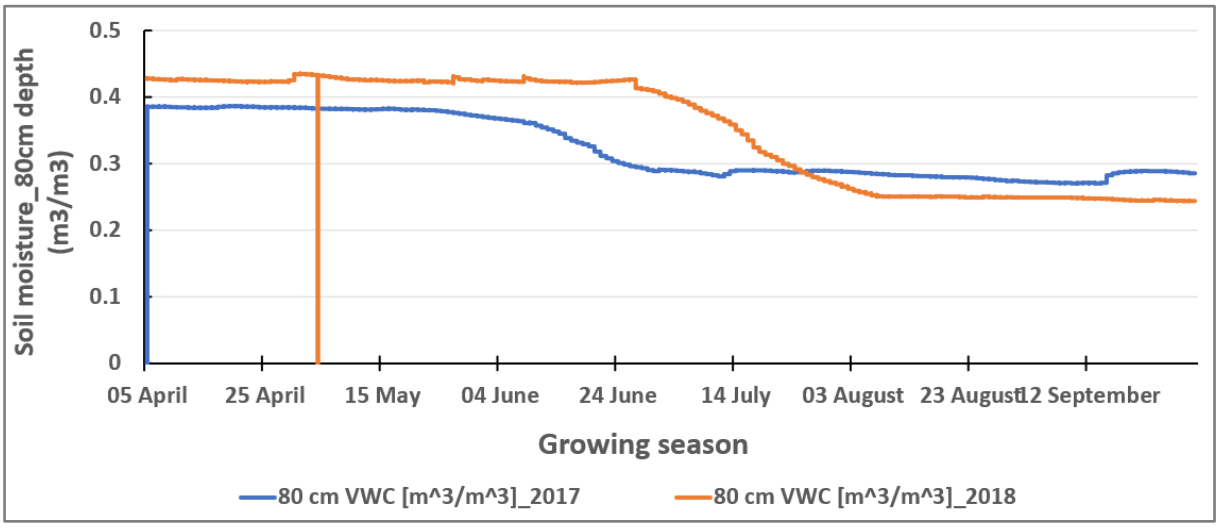

Figure 21: 80cm depth of soil moisture variability of two growing seasons (2017 versus 2018), based on the average data of four stations provided the full dataset, and which are not influenced by the irrigation system.

The 15min soil moisture data have been used to plot figures 17,18,19, 20, and 21. The shallow and deeper layers of soil moisture show that at the beginning of the season, 2018 was wetter than 2017, and it was rather dry in June 2017, which makes sense as it corresponds to the precipitation deficit results, and weather data like rainfall, and vegetation data. Five soil moisture depth layers demonstrate water shortage in 2018 summer compared to the 2017 summer, which meets the expectation.

4.4. Groundwater level

The groundwater level impacts root zone soil moisture which influences crop growth. Ground water heads were collected from Dinoloket (Data en Informatie van de Nederlandse Ondergrond), the link provided in the table5. The instruments (belle sounder and diver data logger) that recorded the data have different recoding times, where the diver is regularly recording daily variation groundwater levels. In contrast, the bell sounder saves measurements inconsistently, based on other literature, because the metadata does not provide the names of instruments used. Unfortunately, some piezometers were not functioning during the study period; others have data gaps from 2016 to 2021; others contain random data and insufficient metadata. Therefore, the five piezometers (B45F1045, B45F1046, B45F1048, B45F1050, and B46C0256) were used to analyze this study because they provided the full daily dataset within the simulation period, well-functioning with sufficient information, and located in the study area. The following figures 22 and 23 are the observations of two piezometers from five available.

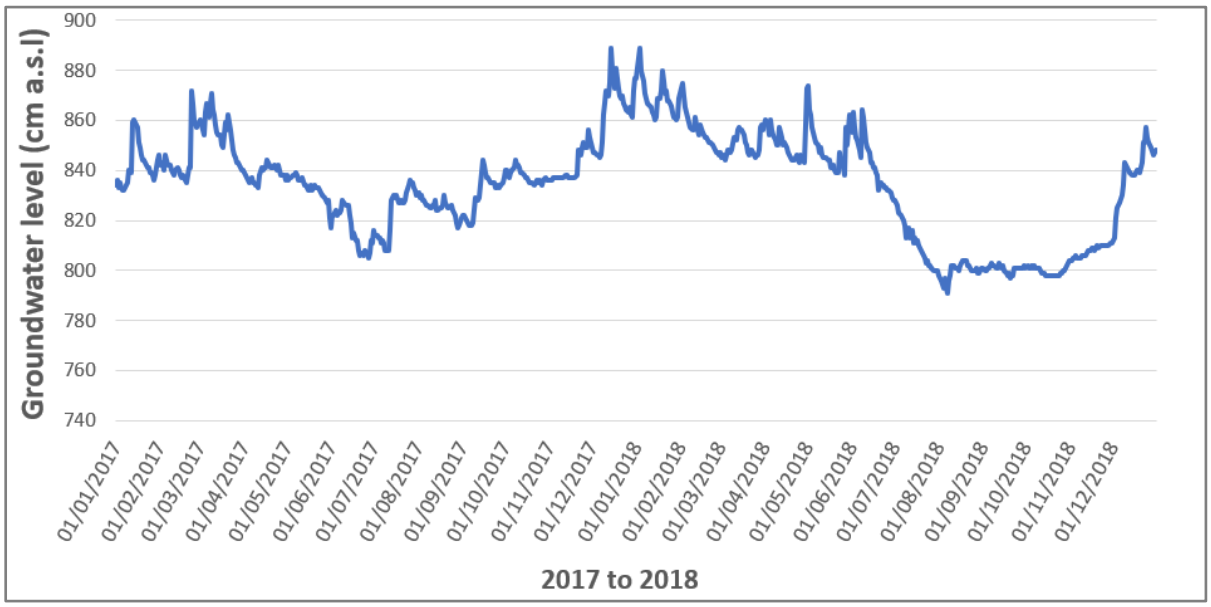

Figure 22: Groundwater level variation of piezometer B45F1045 in the north of the study area; see figure 3

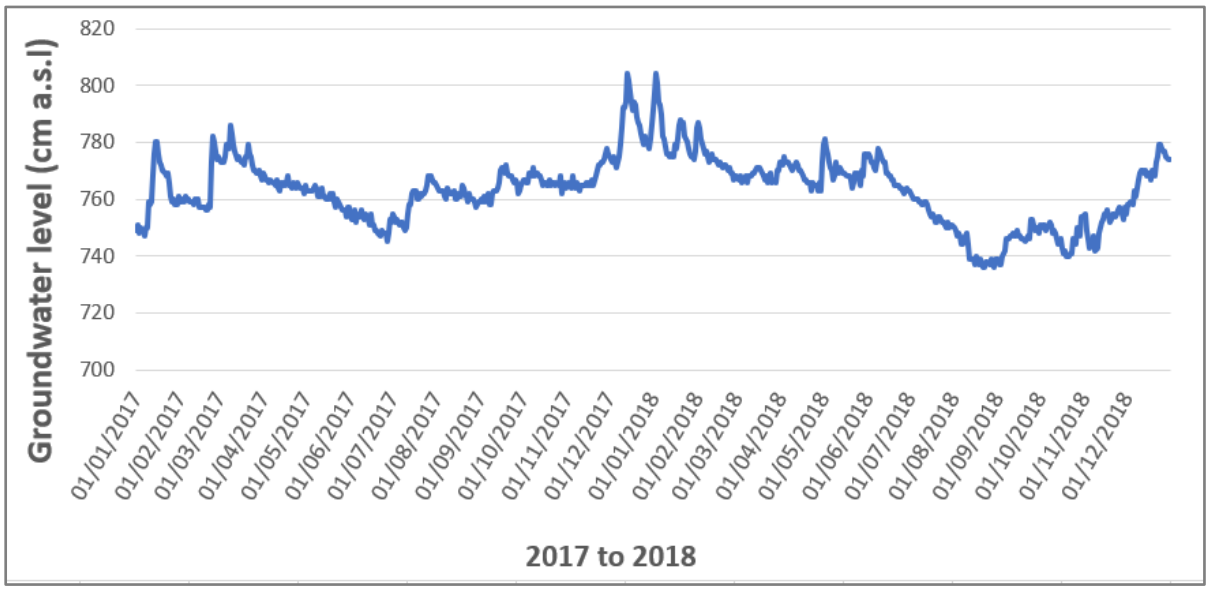

Figure 23: Groundwater level variation of piezometer B45F1050 in the East of the study area; see figure 3

The observations of those two piezometers show the reduction of groundwater level in the 2018 summer compared to the 2017 summer, which was the expectation as the 2018 summer period was dry. This indication is similar to the other three piezometers, which are not plotted, and they have been used in the analysis, where it shows their influence on the root zone soil moisture. See section 5.4.2.1

Piezometer B45F1045 and B45F1050 were chosen to be presented because they are located in a different location in the study area, while the other three remainings are closely located at the same area as B45F1045, see figure 3.

5. RESULTS AND DISCUSSION

5.1. Identification of exceptional year

5.1.1. MODIS NDVI time series

Twenty years of data from 2000 to 2020 have been used to identify a drought year based on the NDVI time series. The following figure shows the NDVI variability of those 20 years.

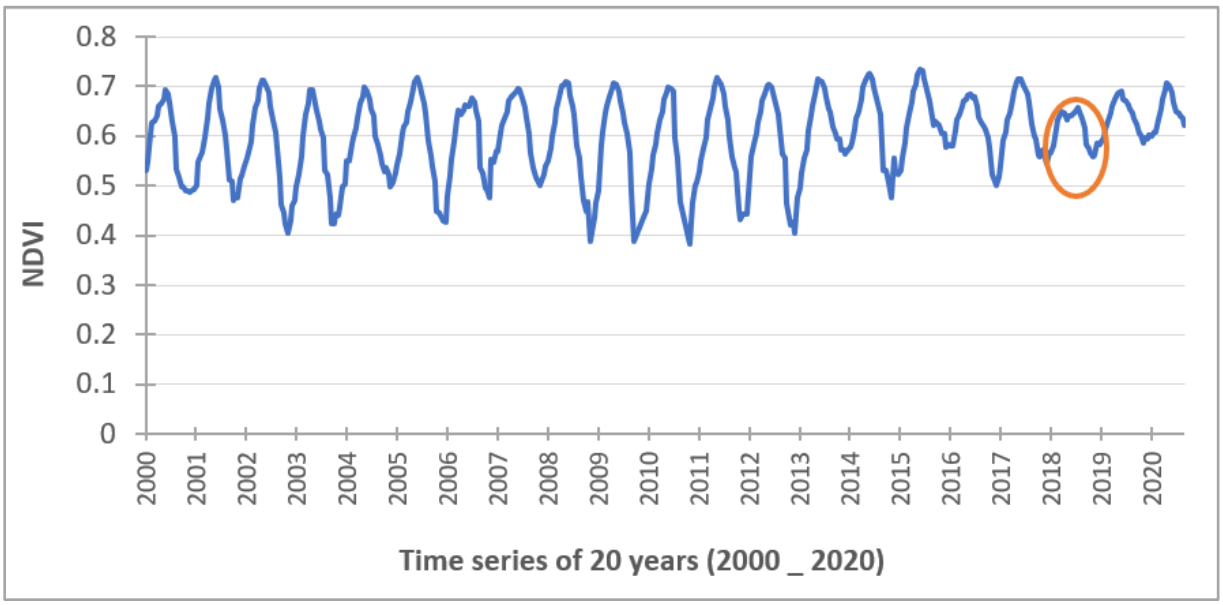

Figure 24: NDVI time series of 20 years in North Brabant_Raam catchment, with the data collected from GEE.

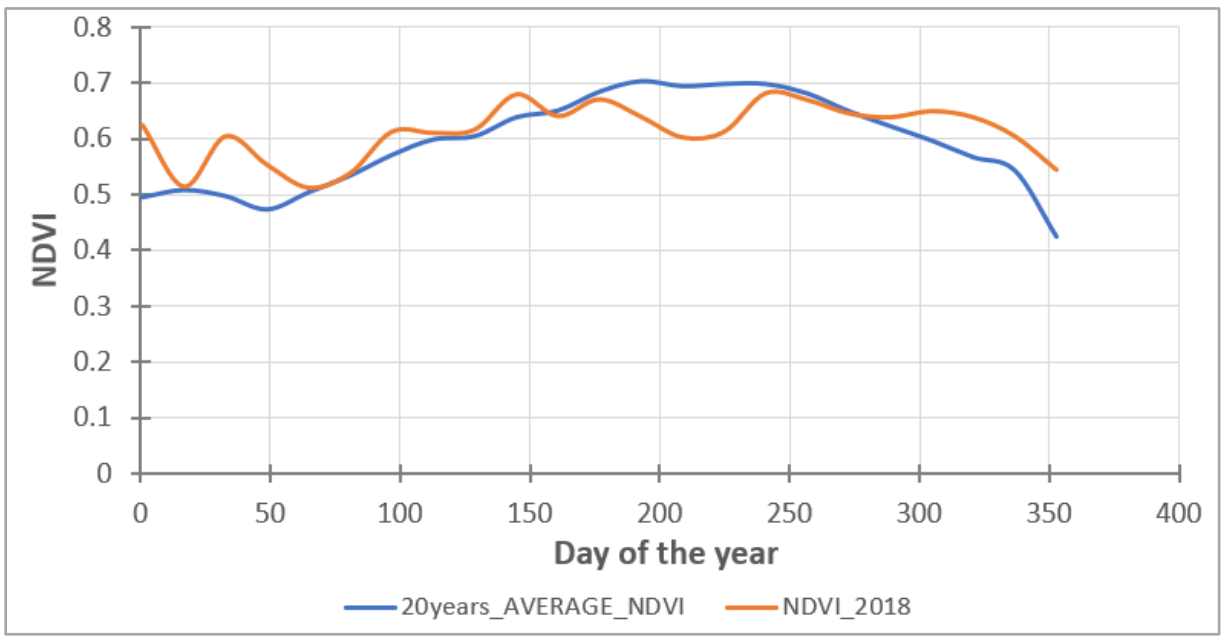

Figure 25: 20 years NDVI average compared to 2018 NDVI of the study area.

According to the NDVI time series analysis done using north Brabant provinces data, It is clear that 2018 was an exceptional year with critical vegetation greenness and density, as shown by the low NDVI value on the resulting figure 24. The three current years (2018, 2019, and 2020) were the dry years in the Netherlands, according to the data provided by KNMI 2020. However, 2018 was more critical than 2019 and 2020 based on the NDVI results above.
Based on the seasonal cycle with peak values in the growing season. In 2018 there was a dip in the peak season, and peak season values were lower than any other year in the time series.

Figure 25 compares the NDVI average of 20years and 2018 NDVI. Still, the 2018 summer (from June to September) was exceptional compared to the average of 20 years. Thus, even though the 2018 NDVI affected the average of 20 years as it included, the 2018 NDVI was still low due to the severity of the 2018 drought (Prins et al., 2018; W. Peters et al., 2020; Buitink et al., 2020).

5.1.2. Precipitation deficit

Daily precipitation deficits of 4 different years have been computed by subtracting cumulative rainfall from cumulative reference evapotranspiration and setting all negative precipitation deficit values to zero (0). Figure 26 presents the precipitation deficit results of four current years.

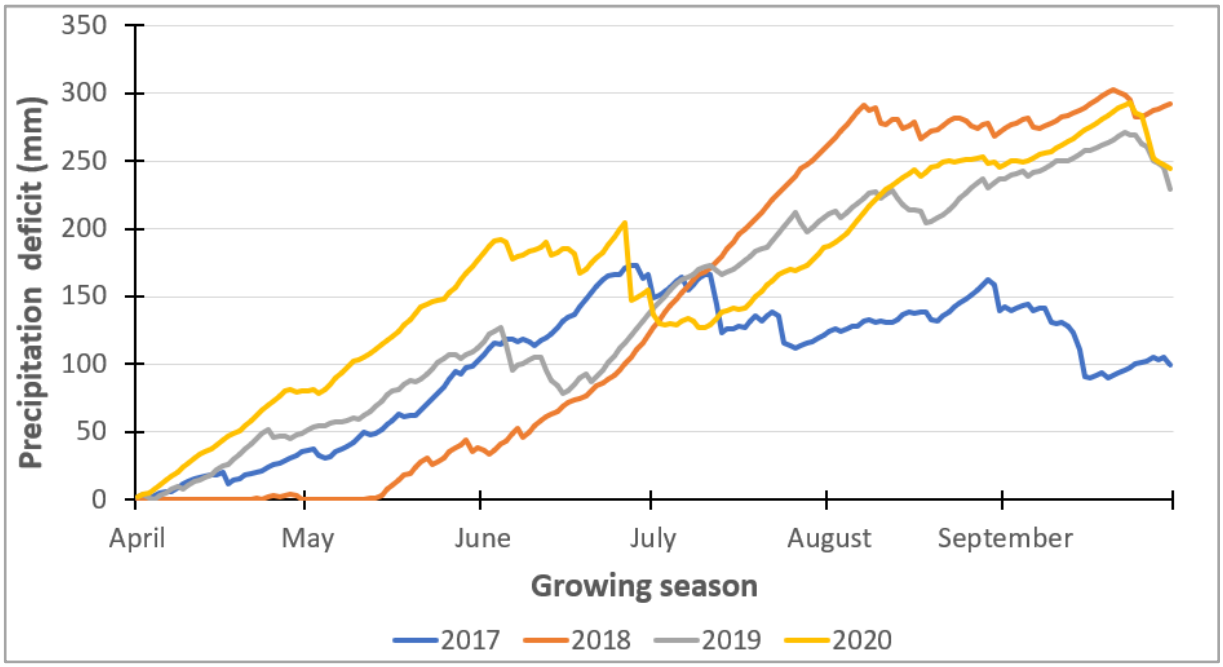

Figure 26: Precipitation deficit of four current years in the study area for drought detection.

The precipitation deficit results from North Brabant_Raam indicate good condition weather at the beginning of the 2018 growing season, which means the planting time was favorable with sufficient soil moisture content due to the adequate rainfall. However, 2018 indicates water shortage in the summer period, mainly from July to September. The 2018 rainfall deficit raised more than 250 mm, which indicates a severe drought(Sluijter et al., 2018). This water shortage affected plants because, in the summer, the plants like potatoes require sufficient water (Aliche et al., 2018). Furthermore, it is the period in which the high photosynthesis process occurred due to adequate sunlight. These results emphasize reducing yield production in 2018, as published by (Centraal Bureau Voor de Statistiek, 2020; Prins et al., 2018).

5.1.3. The temperature difference between the land surface and the air (dTsa)

LST is defined as the brightness temperature of the land surface, and it has a strong relationship with air temperature (Mutiibwa, Strachan, & Albright, 2015). Based on Eq 9, the LST from band 10 was adjusted and converted into degrees Celsius with the data from Landsat 8 collection 2 level 2 of two different growing seasons in the Raam location, at the potato fields. Later, the air temperature from Volkel station, which is recorded at the hour the satellite image was taken, has been subtracted from land surface temperature for evaporation analysis and drought indication. Figure 27 shows the variability of land surface temperature minus air temperature (LST – Ta), which is related to the real situation on the field. The reality of the field is represented by the google earth images corrected in the study period (on 14th August 2017 and 07th August 2018). The date and time of the overpass from LST has mentioned in the legend.

Figure 27: Comparison analysis of LST – Ta or dTsa maps in two growing seasons, with middle google earth image for the real situation on the field during the study period.

The results of LST-Ta, which is known as the temperature difference between the surface and the air (dTsa), provides high dTsa on images (02nd April 2017 and 21st April 2018), mainly in the potato fields because it was during the planting season where the farms reflect as bare soil. The green areas (low dTsa) in those images represent the forests and grass areas, as shown by the google earth image in the middle. dTsa results emphasize the drought in the 2018 summer, where the 26th July 2018 image demonstrates high average dTsa, which is mainly indicated at the potato farms, where during that period, the excellent health of the crop with green reflectance was expected due to the growing stage of the crop. This drought indication is emphasized by the 04th August 2017 image, which is the image of the same period as the one in 2018, but this indicates good crop heath in the potato farms, with low dTsa. The area on which reflect high dTsa (red color) on 04th August 2017 image is at the bore soil area, build-up, and at the agricultural area but covered by plastic properties. See the google earth image in the middle.

5.2. Simulation of Vegetation properties

Among all vegetation data available, the accurate data with free cloud cover and cloud shadow, the potato farms' data which reflect vegetation spectrum, and data obtained from almost the same day for both growing seasons (2017 and 2018) have been used in this study.

The vegetation properties of the potato crop in both years were obtained using inverse modeling with the numerical optimization approach. The simulations of the RTMo were performed using time-series Sentinel2 multi-spectral reflectance of the chosen mentioned data, and it provided ten vegetation properties that were used in the SCOPE model. Three (3) of the simulated vegetation properties, which are more indicate crop stress (LAI, Cw, and Cab), were evaluated whether anomalies in their seasonal dynamics can be used as stress indicators.

5.2.1. Canopy leaf area index (LAI)

Leaf area index (LAI) is defined as the number of square meters of leaves per unit ground surface area and is directly related to photosynthesis(Chen et al., 1997). Therefore, LAI shows the indication of drought when the leaf area declines. The following figures show the variation of LAI during the drought period.

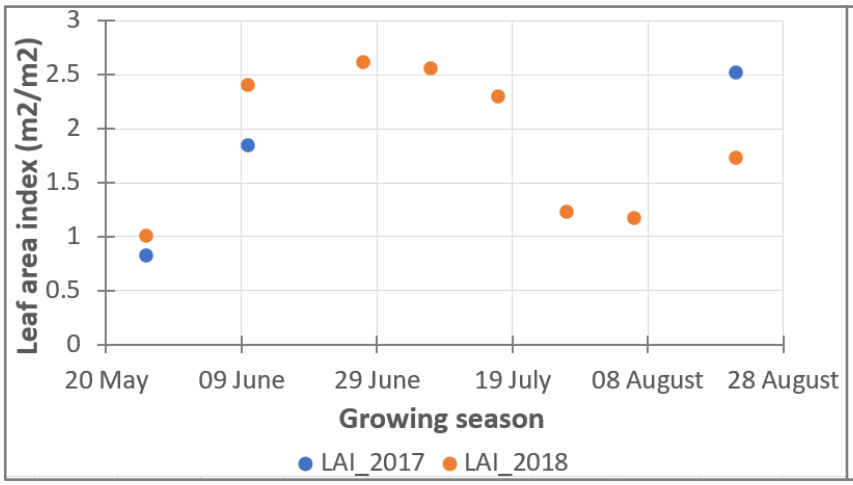

Figure 28: Canopy leaf area index (LAI) of available data in two growing seasons.

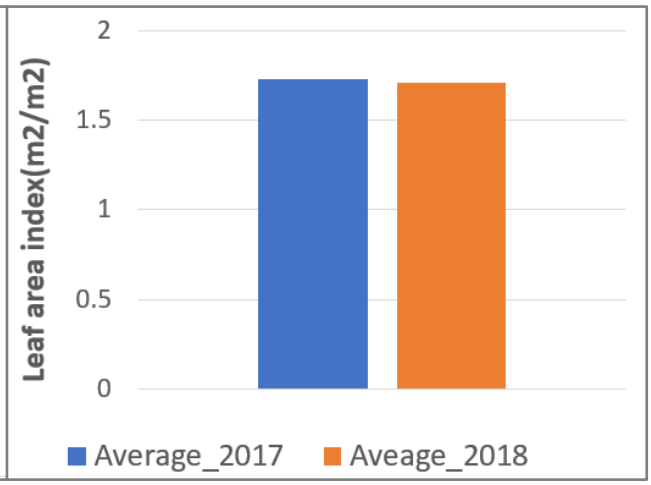

Figure 29: Comparison of mean leaf area index (LAI) of the same days for both years (2017 and 2018).

Leaf area index (LAI) was higher in the spring of 2018, as expected, because the 2017 spring was dry, and the spring of 2018 was wet. The decline comes later (in July), but there are not the 2017 cloud-free images to compare. The comparison analysis between the 2018 growing season that faced drought and the 2017 normal growing season has been done based on 2017 available data; the difference of mean canopy leaf area property of both years was minimal due to the gap of 2017 summer data which would highly contribute.

5.2.2. Leaf water content (Cw)

Leaf water content is retrieved with SCOPE, which has the specific absorption spectrum of water. Cw is used to detect vegetation water stress. The loss of leaf water indicates drought stress (Grzesiak et al., 2006).

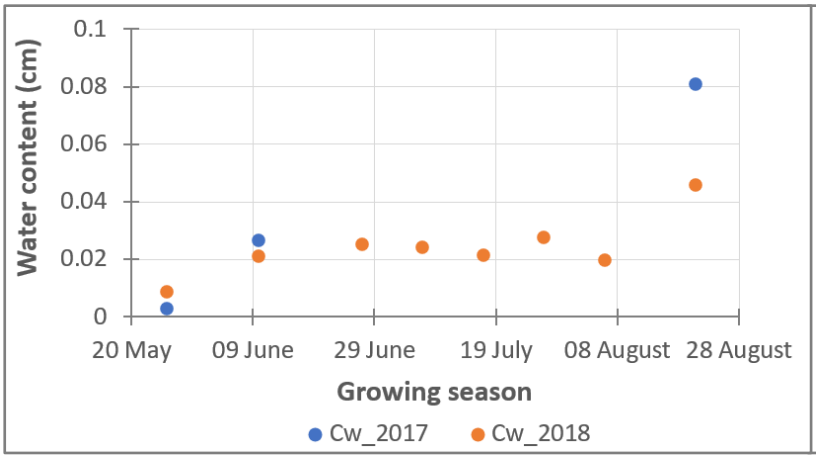

Figure 30: Leaf water content (Cw) 2017 versus 2018 content (Cw) of the same days for both years

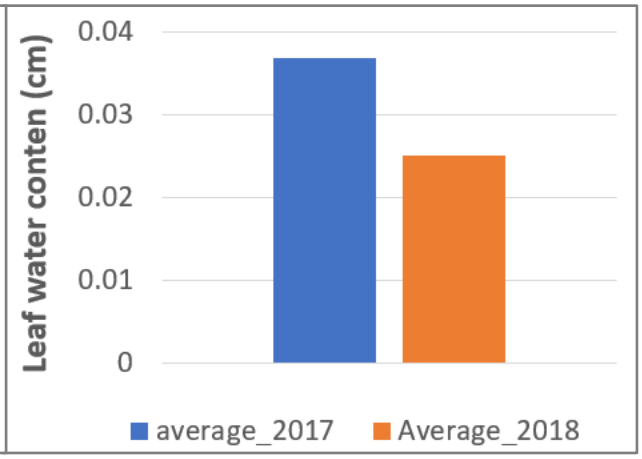

Figure 31: comparison of mean leaf water

Leaf water content in 2018 was lower than in 2017, mainly with figure 31 of average leaf water content, which performed based on the data available in 2017 compared to the same days in 2018. The declination in 2018 mean leaf water content indicates drought stress.

5.2.3. Leaf chlorophyll content (Cab)

Leaf chlorophyll content is a physiological indicator used to calculate the total chlorophyll content of the leaves; this pigment determines the concentration of the crop due to the energy absorption.

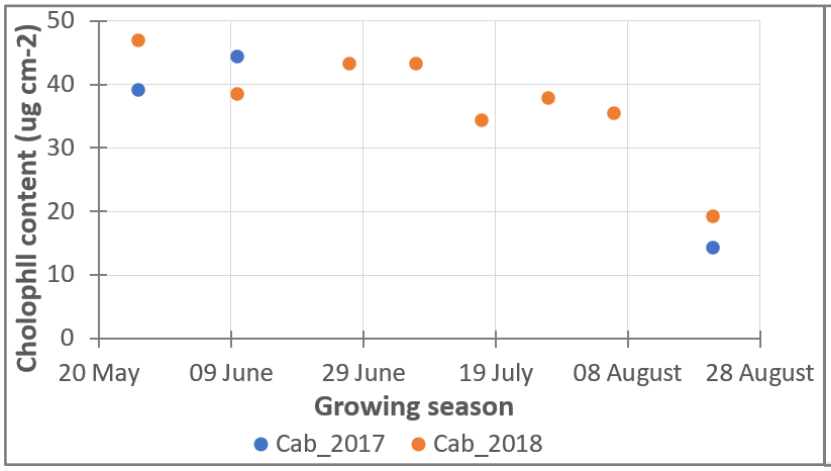

Figure 32: Leaf chlorophyll content (Cab) 2017 and 2018 chlorophyll content (Cab)of the same days for both years

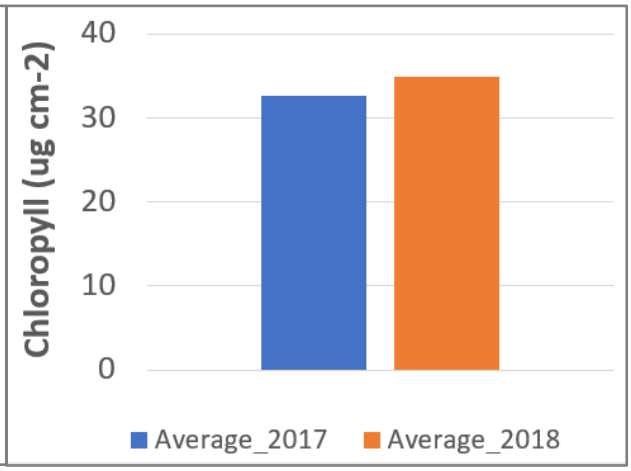

Figure 33: Comparison of mean

At the beginning of the 2018 growing season, the Cab was high because the weather was favorable for the plants with sufficient rainfall and shortwave radiation, but for the following period, Cab is slowly decreased because the plotted graph combines irrigated and non-irrigated farms, that is why the decline is minimal than expected in 2018 summer, see figure 32. However, figure 33 indicates high mean chlorophyll content due to the few data averaged. As 2017 does not have sufficient vegetation data, the comparison made between two years is based on the available data. The summer period data that was expected to reveal the effects of drought are missing; the used one is the beginning and the end of the growing season where 2018 had good weather.

5.3. Simulation of photosynthesis and evapotranspiration.

5.3.1. Photosynthesis

The following photosynthesis result was simulated by the SCOPE model, using the RTMo simulated vegetation properties together with weather data. The model interpolates between days with the 2017 simulation, which had incomplete vegetation properties inputs like LAI and Cab. This means that it has interpolated between 6 June and 20 August 2017. This affected the results, as the summer data expected to reveal the impacts and provide a huge difference between the photosynthesis of two growing seasons. However, due to the severity of the 2018 drought, the available produced satisfactory results with low photosynthesis during the summer drought of 2018 and high photosynthesis in 2017, which was the reference year.

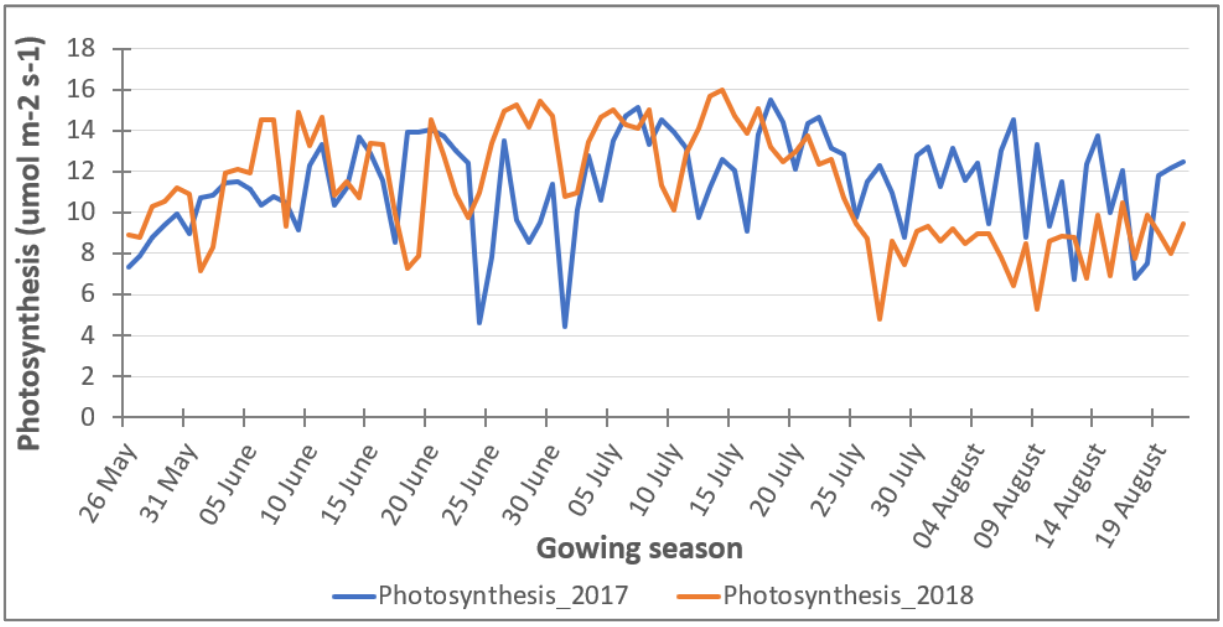

Figure 34: Photosynthesis of two growing seasons, 2017 and 2018, simulated by SCOPE, based on the vegetation and ERA5 weather data.

This result makes sense because at the beginning of the growing season (April to June), the 2018 precipitation was high compared to 2017, as shown in section 4.1.4.3, and the shortwave radiation was sufficient to contribute to high photosynthesis. Based on the analysis made on weather data (section 4.1.4), lack of precipitation combined with high radiation and high temperature in the 2018 summer period (end of June to August) lead to low photosynthesis.

This finding is consistent with the determined precipitation deficit in section 5.1.2, leaf area index simulated and analyzed in section 5.2.1, the information from Centraal Bureau voor de Statistiek, and information

from the literature (W. Peters et al., 2020; Buitink et al., 2020; Prins et al., 2018). The photosynthesis results simulated by SCOPE model is accurate as it meets the expectations.

5.3.1.1. Photosynthesis results compared by leaf area index

The leaf area index is the main factor that determines the photosynthesis stimulated by SCOPE model, which means when the leaf area index declines, it causes less photosynthesis. Briefly, each influences the other as the plants can only make leaves when there is photosynthesis. The following figure 35 shows its correspondence which validates the simulated photosynthesis result.

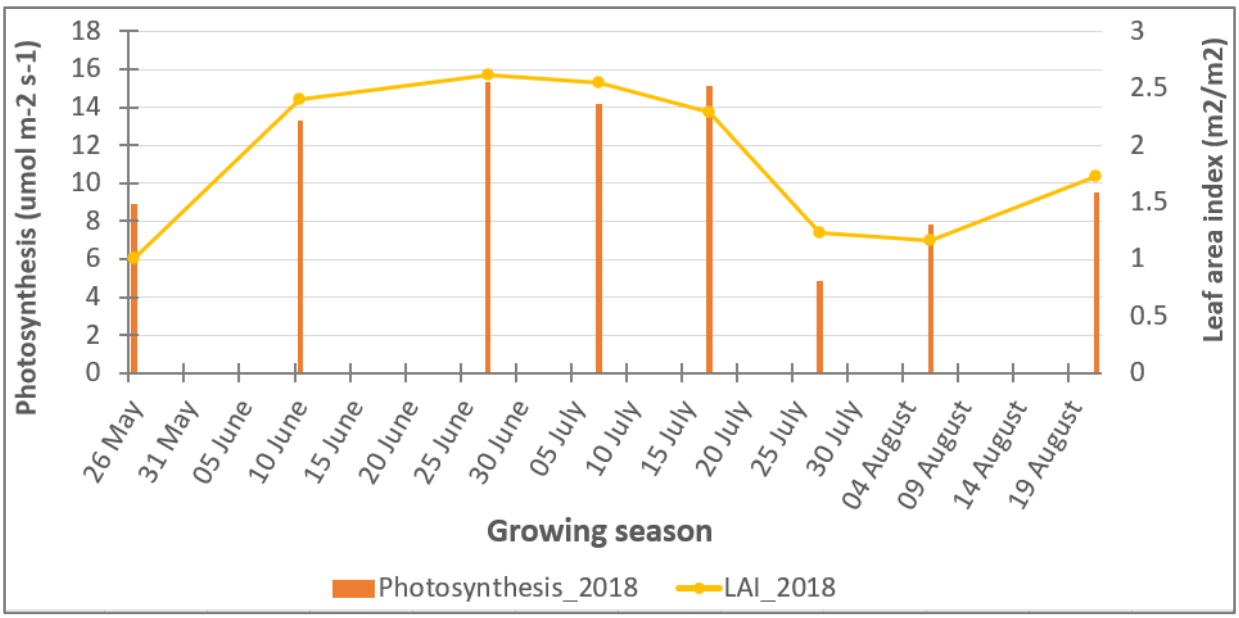

Figure 35: The simulated photosynthesis compared to leaf area index (LAI) of the 2018 growing season.

5.3.2. Actual evapotranspiration (ETa)

Actual evapotranspiration simulated by the SCOPE model is the combination of the latent heat flux from the copy (lEctot) and latent heat flux from the soil (lEstot), which results in the sensible heat flux (lEtot) in Wm-2. Figure 36 shows the ETa of both growing seasons.

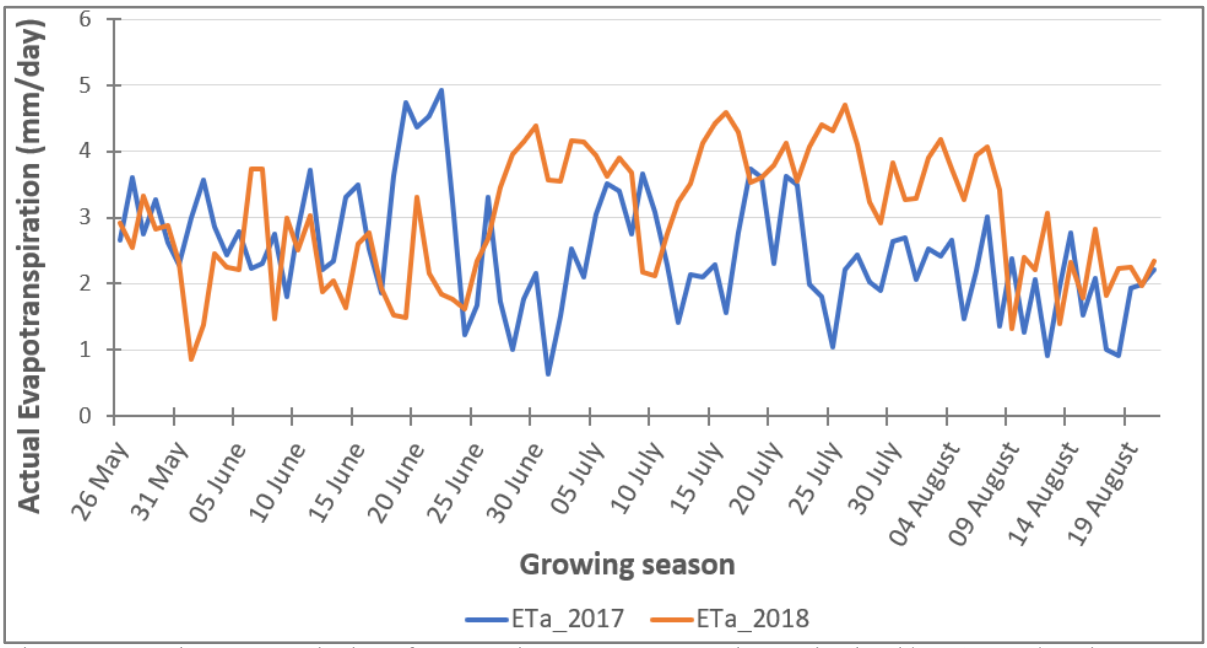

Figure 36: Actual evapotranspiration of two growing seasons, 2017 and 2018 simulated by SCOPE, based on vegetation and ERA5 weather data.

The 2018 actual evapotranspiration was low in the planting season due to the low temperature and irradiance at that time. While in the summer period, it was high based on the high temperature and radiation. Usually, evapotranspiration is closely related to the photosynthesis of plants; however, this result is not the case because both the canopy latent heat flux and the soil latent heat flux were critical while they were lack of soil moisture content due to the low precipitation, see section 4.3. Consequently, this may be caused by the SCOPE model, which keeps track of a water budget, and there is no limitation by soil moisture content on soil evaporation, transpiration, and photosynthesis. For this reason, the soil evaporation continued in the SCOPE simulation during the drought, which is not realistic because, in reality, the low soil moisture would restrict soil evaporation. Based on the minimal soil moisture content during the 2018 summer, see section 4.3, the soil evaporation would be limited.

5.3.2.1. Latent heat flux from the canopy (lEctot)

The lEctot simulated by SCOPE reacted to the presence of high temperature in the 2018 summer, which causes high transpiration. Therefore, the plants faced a water shortage as the water evaporated was from the canopy while the water recharge (rainfall and groundwater) was low; see sections 4.1.4.3 and 4.4. Figure 37 shows the situation of vegetation transpiration during the 2017 and 2018 growing seasons, where the plant transpiration during the 2018 summer was high compared to 2017, which influenced the high temperature in the 2018 summer.

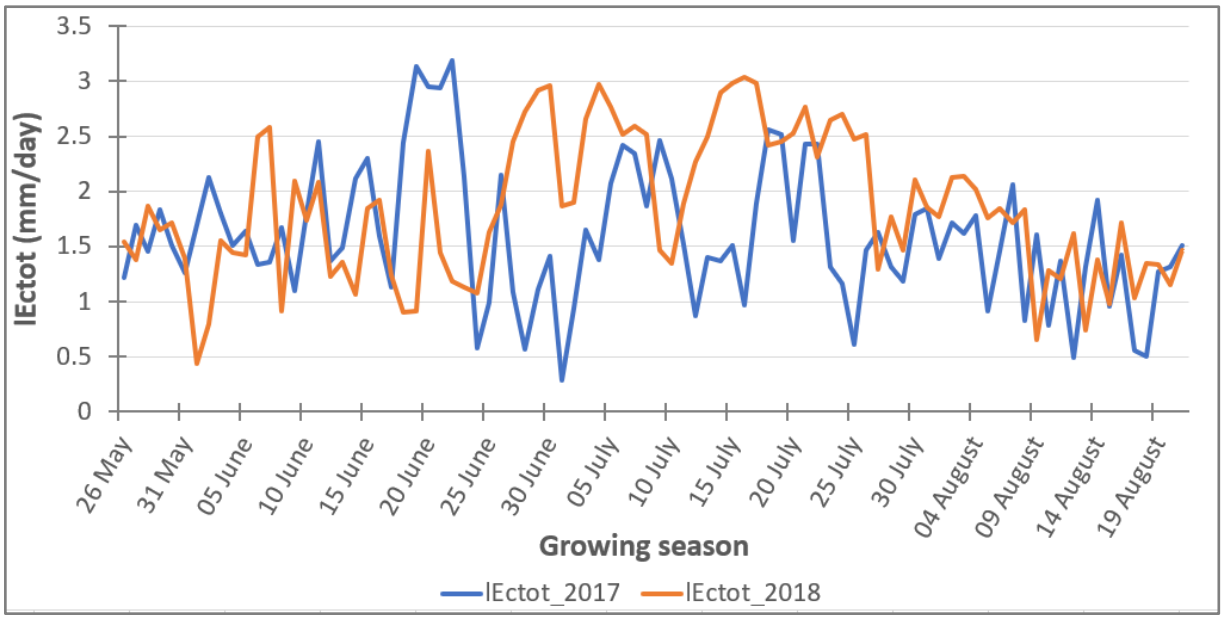

Figure 37: Latent heat flux from the canopy of two growing seasons, 2017 and 2018 simulated by SCOPE, based on vegetation and ERA5 weather data.

5.4. Soil moisture content

Among 15 soil moisture stations in the raam catchment, seven of them shown the data gaps during the study period, the eight (station 01, 02, 03, 04, 07, 12, 14, and 15) stations with full of the dataset in two growing seasons are the ones used for analysis and validation process. Five depths have been considered where the top ones (5cm and 10cm) compared by rainfall and deeper ones with groundwater after estimation of root zone soil moisture.

5.4.1. Shallow Soil moisture compared to precipitation

Figure39 and figure35 combine the station 01, 02, and 03; It shows the variability of the shallow in situ soil moisture due to the influence of precipitation recoded from the Volkel station located in the catchment.

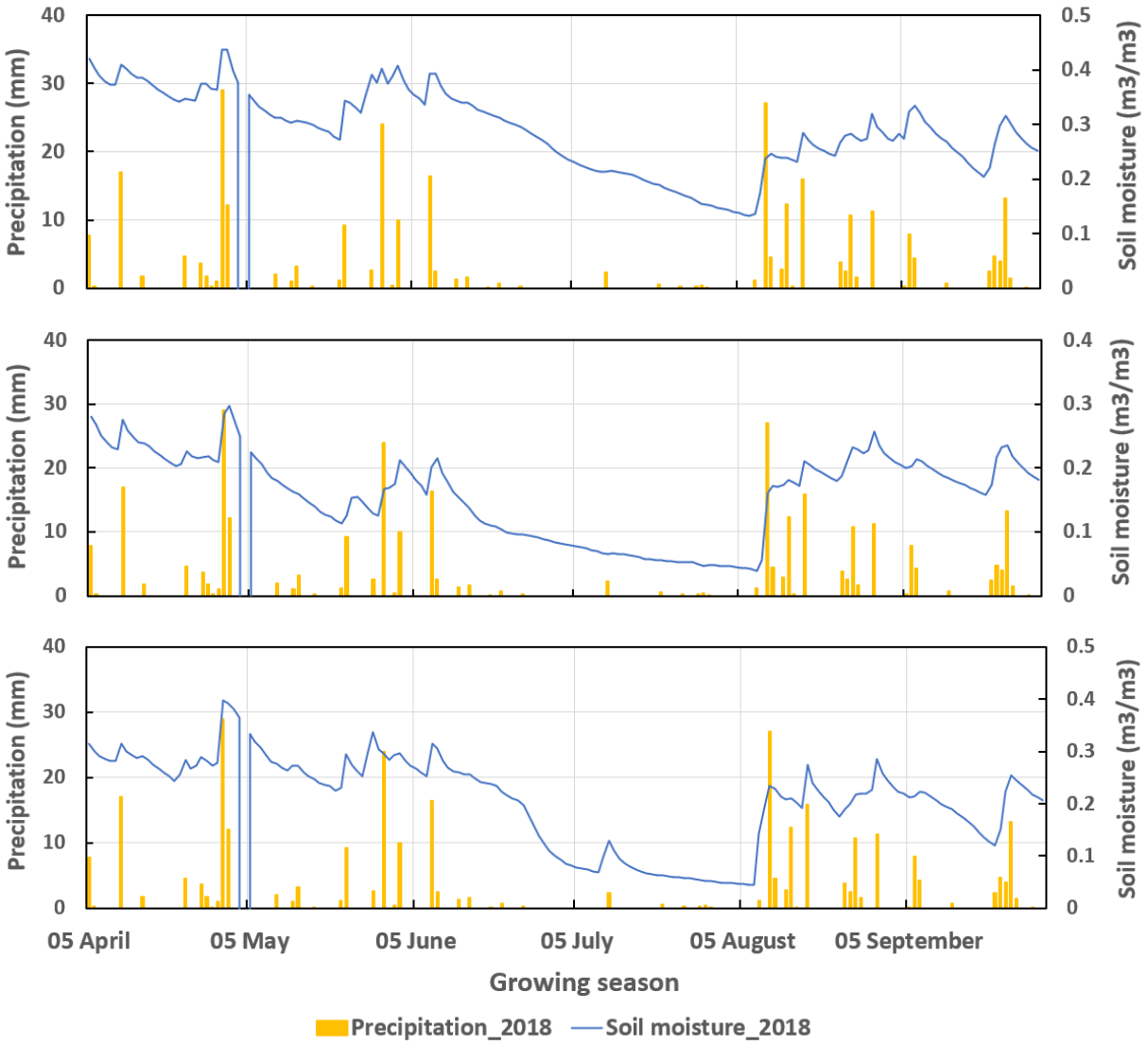

Figure 38:Daily mean surface soil moisture variation, of station 01, 02, and 04 respectively, at 5cm depth which influenced by the precipitation.

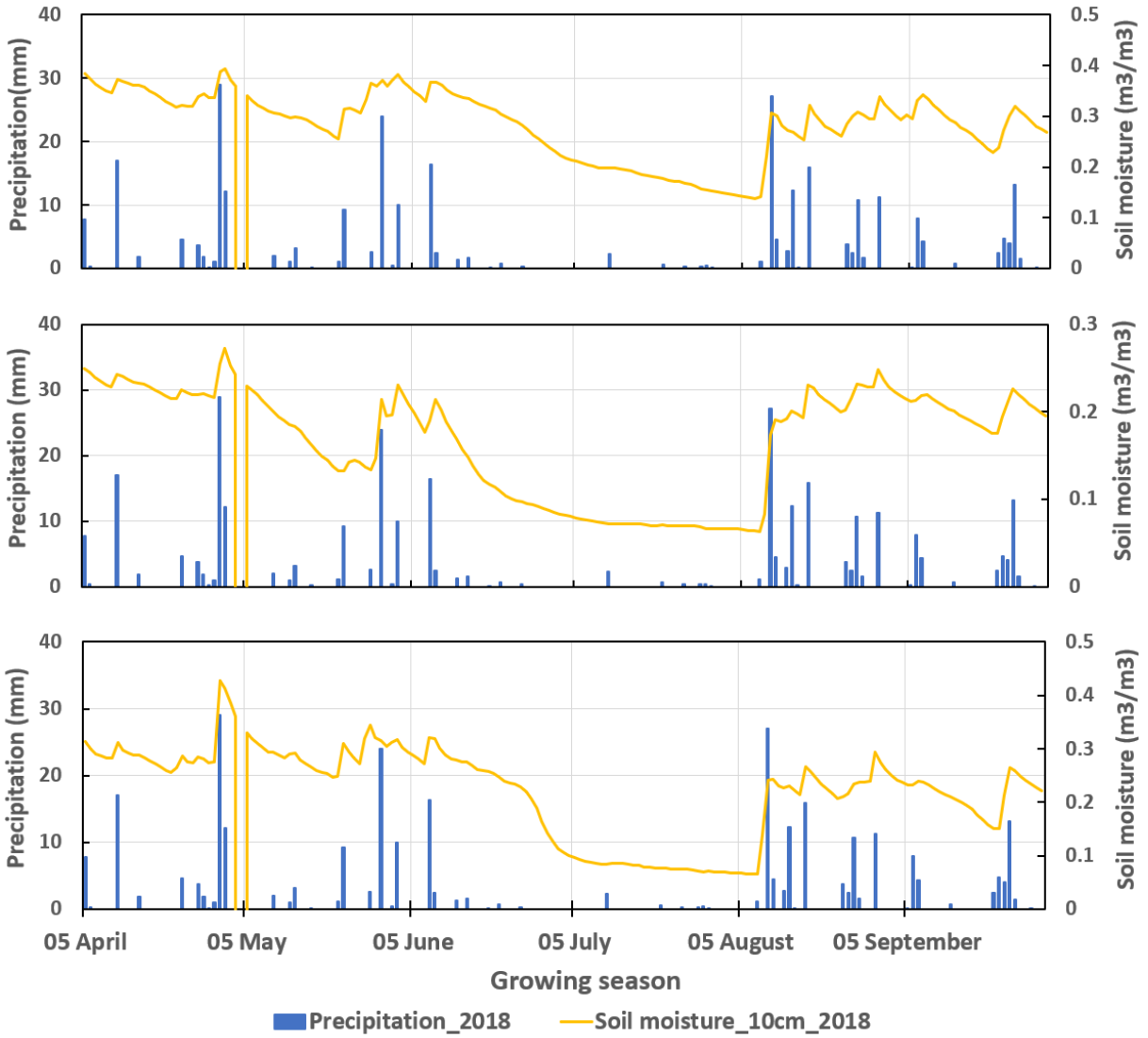

Figure 39: Daily mean soil moisture variation, of station 01, 02, and 04 respectively, at 10cm depth which influenced by the precipitation.

Top layers of soil moisture (5cm and 10cm) are influenced by rainfall, as shown by Figures 39 and 40, where at the beginning and the end of the growing season, the soil moisture content was high due to sufficient rainfall. However, during the summer period from June to August, the soil moisture content declined due to the precipitation shortage, this influenced drought.

Figure 41 shows the variability of surface soil moisture content based on irrigation. The variability of shallow soil moisture content at stations 14 and 15 depends on rainfall at the beginning of the growing season and irrigation during the summer period. The stations are located in the area where the irrigation system is high; that is why the soil moisture content in figure 41 suddenly rises and drops (ups and down)

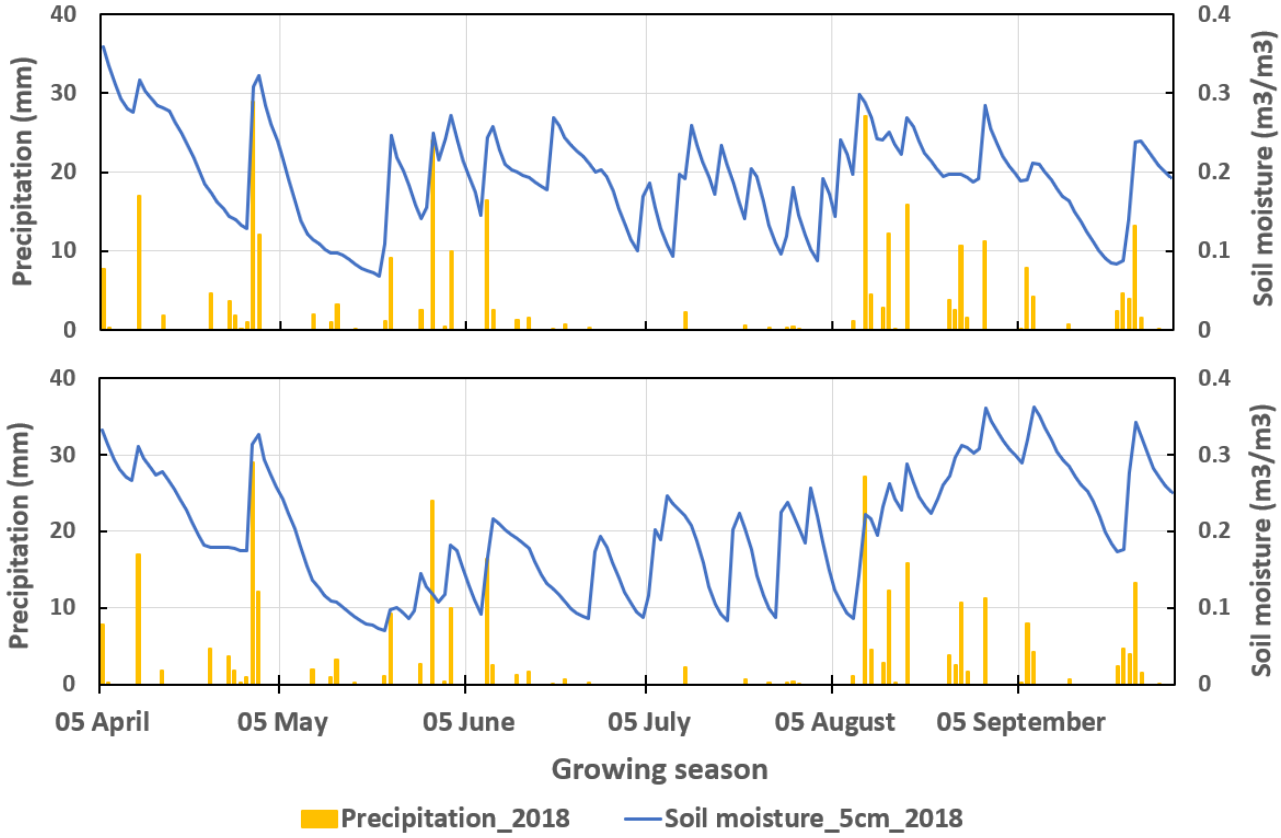

Figure 40:Daily mean shallow soil moisture of stations 14, and 15 respectively at 5cm depth which influenced by the precipitation and irrigation.

The following google earth pictures of august 2018 show the ongoing irrigation activity around station14 and 15, which justify the reaction or reflectance (ups and down) at the sttions.

Figure 41: google earth pictures of august 2018 show the ongoing irrigation activity at the 14 and 15 stations location.

5.4.2. Root zone soil moisture (RZSM)

Based on the weighted method and Eq 11 explained in section 4.3, the root zone soil moisture of 40 cm and 80 cm depth were calculated for comparative analysis. Figures 43 and 44 show the variability of the soil moisture at both depths in two growing seasons. The following graphs are an example of the root zone soil moisture (RZSM) at station 01 for both depths.

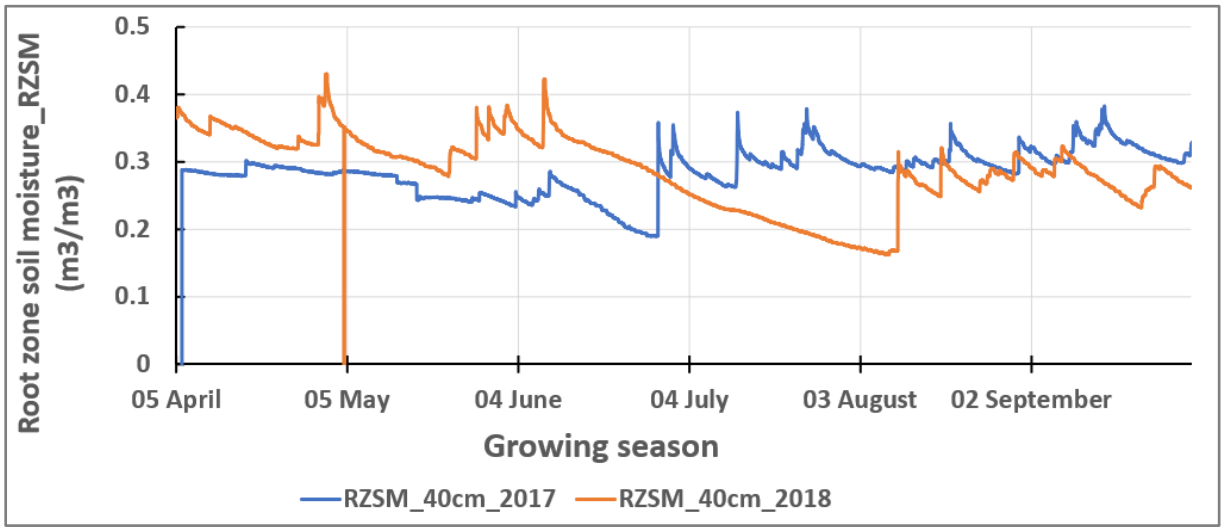

Figure 42: root zone soil moisture of two growing seasons (2017 versus 2018) at 40cm depth.

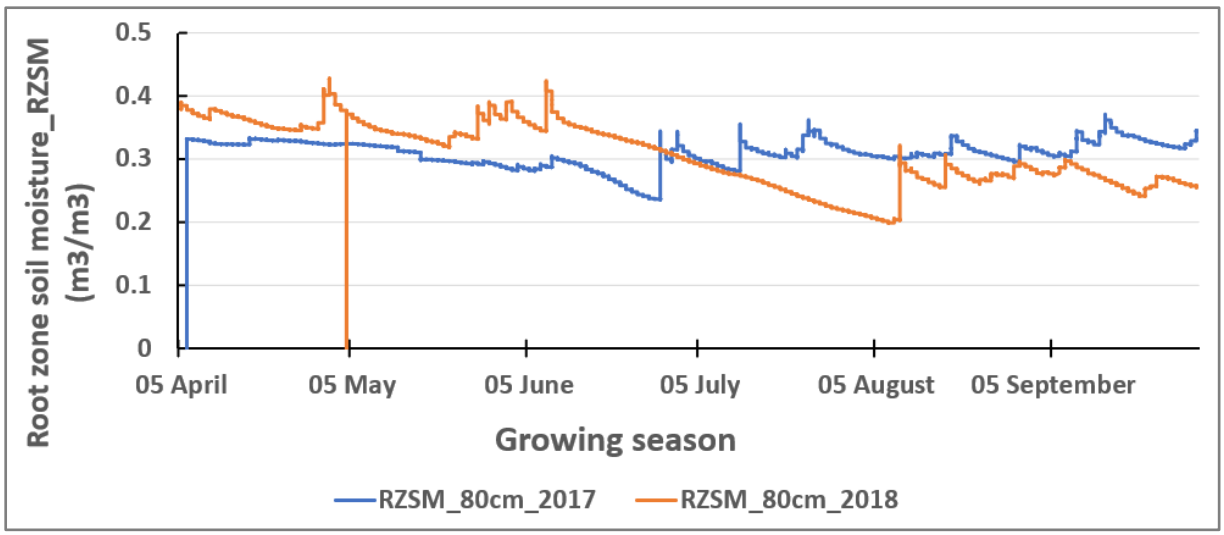

Figure 43: root zone soil moisture of two growing seasons (2017 versus 2018) at 80cm depth

Figures 43 and 44 show the decline of root zone soil moisture in the 2018 summer period compared to 2017; this indication is valid as there was a drought in that period. Therefore, these root zone soil moisture (RZSM) content results prove the simulated photosynthesis as both (RZSM and photosynthesis) indicate good condition at the beginning of the 2018 growing season and drought in the summer.
This result is reliable as the root zone soil moisture is the main physical process affecting photosynthesis and developing drought(All, 1996).

5.4.2.1. Variability of root zone soil moisture based on groundwater

The daily dataset of monitoring wells that recorded automatically have been obtained from Dinoloket and used to analyze the groundwater level fluctuation. The Piezometers B45F1045, B45F1050, and B46C0256 located in the study area have been selected and used, where their hydraulic heads were compared with the root zone soil moisture. Figure 45 shows the variability of the root zone soil moisture influenced by groundwater level, where the changes were gradual except in summer when there was drought.

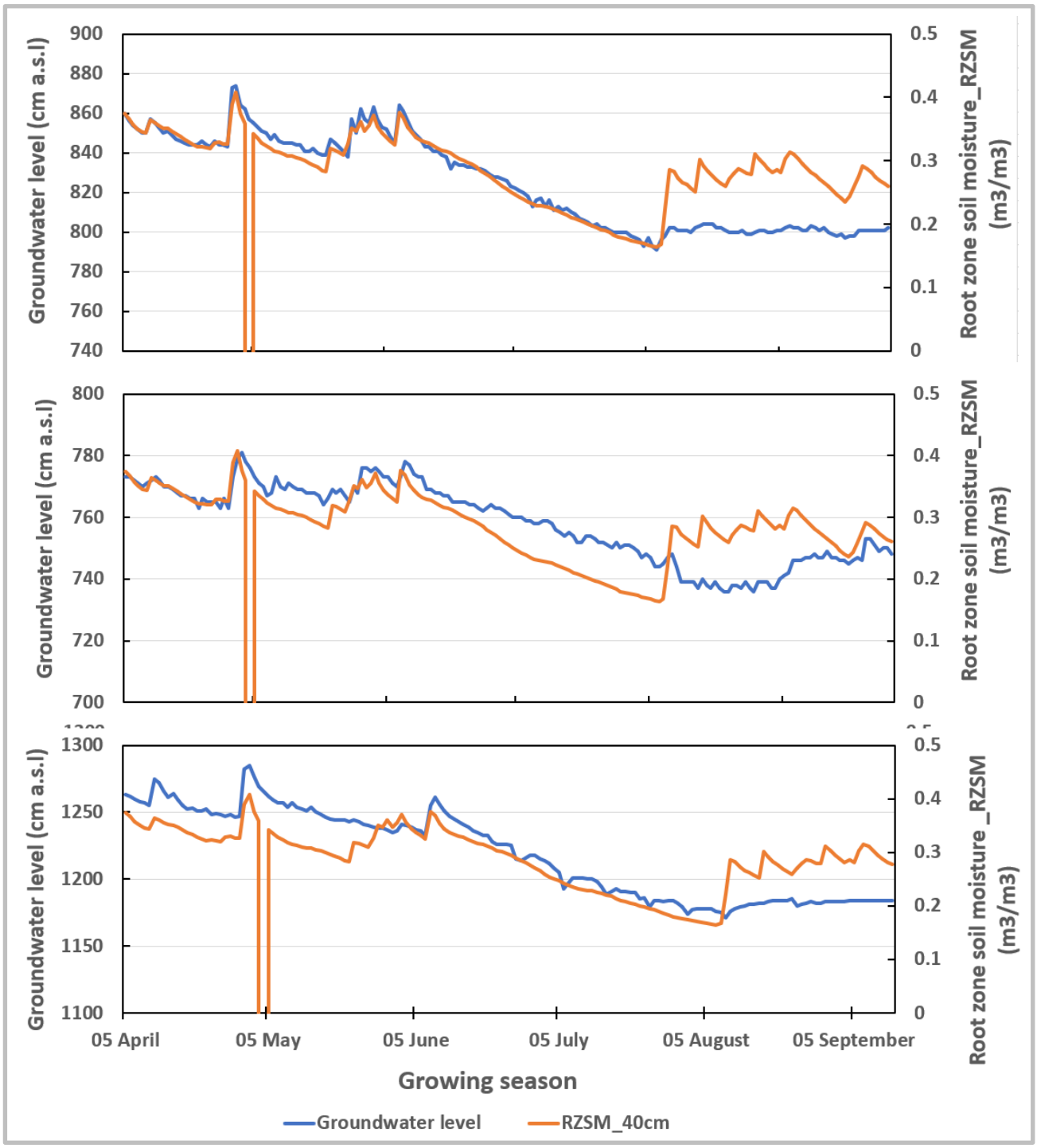

Figure 44: Daily mean root zone soil moisture of 40cm at station 01 compared to the groundwater level from piezometers B45F1045, B45F1050, and B46C0256.

Kumar & Minhas (1999); Muthoni & Kabira (2016); Aliche et al. (2018) concluded the tuber bulking growing stage of potato as the highly affected by root zone soil moisture deficit. The water shortage impacts photosynthesis, reduces the leaf expansion rate, prevents the development of new leaves, influences plant senescence, affects the tube size, impacts potato quality, and then reduces tuber yield production (Ramírez et al., 2014).

The findings of this study emphasize that the tuber bulking stage of potato is the most affected by drought, as concluded by the different researches. During the growing season of 2018, the period in which the soil moisture reduces is the same as when the LAI reduced, and the photosynthesis as well, and same period rainfall deficit was high, and groundwater level was decreased; see section5. This period covers the tuber bulking stage of potato as it is on the 90th days of the growing season.

It is particularly relevant that the reduction of LAI coincided in time with the high precipitation deficit and the tuber bulking stage during the growing season of 2018. At the same period, the soil moisture reduces as well, the photosynthesis was low, and groundwater level was decreased; see section5.

When the soil moisture deficit becomes higher, the water available for plant transpiration decreases, which leads to drought plant stress (Bayat et al., 2016). In addition, due to the SCOPE model, declination of leaf area index results in less photosynthesis. Still, usually less photosynthesis affects the expansion rate of leaves, which means each influences the other. This process negatively impacts plant growth rate mainly when it is combined with high evapotranspiration (Hui-Mean et al., 2018). based on the analysis and results of this study, those mentioned scenarios happened during the tuber bulking stage period, which concludes that is the stage on which is highly affected by the drought.

6. CONCLUSION AND RECOMMENDATION

6.1. Conclusion

This study aimed to develop a method to monitor drought stress in potatoes and differentiate this from other effects such as diseases, wildfire, insects, pesticides, lack of fertilizers, and flood by using the multiple indices and consideration of physical processes related to drought. This was achieved using remote sensing data, combined with meteorological data, and the vegetation properties simulated by RTMo based on the sentinel-2 reflectance, field measurements of soil moisture and groundwater level data. Those reflectance data have been collected from eighty-eight (88) potato farms and used in the SCOPE to simulate photosynthesis and evapotranspiration of two growing seasons (2017 and 2018) in the Raam catchment, then validated with in situ data.

Hence, after analyzing the simulated drought-related variables, it was found that they have a good match with the observed in situ soil moisture and groundwater heads and with the leaf area index where all of them indicate drought in the 2018 summer. This concludes the accuracy of simulated results provided by satellite data, as this study was based on the reflectance data collected from sentinel-2. Concerning the specific objective and research questions of this study, the following conclusion can be drawn from the result and discussion chapter :

i) 2018 has been concluded as an exceptional year based on the performance of the 20 years NDVI time series of the study area, the computation of precipitation deficit of four current years, and the comparison of the land surface temperature minus air temperature (LST – Ta) of two growing seasons. This time series and comparison analysis concluded the 2018 summer as the driest period, even more than the 2019 and 2020, which were also the dry years in the Netherlands. See section 5.1.1, 5.1.2, and 5.1.3

ii) The multi-spectral reflectance data retrieved from Sentinel-2 with the help of google earth engine (GEE) have been used in RTMo to simulate vegetation properties, and the anomalies in their seasonal dynamics concluded as drought stress indicators. It is particularly relevant that the reduction of LAI coincided in time with the high precipitation deficit and the tuber bulking stage. See section 5.1.2 and 5.2.1

iii) Vegetation properties simulated by RTMo, combined with weather data from ERA5, have been used in the SCOPE model to simulate photosynthesis and evapotranspiration. The results show the severity and duration of the 2018 drought, based on the comparative analysis done with the 2017 regular year and based on the comparision done using in situ soil moisture, rainfall, leaf area index, and groundwater level.

iv) Based on the findings of this study presented in section 5, it can be concluded that the tuber bulking growing stage of potato is highly affected by drought as both the severity and duration of the 2018 drought, which is negatively impacted the crop production, occurred in the period of tuber bulking stage.

This study observed that satellite-derived data such as sentinel-2 data could sufficiently identify and characterize the occurrence and duration of drought during the growing period, but the reliability of the interpretation improves when validated with in situ data. Therefore, sentinel-2 data is trustable to the agricultural drought monitoring as it provides the data of high spatial resolution and helps to be more specific.

This study utilized the comparison analysis of evapotranspiration (2017 and 2018), the relationship between leaf area index (LAI), and photosynthesis which can be applied for forecasting the yield reduction in case of a drought situation. Therefore, based on the study findings and comparison analysis, there was a significant positive relationship between LAI and photosynthesis, rainfall and topsoil moisture content, as well as root zone soil moisture and shallow groundwater tables. This can be used in agricultural drought monitoring and early warning the authorities and decision-maker for the effective drought mitigation measures to the onset of drought as part of preparedness and strategic planning to face the drought. The applied method has been successful for drought assessment and detection of vegetation stress, as proved by the obtained results.

6.2. Limitations and Recommendation

This study relied on sentinel-2 data. The multi-spectral information obtained from sentinel-2 using Google Earth Engine had many data gaps due to the cloud cover and shadow, which affected data collection, mainly in the 2017 growing season. The reflectance data obtained for 2017 was less than that of 2018, and it becomes very less after the processing of the data, which based on the growth stage of the potato because the data used were the ones that showed vegetation spectral in order to avoid using bare soil data in vegetation stress analysis. That issue of using few data may have introduced uncertainties in the retrieval process. For example, it is unrealistic for 2018 to record a high average leaf chlorophyll content (Cab) 2018, as shown in Figure33. This could be caused by averaging only data of beginning and end of the growing season while knowing very well that the drought happened in summer as shown by rainfall deficit and other indicators, mean the sufficient summer data of 2017 would impact the results and show a huge difference between two growing seasons.

The study was about monitoring agriculture drought based on sentinel-2 data and meteorological data. If there were other stresses like stomatal closure, it wouldn't be observed as there were not any information on soil moisture use in the SCOPE model; otherwise, the more stress factor with soil moisture is needed. The next improvement version of SCOPE is recommended to keep track of limitation by soil moisture content on soil evaporation, transpiration, and photosynthesis.

Leaf temperature is a good indicator of drought stress, and it is retrieved from the thermal band. Therefore, the lack of a thermal band in the Sentinel-2 image collection prevents leaf temperature from being used.

The same potato farms for both years (2017 and 2018) couldn't be used in the analysis due to crop planting rotations in the Netherlands, which means it is impossible to get the same farm of a similar crop type in two consecutive years. But the farms used for both years are close to each other to minimize the errors.

Among the 15 in situ soil moisture stations in the Raam catchment, seven of them showed data gaps during the study period. The data gaps in stations 9, 10, and 12 prevent them from being used in the analysis while they were located within potato farms. Using the data from those stations within potato farms would provide more accurate results than using those at 5 to 9km far from the focussed area. The management is recommended to do the follow-up or maintenance of the stations for better consecutive data.

In the Raam catchment, several piezometers have data gaps. Others are recording random data, where only a one-day dataset represents the whole month, and some piezometers are not working. In the study area, only five piezometers are provided a full daily dataset of the simulation period; four of them are very close to each other, as shown in the study area map (figure 3). It would be better to use the piezometers, which are well distributed in the study area. The management is recommended to replace those not working and install more piezometers that record the daily data and take care of their distribution.

LIST OF REFERENCES

Aliche, E. B., Oortwijn, M., Theeuwen, T. P. J. M., Bachem, C. W. B., Visser, R. G. F., & van der Linden, C. G. (2018). Drought response in field grown potatoes and the interactions between canopy growth and yield. *Agricultural Water Management*, *206*(April), 20–30. https://doi.org/10.1016/j.agwat.2018.04.013

All, U. T. C. (1996). *Physical Processes Involved in the 1988 Drought and 1993 Floods in North America Author (s): Kevin E . Trenberth and Christian J . Guillemot Published by : American Meteorological Society Stable URL : https://www.jstor.org/stable/26201317 REFERENCES Lin*. *9*(6), 1288–1298.

Allen, R. G., Pereira, L. S., Raes, D., & Smith, M. (1998). Crop evapotraspiration guidelines for computing crop water requirements. In *FAO Irrigation & drainage Paper 56. FAO, Food and Agriculture Organization of the United Nations,Roma*.

Allen, Richard G., PEREIRA, Luis S., RAES, Dirk and SMITH, M. (1998). FAO Irrigation and Drainage Paper Crop by. *Irrigation and Drainage*, *300*(56), 300. Retrieved from http://www.kimberly.uidaho.edu/water/fao56/fao56.pdf

Badeck, F.-W., Bondeau, A., Böttcher, K., Doktor, D., Lucht, W., Schaber, J., & Sitch, S. (2004). *Research review Responses of spring phenology to climate change*. https://doi.org/10.1111/j.1469-8137.2004.01059.x

Bayat, B., van der Tol, C., & Verhoef, W. (2016). Remote sensing of grass response to drought stress using spectroscopic techniques and canopy reflectance model inversion. *Remote Sensing*, *8*(7), 1–24. https://doi.org/10.3390/rs8070557

Bayat, B., van der Tol, C., Yang, P., & Verhoef, W. (2019). Extending the SCOPE model to combine optical reflectance and soil moisture observations for remote sensing of ecosystem functioning under water stress conditions. *Remote Sensing of Environment*, *221*(August 2018), 286–301. https://doi.org/10.1016/j.rse.2018.11.021

Beersma, J. J., & Adri Buishand, T. (2004). Hydrology: Drought; 1818 Hydrology: Evapotranspiration; 1854 Hydrology: Precipitation (3354); 1860 Hydrology: Runoff and streamflow; Citation: Beersma. *Water Resour. Res*, *40*, 12508. https://doi.org/10.1029/2004WR003265

Beersma, J. J., & Buishand, T. A. (2007). Drought in the Netherlands - Regional frequency analysis versus time series simulation. *Journal of Hydrology*, *347*(3–4), 332–346. https://doi.org/10.1016/j.jhydrol.2007.09.042

Benninga, H. J. F., Carranza, C. D. U., Pezij, M., Van Santen, P., Van Der Ploeg, M. J., Augustijn, D. C. M., & Van Der Velde, R. (2018). The Raam regional soil moisture monitoring network in the Netherlands. *Earth System Science Data*, *10*(1), 61–79. https://doi.org/10.5194/essd-10-61-2018

Beukema, & Van Der Zaag, D. E. (1990). Introduction to potato production. In *1990 Ed* (Vol. 2).

Bhavani, P., Roy, P. S., Chakravarthi, V., & Kanawade, V. P. (2017). Satellite Remote Sensing for Monitoring Agriculture Growth and Agricultural Drought Vulnerability Using Long-Term (1982–2015) Climate Variability and Socio-economic Data set. *Proceedings of the National Academy of Sciences India Section A - Physical Sciences*, *87*(4), 733–750. https://doi.org/10.1007/s40010-017-0445-7

Boken, V. K. (2009). Improving a drought early warning model for an arid region using a soil-moisture index. *Applied Geography*, *29*(3), 402–408. https://doi.org/10.1016/j.apgeog.2008.12.006

Borzuchowski, J., & Schulz, K. (2010). Retrieval of leaf area index (LAI) and soil water content (WC) using hyperspectral remote sensing under controlled glass house conditions for spring barley and sugar beet. *Remote Sensing*, *2*(7), 1702–1721. https://doi.org/10.3390/rs2071702

Bressers, H., & Bressers, N. (2016). Governance for Drought Resilience. In *Governance for Drought Resilience*. https://doi.org/10.1007/978-3-319-29671-5

Buitink, J., Swank, A. M., van der Ploeg, M., Smith, N. E., Benninga, H.-J. F., van der Bolt, F., … Teuling, A. J. (2020). Anatomy of the 2018 agricultural drought in The Netherlands using in situ soil moisture and canopy nearinfrared reflectance satellite imagery. *Hydrology and Earth System Sciences*, (August), 1–17.

Carranza, C., Nolet, C., Pezij, M., & van der Ploeg, M. (2021). Root zone soil moisture estimation with Random Forest. *Journal of Hydrology*, *593*(November 2020), 125840. https://doi.org/10.1016/j.jhydrol.2020.125840

Chen, J. M., Rich, P. M., Gower, S. T., Norman, J. M., & Plummer, S. (1997). Leaf area index of boreal forests: Theory, techniques, and measurements. *Journal of Geophysical Research Atmospheres*, *102*(24), 29429–29443. https://doi.org/10.1029/97jd01107

Chen, Y., Sun, L., Wang, W., & Pei, Z. (2019). Application of sentinel 2 data for drought monitoring in Texas, America. *2019 8th International Conference on Agro-Geoinformatics, Agro-Geoinformatics 2019*, 2019–2022. https://doi.org/10.1109/Agro-Geoinformatics.2019.8820491

Dagnenet, M. (2019). *Satellite remote sensing for soil moisture estimation : Gumara catchment , Satellite Remote Sensing for Soil Moisture Estimation : Gumara Catchment , Ethiopia Dagnenet Fenta Mekonnen*. (November).

Dai, A. (2013). Increasing drought under global warming in observations and models. In *Nature Climate Change* (Vol. 3). https://doi.org/10.1038/nclimate1633

Dash, P., Göttsche, F. M., Olesen, F. S., & Fischer, H. (2002). Land surface temperature and emissivity estimation from passive sensor data: Theory and practice-current trends. *International Journal of Remote Sensing*, *23*(13), 2563–2594. https://doi.org/10.1080/01431160110115041

De Wit, A. J. W., & Clevers, J. G. P. W. (2004). Efficiency and accuracy of per-field classification for operational crop mapping. *International Journal of Remote Sensing*, *25*(20), 4091–4112. https://doi.org/10.1080/01431160310001619580

Do Amaral Cunha, A. P. M., Marchezini, V., Lindoso, D. P., Saito, S. M., & Dos Santos Alvalá, R. C. (2019). The challenges of consolidation of a drought-related disaster risk warning system to Brazil. *Sustentabilidade Em Debate*, *10*(1), 43–59. https://doi.org/10.18472/SustDeb.v10n1.2019.19380

Dumedah, G., Walker, J. P., & Merlin, O. (2015). Root-zone soil moisture estimation from assimilation of downscaled Soil Moisture and Ocean Salinity data. *Advances in Water Resources*, *84*, 14–22. https://doi.org/10.1016/j.advwatres.2015.07.021

Fahad, S., Bajwa, A. A., Nazir, U., Anjum, S. A., Farooq, A., Zohaib, A., … Huang, J. (2017). Crop production under drought and heat stress: Plant responses and management options. *Frontiers in Plant Science*, *8*(June), 1–16. https://doi.org/10.3389/fpls.2017.01147

Fathi, A., & Tari, D. B. (2016). Effect of Drought Stress and its Mechanism in Plants. *International Journal of Life Sciences*, *10*(1), 1–6. https://doi.org/10.3126/ijls.v10i1.14509

Feyen, L., & Dankers, R. (2009). Impact of global warming on streamflow drought in Europe. *Journal of Geophysical Research Atmospheres*, *114*(17), 1–17. https://doi.org/10.1029/2008JD011438

Gao, B.-C. (1995). Normalized difference water index for remote sensing of vegetation liquid water from space. *Imaging Spectrometry*, *2480*(June 1995), 225. https://doi.org/10.1117/12.210877

Gao, B. C. (1996). NDWI - A normalized difference water index for remote sensing of vegetation liquid water from space. *Remote Sensing of Environment*, *58*(3), 257–266. https://doi.org/10.1016/S0034-4257(96)00067-3

Grzesiak, M. T., Grzesiak, S., & Skoczowski, A. (2006). Changes of leaf water potential and gas exchange during and after drought in triticale and maize genotypes differing in drought tolerance. *Photosynthetica*, *44*(4), 561–568. https://doi.org/10.1007/s11099-006-0072-z

Harmsen, E. W., Miller, N. L., Schlegel, N. J., & Gonzalez, J. E. (2009). *Seasonal climate change impacts on evapotranspiration, precipitation deficit and crop yield in Puerto Rico*. https://doi.org/10.1016/j.agwat.2009.02.006

Hayes, M., Svoboda, M., Wall, N., & Widhalm, M. (2011). The lincoln declaration on drought indices: Universal meteorological drought index recommended. *Bulletin of the American Meteorological Society*, *92*(4), 485–488. https://doi.org/10.1175/2010BAMS3103.1

Hiemstra, P., & Sluiter, R. (2011). Interpolation of Makkink Evaporation in the Netherlands. *De Bilt, 2011 | Technical Report; TR-327*, 78. Retrieved from http://www.numbertheory.nl/files/report_evap.pdf

Hijmans, R. J. (2003). The effect of climate change on global potato production. *American Journal of Potato Research : An Official Publication of the Potato Association of America*, *80*(4), 8–280. https://doi.org/10.1016/S0308-521X(02)00081-1

Holzman, M. E., Rivas, R., & Piccolo, M. C. (2014). Estimating soil moisture and the relationship with crop yield using surface temperature and vegetation index. *International Journal of Applied Earth Observation and Geoinformation*, *28*(1), 181–192. https://doi.org/10.1016/j.jag.2013.12.006

Huang, J., Zhuo, W., Li, Y., Huang, R., Sedano, F., Su, W., … Zhang, X. (2020). Comparison of three remotely sensed drought indices for assessing the impact of drought on winter wheat yield. *International Journal of Digital Earth*, *13*(4), 504–526. https://doi.org/10.1080/17538947.2018.1542040

Hui-Mean, F., Yusop, Z., & Yusof, F. (2018). Drought analysis and water resource availability using standardised precipitation evapotranspiration index. *Atmospheric Research*, *201*(August 2017), 102–115. https://doi.org/10.1016/j.atmosres.2017.10.014

JRC European Commission. (2011). NDWI (Normalized Difference Water Index).

Karnieli, A., Bayasgalan, M., Bayarjargal, Y., Agam, N., Khudulmur, S., & Tucker, C. J. (2006). Comments on the use of the Vegetation Health Index over Mongolia. *International Journal of Remote Sensing*,

27(10). https://doi.org/10.1080/01431160500121727
Kashyap, P. S., & Panda, R. K. (2001). Evaluation of evapotranspiration estimation methods and development of crop-coefficients for potato crop in a sub-humid region. *Agricultural Water Management*, *50*(1), 9–25. https://doi.org/10.1016/S0378-3774(01)00102-0
Keyantash, J. (2002). An Evaluation of a Drought. *American Meteorological Society*, (August), 1167–1180.
Kim, J. S., Park, S. Y., Lee, J. H., Chen, J., Chen, S., & Kim, T. W. (2021). Integrated drought monitoring and evaluation through multi-sensor satellite-based statistical simulation. *Remote Sensing*, *13*(2), 1–18. https://doi.org/10.3390/rs13020272
KNMI. (2020). Background information rainfall deficit.
Kumar, D., & Minhas, J. S. (1999). Effect of water stress on photosynthesis, productivity and water status in potato*. *Journal Indian Potato Association*, *01*(26), 7–10.
Li, Z. L., Tang, R., Wan, Z., Bi, Y., Zhou, C., Tang, B., … Zhang, X. (2009). A review of current methodologies for regional Evapotranspiration estimation from remotely sensed data. *Sensors*, *9*(5), 3801–3853. https://doi.org/10.3390/s90503801
Livada, I., & Assimakopoulos, V. D. (2007). Spatial and temporal analysis of drought in Greece using the Standardized Precipitation Index (SPI). *Theoretical and Applied Climatology*, *89*(3–4), 143–153. https://doi.org/10.1007/s00704-005-0227-z
Mallin, M. A., Paerl, H. W., Rudek, J., & Bates, P. W. (1993). Regulation of estuarine primary production by watershed rainfall and river flow. *Marine Ecology Progress Series*, *93*(1–2), 199–203. https://doi.org/10.3354/meps093199
Mane, S. P., Robinet, C. V., Ulanov, A., Schafleitner, R., Tincopa, L., Gaudin, A., … Grene, R. (2008). Molecular and physiological adaptation to prolonged drought stress in the leaves of two Andean potato genotypes. *Functional Plant Biology*, *35*(8), 669–688. https://doi.org/10.1071/FP07293
Mckee, T. B., Doesken, N. J., & Kleist, J. (1993). THE RELATIONSHIP OF DROUGHT FREQUENCY AND DURATION TO TIME SCALES. In *Eighth Conference on Applied Climatology*.
Meroni, M., Fasbender, D., Rembold, F., Atzberger, C., & Klisch, A. (2019). Near real-time vegetation anomaly detection with MODIS NDVI: Timeliness vs. accuracy and effect of anomaly computation options. *Remote Sensing of Environment*, *221*(June 2018), 508–521. https://doi.org/10.1016/j.rse.2018.11.041
Milly, P. C. D., & Dunne, K. A. (2016). Potential evapotranspiration and continental drying. *Nature Climate Change*, *6*(10), 946–949. https://doi.org/10.1038/nclimate3046
Mishra, A. K., & Singh, V. P. (2011). *Drought modeling-A review*. https://doi.org/10.1016/j.jhydrol.2011.03.049
Muthoni, J., & Kabira, J. N. (2016). Potato Production under Drought Conditions: Identification of Adaptive Traits. *International Journal of Horticulture*, (January 2016). https://doi.org/10.5376/ijh.2016.06.0012
Mutiibwa, D., Strachan, S., & Albright, T. (2015). Land Surface Temperature and Surface Air Temperature in Complex Terrain. *IEEE Journal of Selected Topics in Applied Earth Observations and Remote Sensing*, *8*(10), 4762–4774. https://doi.org/10.1109/JSTARS.2015.2468594
Pablos, M., Martínez-Fernández, J., Piles, M., Sánchez, N., Vall-llossera, M., & Camps, A. (2016). Multi-temporal evaluation of Soil Moisture and land surface temperature dynamics using in situ and satellite observations. *Remote Sensing*, *8*(7). https://doi.org/10.3390/rs8070587
Peng, C., Di, L., Deng, M., Han, W., & Yagci, A. (2013). A comprehensive agricultural drought stress monitoring method integrating MODIS and weather data: A case study of Iowa. *2013 2nd International Conference on Agro-Geoinformatics: Information for Sustainable Agriculture, Agro-Geoinformatics 2013*, 147–152. https://doi.org/10.1109/Argo-Geoinformatics.2013.6621898
Pereira, L. S., Perrier, A., Allen, R. G., & Alves, I. (1999). Evapotranspiration: Concepts and Future Trends. *Journal of Irrigation and Drainage Engineering*, *125*(2), 45–51. https://doi.org/10.1061/(asce)0733-9437(1999)125:2(45)
Peters, A. J., Walter-Shea, E. A., Ji, L., Viña, A., Hayes, M., & Svoboda, M. D. (2002). Drought monitoring with NDVI-based Standardized Vegetation Index. *Photogrammetric Engineering and Remote Sensing*, *68*(1), 71–75.
Peters, W., Bastos, A., Ciais, P., & Vermeulen, A. (2020). A historical, geographical and ecological perspective on the 2018 European summer drought: Perspective on the 2018 European drought. *Philosophical Transactions of the Royal Society B: Biological Sciences*, *375*(1810). https://doi.org/10.1098/rstb.2019.0505
Pettorelli, N. (2019). Satellite Remote Sensing and the Management of Natural Resources. *Satellite Remote*

Sensing and the Management of Natural Resources. https://doi.org/10.1093/oso/9780198717263.001.0001
Pettorelli, N., Vik, J. O., Mysterud, A., Gaillard, J. M., Tucker, C. J., & Stenseth, N. C. (2005). Using the satellite-derived NDVI to assess ecological responses to environmental change. *Trends in Ecology and Evolution*, *20*(9), 503–510. https://doi.org/10.1016/j.tree.2005.05.011
Philip, S. Y., Kew, S. F., Van Der Wiel, K., Wanders, N., Jan Van Oldenborgh, G., & Philip, S. Y. (2020). Regional differentiation in climate change induced drought trends in the Netherlands. *Environmental Research Letters*, *15*(9). https://doi.org/10.1088/1748-9326/ab97ca
Prins, H., Jager, J., Stokkers, R., & van Asseldonk, M. (2018). *Damage to Dutch agricultural and horticultural crops as a result of the drought in 2018*. (Table 1), 1–7. Retrieved from http://edepot.wur.nl/458511
Ramírez, D. A., Yactayo, W., Gutiérrez, R., Mares, V., De Mendiburu, F., Posadas, A., & Quiroz, R. (2014). Chlorophyll concentration in leaves is an indicator of potato tuber yield in water-shortage conditions. *Scientia Horticulturae*, *168*(February), 202–209. https://doi.org/10.1016/j.scienta.2014.01.036
Ruíz, A. A. B. (2015). *Methods and tools for drought analysis and managment* (Vol. 3). Retrieved from http://repositorio.unan.edu.ni/2986/1/5624.pdf
Sage, R. F., & Kubien, D. S. (2007). The temperature response of C3 and C4 photosynthesis. *Plant, Cell and Environment*, *30*(9), 1086–1106. https://doi.org/10.1111/j.1365-3040.2007.01682.x
Serrano, J., Shahidian, S., & da Silva, J. M. (2019). Evaluation of normalized difference water index as a tool for monitoring pasture seasonal and inter-annual variability in a Mediterranean agro-silvo-pastoral system. *Water (Switzerland)*, *11*(1). https://doi.org/10.3390/w11010062
Sheffield, J., Wood, E. F., & Roderick, M. L. (2012). Little change in global drought over the past 60 years. *Nature*, *491*(7424), 435–438. https://doi.org/10.1038/nature11575
Sluijter, R., Plieger, M., Oldenborgh, G. J. van, Beersma, J., & de Vries, H. (2018). Een analyse op basis van het potentiële neerslagtekort. *Knmi*.
Sur, C., Park, S.-Y., Kim, T.-W., & Lee, J.-H. (2019a). Remote Sensing-based Agricultural Drought Monitoring using Hydrometeorological Variables. *KSCE Journal of Civil Engineering*, *23*(12), 5244–5256. https://doi.org/10.1007/s12205-019-2242-0
Sur, C., Park, S. Y., Kim, T. W., & Lee, J. H. (2019b). Remote Sensing-based Agricultural Drought Monitoring using Hydrometeorological Variables. *KSCE Journal of Civil Engineering*, *23*(12), 5244–5256. https://doi.org/10.1007/s12205-019-2242-0
Thornes, J. E. (2002). IPCC, 2001: Climate change 2001: impacts, adaptation and vulnerability, Contribution of Working Group II to the Third Assessment Report of the Intergovernmental Panel on Climate Change, edited by J. J. McCarthy, O. F. Canziani, N. A. Leary, D. J. Dokken a. *International Journal of Climatology*, *22*(10), 1285–1286. https://doi.org/10.1002/joc.775
Tol, C. Van Der, Verhoef, W., Timmermans, J., Verhoef, A., & Su, Z. (2009). An integrated model of soil-canopy spectral radiance observations, photosynthesis, fluorescence, temperature and energy balance. *Biogeosciences Discussions*, *6*(3), 6025. https://doi.org/10.5194/bgd-6-6025-2009
U.S. Geological Survey. (2020). Landsat 8 Level 2 Science Product (L2SP) Guide. *Nasa*, *2*(May). Retrieved from https://prd-wret.s3.us-west-2.amazonaws.com/assets/palladium/production/atoms/files/LSDS-1619_Landsat8-C2-L2-ScienceProductGuide-v2.pdf
Van Der Tol, C., Verhoef, W., Timmermans, J., Verhoef, A., & Su, Z. (2009). An integrated model of soil-canopy spectral radiances, photosynthesis, fluorescence, temperature and energy balance. *Biogeosciences*, *6*(12), 3109–3129. https://doi.org/10.5194/bg-6-3109-2009
Vasquez-Robinet, C., Mane, S. P., Ulanov, A. V., Watkinson, J. I., Stromberg, V. K., De Koeyer, D., … Grene, R. (2008). Physiological and molecular adaptations to drought in Andean potato genotypes. *Journal of Experimental Botany*, *59*(8), 2109–2123. https://doi.org/10.1093/jxb/ern073
Vicente-Serrano, S. M., Beguería, S., & López-Moreno, J. I. (2010). A multiscalar drought index sensitive to global warming: The standardized precipitation evapotranspiration index. *Journal of Climate*, *23*(7), 1696–1718. https://doi.org/10.1175/2009JCLI2909.1
Weijers, R. (2020). *Drought indicators in The Netherlands*. (July), 204. Retrieved from https://repository.tudelft.nl/islandora/object/uuid:3c915a71-95ee-462d-99fc-eaa2fd167765
White, M. A., Thornton, P. E., & Running, S. W. (1997). A continental phenology model for monitoring vegetation responses to interannual climatic variability. *Global Biogeochemical Cycles*, *11*(2), 217–234. https://doi.org/10.1029/97GB00330
Wilhite, D. a. (2011). Quantification of Agricultural Drought for Effective Drought Mitigation and

Preparedness: Key Issues and Challenges. *Agricultural Drought Indices Proceedings of a WMO Expert Meeting Held in Murcia, Spain*, (June), 15.
Wilhite, D. A., & Glantz, M. H. (2019). Understanding the drought phenomenon: The role of definitions. *Planning for Drought: Toward A Reduction of Societal Vulnerability*, 11–27. https://doi.org/10.4324/9780429301735-2
Wösten, H., De Vries, F., Hoogland, T., Massop, H. T. L., Veldhuizen, A. A., Vroon, H., … Bolman, A. (2013). BOFEK2012, de nieuwe, bodemfysische schematisatie van Nederland [BOFEK2012; the new soil physical schematization of the Netherlands, in Dutch]. *Alterra Report*, *2387*, 92. Retrieved from http://edepot.wur.nl/247678
Wu, B., Ma, Z., & Yan, N. (2020). Agricultural drought mitigating indices derived from the changes in drought characteristics. *Remote Sensing of Environment*, *244*(January), 111813. https://doi.org/10.1016/j.rse.2020.111813
Yang, P., Prikaziuk, E., Verhoef, W., & van der Tol, C. (2020). SCOPE 2.0: A model to simulate vegetated land surface fluxes and satellite signals. *Geoscientific Model Development Discussions*, (October), 1–26. https://doi.org/10.5194/gmd-2020-251
Zhang, J., Gao, S., Chen, H., Yu, J., & Tang, Q. (2015a). *Retrieval of the land surface-air temperature difference from high spatial resolution satellite observations over complex surfaces in the Tibetan Plateau*. https://doi.org/10.1002/2015JD023395
Zhang, J., Gao, S., Chen, H., Yu, J., & Tang, Q. (2015b). Retrieval of the land surface-air temperature difference from high spatial resolution satellite observations over complex surfaces in the Tibetan Plateau. *Journal of Geophysical Research*, *120*(16), 8065–8079. https://doi.org/10.1002/2015JD023395
Zhang, L., Yao, Y., Bei, X., Jia, K., Zhang, X., Xie, X., … Chen, X. (2019). Assessing the remotely sensed evaporative drought index for drought monitoring over Northeast China. *Remote Sensing*, *11*(17). https://doi.org/10.3390/rs11171960
Zheng, Q., Huang, W., Cui, X., Shi, Y., & Liu, L. (2018). New spectral index for detecting wheat yellow rust using sentinel-2 multispectral imagery. *Sensors (Switzerland)*, *18*(3), 1–19. https://doi.org/10.3390/s18030868
Zhou, X., Wang, P., Tansey, K., Zhang, S., Li, H., & Wang, L. (2020). Developing a fused vegetation temperature condition index for drought monitoring at field scales using Sentinel-2 and MODIS imagery. *Computers and Electronics in Agriculture*, *168*(17), 105144. https://doi.org/10.1016/j.compag.2019.105144

7. APPENDIX

7.1. Correlation between ERA5 data and KNMI data

The weather data used in the study are the climate reanalysis data, produced by an atmospheric circulation model. ERA5 meteorological variables have been used in the study because there were some variables required by the SCOPE model that are not available from KNMI (Royal Dutch Meteorological Institute), for example, Integrated incoming longwave radiation (Rli).

However, the ERA5 data are global with 10 km resolution but are accurate, and almost similar to the ones provided by KNMI. The following figures show the correlation analysis between KNMI and ERA5 data:

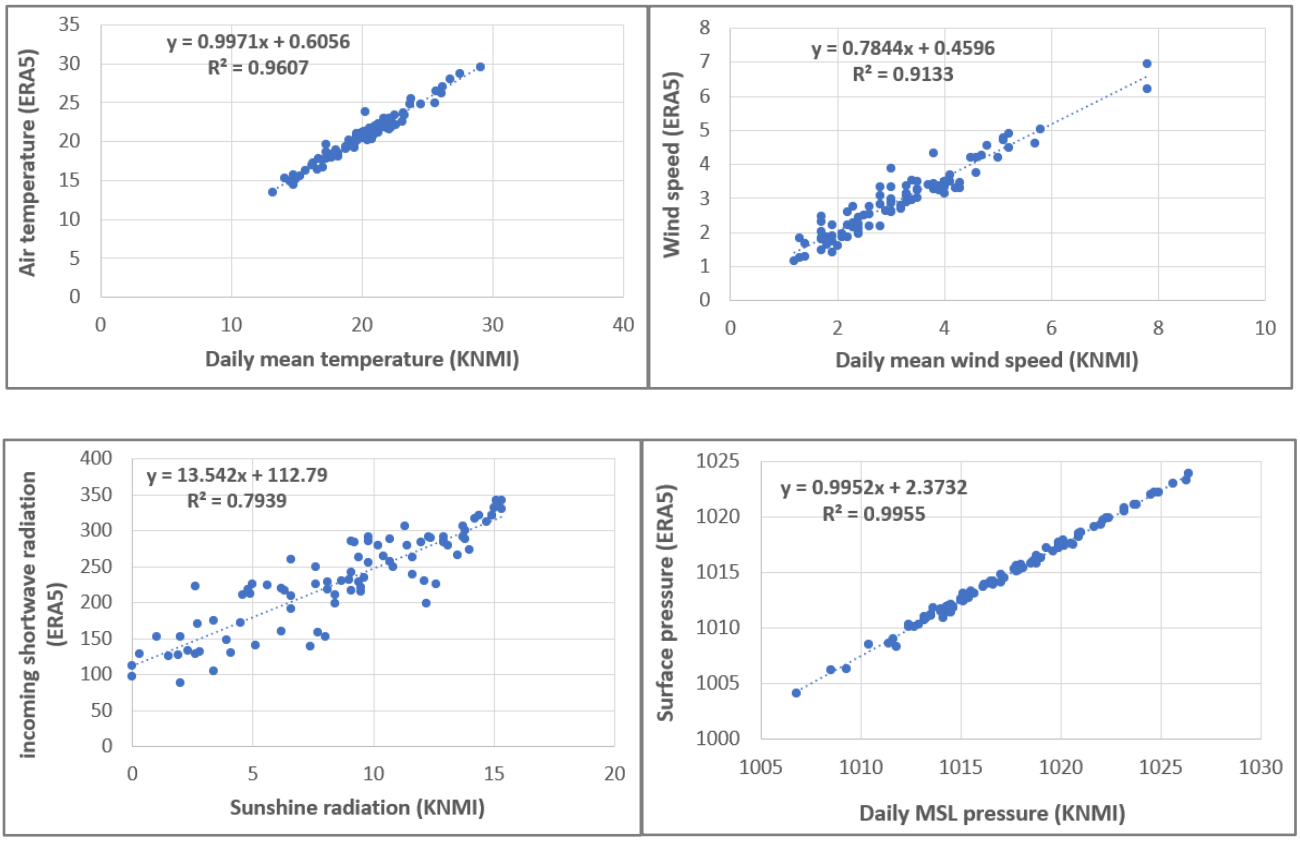

Figure 45: The correlation analysis between KNMI and ERA5 variables, based on the 2018 data.

7.2. Volumetric soil moisture measurements

The following figures show the 15min volumetric soil moisture measurements of all depths (5, 10, 20, 40, and 80cm) for the stations with full dataset 01, 02, 03, 04, 12, 14, and 15 respectively, availability of high soil moisture in the 2018 summer period at the station 14 and 15 is due to the irrigation as shown on figure 42.